



ISAS - INTERNATIONAL SCHOOL FOR ADVANCED STUDIES

Attestato di Ricerca

"Doctor Philosophiae"

THEORY OF THE STRUCTURE OF CHARGED LIQUIDS AND
SOME APPLICATIONS

CANDIDATO:

Giorgio Pastore

RELATORE:

Prof. M.P. Tosi

Anno Accademico 1984/85

TRIESTE

**SISSA - SCUOLA
INTERNAZIONALE
SUPERIORE
DEI STUDI AVANZATI**

TRIESTE
Strada Costiera 11

THEORY OF THE STRUCTURE OF CHARGED LIQUIDS
AND SOME APPLICATIONS

Thesis submitted for the degree of "Doctor Philosophiae"
at the International School for Advanced Studies, Trieste, Italy

Candidato : Giorgio Pastore

Relatore : Prof. Mario P. Tosi

Classe : Fisica

Settore : Stati Condensati della Materia

Anno Accademico 1984/85

ACKNOWLEDGMENTS

I would like to express my gratitude to Prof. M.P.Tosi for his supervision and assistance throughout this research, as well as for his help in the preparation of this manuscript.

I acknowledge the long and fruitful collaboration with Dr.P.Ballone during these years as well as his help in the preparation of the typed version of this thesis.

I also wish to thank Dr.M.Rovere and Dr.G.Senatore for many useful discussions.

The present thesis is an introduction to and a critical discussion of the following papers:

P. Ballone, G. Pastore, M. Rovere, M. P. Tosi "Liquid Structure and Freezing of the Two-Dimensional Classical Electron Fluid" J. Phys. C 18, 4011 (1985)

P. Ballone, G. Pastore, M. Rovere, M. P. Tosi "Structure and Crystallization of the 2-D Classical Electron Fluid" in Festkoerperprobleme XXV (1985) p. 539

G. Pastore, G. Senatore, M. P. Tosi "Electric Resistivity and Structure of Liquid Alkali Metals and Alloys as Electron-Ion Plasmas" Physica 111B, 283 (1981)

G. Pastore, M. P. Tosi "Structure Factor of Liquid Alkali Metals Using a Classical-Plasma Reference System" Physica 124B, 383 (1984)

P. Ballone, G. Pastore, M. P. Tosi "Structure and Thermodynamic Properties of Molten Rubidium Chloride" J. Phys. C 17, L333 (1984)

P. Ballone, G. Pastore, M. P. Tosi "Structure and Thermodynamic Properties of Molten Alkali Chlorides" J. Chem. Phys. 81, 3174 (1984)

G. P. Malescio, G. Pastore, P. Ballone, M. P. Tosi "Evidence for Many-Body Interactions in the Structure of Molten Alkali

Chlorides" Phys. Chem. Liq. 15, 31 (1985)

G. Pastore, P. Ballone, M. P. Tosi "Structure and
Thermodynamic Properties of Molten Strontium Chloride"
J. Phys. C (1985) in press

G. Pastore, P. V. Giaquinta, J. S. Thakur, M. P. Tosi "Ionic
Pairing in Binary Liquids of Charged Hard Spheres with
Non-Additive Diameters" J. Chem. Phys. (1985) in press

I N D E X

INTRODUCTION		p. 13
CHAPTER 1. THEORETICAL BACKGROUND		
1.0	Introduction	p. 1
1.1	The microscopic structure and its experimental connections	p. 1
1.2	The static correlation functions of liquids	p. 7
1.3	Approximate theories	p. 20
CHAPTER 2. MODEL SYSTEMS FOR COULOMB LIQUIDS.		
2.0	Why model systems?	p. 36
2.1	The three-dimensional One-Component Plasma	p. 38
2.2	The two-dimensional One-Component Plasma	p. 48
2.3	Charged hard spheres	p. 58
CHAPTER 3. LIQUID METALS.		
3.0	Introduction	p. 65
3.1	Physics of the liquid alkali metals and their alloys	p. 66
3.2	Alkali metals and their alloys	

	as Electron-Ion Plasmas	p. 70
3.3	Electric resistivity calculations	p. 72
3.4	Beyond the RPA treatment of the pure alkali metals	p. 76
CHAPTER 4. MOLTEN SALTS		
4.0	Introduction	p. 81
4.1	Experimental data, primitive model and refined potentials	p. 81
4.2	Theory of the structural and thermodynamic properties of molten alkali chlorides and strontium chloride	p. 84
4.3	Comparison with the experiments	p. 90

APPENDICES

BIBLIOGRAPHY

INTRODUCTION

The study of the liquid state has drawn increasing attention from both a technological and a basic viewpoint. On one side, a knowledge of the behavior of specific systems and a general picture of the liquid state have widespread usefulness for chemists, electrochemists, astrophysicists and biologists; on the other, the special conditions of this state of the matter (high couplings but no simplification from order) have motivated a lot of experimental and theoretical work to unravel the complexity of such a many-body problem.

Great effort in modern liquid state physics has gone into the determination of liquid structure. Exactly as for solids, a previous knowledge of the microscopic arrangement of the atoms is at the basis of understanding the other physical properties of the system. For this reason the development of experimental techniques for structure determinations has played an important role in the building of the modern picture of this state.

A quantitative evaluation of the thermodynamic quantities of a liquid from the measured structure requires the knowledge of the interparticle interactions. Since the structure itself is determined by the interactions, the theory is faced with the problem of a consistent evaluation of thermodynamics and structure from given interatomic forces which themselves need careful independent study.

Extensive studies of some model liquids, allowed by the progress of computer simulation techniques, have been the bootstrap for the developments of quantitative theories of

the structure. For simple one-component fluids an impressive improvement of the theoretical methods has been achieved in the last decade. Multicomponent charged liquids show a higher degree of structural complexity and the development of quantitative theories is more demanding than a trivial implementation of established techniques.

This thesis aims to be a detailed introduction to and a critical discussion of the work that we have done to develop suitable techniques for such liquids. We have carried out quantitative calculations of thermodynamic and structural properties of widely different charged liquids (molten salts, liquid alkali metals and their alloys, a two dimensional layer of electrons on the surface of liquid helium and some related model systems like classical jellia and charged-hard-spheres liquids).

We regard as the main result of our work the development of theoretical techniques of remarkable accuracy, this being a crucial prerequisite for a meaningful quantitative discussion of physical properties and for contact with experiment.

Each chapter in this thesis begins with a general introduction to set up the scenario in which the discussion of the known results and of our original contributions are embedded. Our results are usually discussed in a self-contained way but a copy of the related papers has been put in a physically separate appendix.

Ch. 1 is mainly a summary of the theoretical tools, as developed in the literature, from which we have started. In chapter 2 we discuss some important model systems: the

classical jellia and the liquid of charged-hard-spheres. In the case of the 3-dimensional one-component plasma (classical jellium) we summarize the known exact results and we compare the performances of the best available approximate theories for the structure. Beside its intrinsic interest, this discussion is useful for the following chapter on liquid alkali metals and to introduce the methods used to deal with the two-dimensional one-component plasma [1] which models an electron layer on the surface of liquid helium. For this system we present a very accurate determination of the static structure which allows us to describe the freezing transition within the density wave theory of freezing. Again in the context of very idealized model systems we present the liquid of charged hard spheres and our own contribution [2] to the investigations of effects of size non-additivity, in relation to structural studies of some electrolyte solutions.

Ch. 3 mainly concerns the electron-ion plasma approach to liquid alkali metals. Our contribution to this problem is twofold: we have checked the accuracy of the lowest order approximation to the coupled system of electrons and ions through resistivity calculations [3] and successfully implemented an extension of this RPA theory [4] to obtain very good agreement with computer simulation and to describe the observed structure in terms of the basic constituents of the liquid metal (ions and electrons).

The last chapter is about molten salts. The technological interest for such systems is very high and extensive experimental characterizations have been

presented in the physical and physico-chemical literature. Due to the complex chemical-bonding behavior of these systems, a truly microscopic description is confined to the simplest salts i. e. those for which the ionic character of the interaction is dominant: alkali halides and, to some extent, the alkaline-earth halides. After the usual introduction to the subject, we shall describe our treatment of the theory of structure [5,6,7] for these liquids. This is a suitable extension to multicomponent charged fluids of the modified hypernetted chain integral equation (MHNC) as successfully developed for monocomponent fluids by Lado, Rosenfeld and Ashcroft. The comparison between our MHNC results and the computer simulation is very satisfying. Hence we can use the theory to get some insight in the observed discrepancies between experiments and computer simulation [8] and therefore to attempt a microscopic picture for more complex salts [9].

CHAPTER 1. THEORETICAL BACKGROUND.

1.0 Introduction.

In the following sections we shall summarize the relevant results of the theory of liquids that we shall be using extensively in the next chapters. The main emphasize has been put on the connection with the measurements and on the theoretical topics closest to the techniques we have used in our investigations. More detailed discussion of the subject herewith presented can be easily found in the literature [10].

In the part 1.1 we shall introduce the "experimental" description of the liquid structure by defining the correlation functions in terms of the response of the system to some external probe. In the part 1.2 we shall change viewpoint and we shall characterize the same functions as equilibrium properties of the unperturbed system making connection with the statistical mechanics formalism. Up to this level the theory is completely general but formal. In the last part we shall illustrate the most important approximate schemes used in the study of the static liquid structure.

1.1 The microscopic structure and its experimental connections.

Since the first experimental determinations of the microscopic structure in condensed matter, it has been realized that the structural information is essential to understand the physical behavior of the dense systems. At the extent in which the structure is determined by the interparticle interactions it carries a precise information on the hamiltonian of the system. On the other side its knowledge is essential to understand the

thermodynamic and transport properties as well as the electronic structure of the liquids.

The most powerful methods of investigation of the microscopic structure of the matter are the scattering experiments. For detailed accounts of the experimental techniques we refer to the literature [11]. Here we simply try to draw, in an approximate way, a map of the experimental methods with particular emphasize on two points: the connection between the measurements and the theoretical language of the correlation functions and the possibilities and limitations of nowadays experiments.

A very useful and enlighting way of looking at the scattering experiments is to consider them as a way of getting the properties of the unperturbed system through its response to external perturbations [12].

The formal basis for this aim is the so called fluctuation and dissipation theorem (F.D.T.) [13, 14] which states that the response of a thermodynamic system to a "weak" external perturbation is directly connected to the correlations between spontaneous fluctuations of the system at the equilibrium. The linear response function $\chi_{AB}(\underline{k}, \omega)$ defined by:

$$\delta \langle A \rangle(\underline{k}, \omega) = \sum_B \chi_{AB}(\underline{k}, \omega) \phi_B(\underline{k}, \omega) \quad 1.1$$

where $\delta \langle A \rangle(\underline{k}, \omega)$ is the first order variation of the equilibrium average of the observable A as consequence of the external perturbation fields $\phi_B(\underline{k}, \omega)$ of wavelenght \underline{k} and frequency ω which couple to the observables B. The F.D.T. connects the functions χ_{AB} to the correlation functions between A and B: for classical systems we have [13]

$$\text{Im} \chi_{AB}(\underline{k}, \omega) = \frac{\omega}{2k_B T} S_{AB}(\underline{k}, \omega) \quad 1.2$$

where

$$S_{AB}(\underline{k}, \omega) = \int d\underline{r} e^{i\underline{k} \cdot \underline{r}} \int d\underline{r}' e^{i\underline{\omega} \cdot \underline{r}'} \left\langle (A(\underline{r}, t) - \langle A(\underline{r}, t) \rangle) (B(\underline{r}', 0) - \langle B(\underline{r}', 0) \rangle) \right\rangle \quad 1.3$$

and for static properties

$$S_{AB}(\underline{k}) = \int \frac{d\omega}{2\pi} S_{AB}(\underline{k}, \omega) = -k_B T \int \frac{d\omega}{2\pi} \frac{\text{Im} \chi_{AB}(\underline{k}, \omega)}{\omega} = -\frac{k_B T}{\rho} \chi_{AB}(\underline{k}) \quad 1.4$$

$\chi_{AB}(\underline{k})$ being defined as $\text{Re} \chi_{AB}(\underline{k}, \omega=0)$

Since in discussing the thermodynamic and structural properties we are interested in the average density fluctuation distribution, we need a probe which couples to these fluctuations.

The scattering of particles gives us such a probe. The analysis of the scattering of a radiation beam by many centers of diffusion shows that the measurable cross section does contain informations on the average positions of the scatterers. The relevant connection is summarized by [15]

$$\frac{d\sigma}{d\Omega dE} = N \sum_{i,j} f_i(\underline{k}) f_j(\underline{k}) S_{ij}(\underline{k}, \omega) \quad 1.5$$

where $f_i(\underline{k})$ is the form factor for the center of scattering of kind i , N the total number of them and $S_{ij}(\underline{k}, \omega)$ are the dynamic partial structure factors (van Hove functions).

Since for different radiations, like electrons, X-ray, neutrons etc., from the currently available sources, we have different relations between the transferred momentum and the transferred energy, they will explore different (in some cases overlapping) regions in the (\underline{k}, ω) space. Hence, for example, the nowadays X-ray techniques are not able to give informations about the dynamic structure (ω dependence).

The X-ray scattering in the original form is also unable to give separately the partial structure factors in multicomponent systems. In the case of a n component

mixture at least $n(n+1)/2$ experiments have to be performed, varying the form factors, to get a solvable system of linear equations in the $n(n+1)/2$ unknown partial structure factors.

The first and more popular technique used to change the form factors has been the isotope substitution [16] in connection with neutron experiments. If we have a sufficient number of isotopes with sufficiently different form factors, we can repeat the neutron diffraction with chemically equivalent samples whose scattering properties are different. Accurate data reduction techniques have been developed [17] to separate the partial $S_{ij}(k, \omega)$.

Many other techniques have been explored in recent years to change the form factors in the 1.5 like combination of X-ray and neutron isotopic substitution [18], X-ray anomalous scattering [19,20] or combined X-ray, neutron and electron scattering [21]. This last technique looks particularly interesting when we realize that the centers of scattering are electrons for X-ray and electrons and nuclei for neutrons.

In principle, looking at a metal as a two component system (valence electrons and ions), it would be possible to separate the diffracted intensities into ion-ion, electron-ion and electron-electron components [22]. However, notwithstanding the theoretical correctness of the argument and the claims of partial experimental confirms [23] we have to note that it is not definitely clear if it is possible to have unambiguous informations from this method within the current experimental precision [24,21].

More in general it is difficult to assess the exact accuracy of the experimental structure factors. Many

approximate corrections, necessary to go from the rough intensity data to the final $S(k)$, will add some uncertainty to the final result; furthermore some details like the heights of peaks of the structure factors will be affected more than others from the experimental resolution of different arrangements.

Whenever it is not easy to decide what is the most accurate experimental result, a good practice would be to look at the structure factors globally without putting too much emphasis on single points [25]. To illustrate this point in fig. 1 we show the difference of measured $S(k)$ for liquid sodium and potassium between the X-ray data of van der Lugt et al. [26] and that of Greenfield et al. [27].

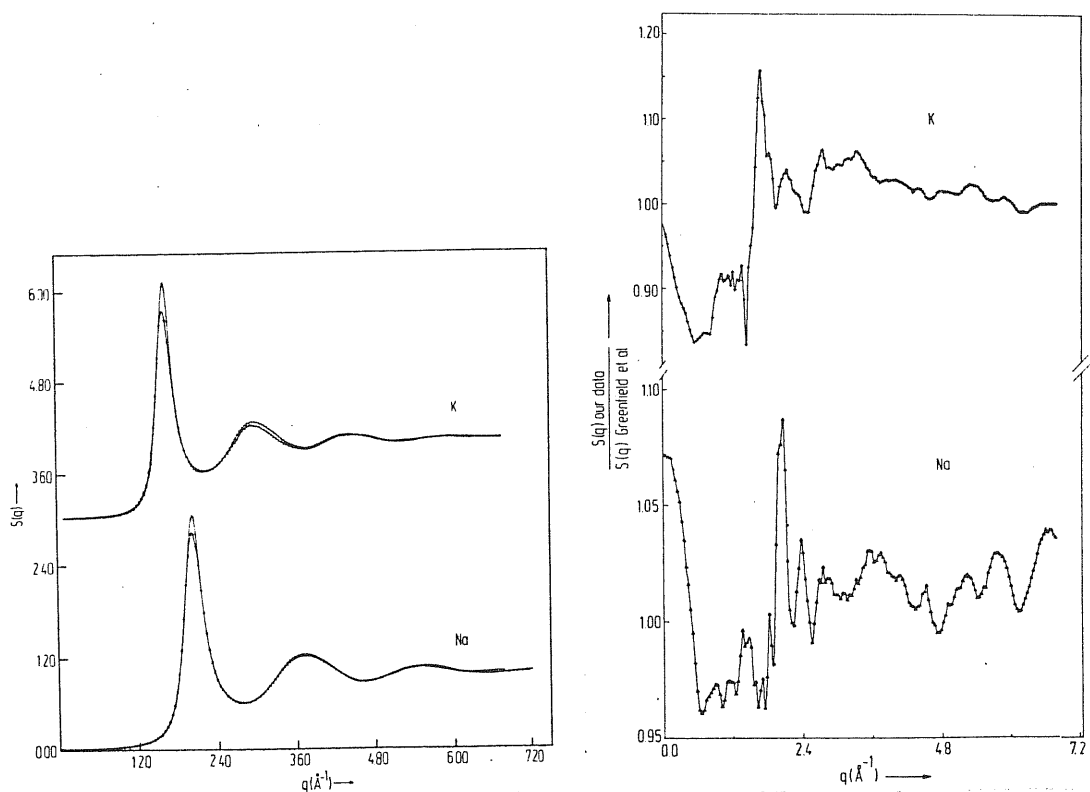


fig. 1. Comparison of the X-ray structure factors and their ratios for Na at 373 K and K at 338 K obtained by Greenfield et al. [27] and Hujiben et al. [26] (higher curves). From [26].

As it is seen the differences are inside the 5% except in the region of small k 's and near the first peak where probably the better resolutive power of the van der Lugt's geometry is playing a crucial role [25]. In any case the 5% can be taken as an estimation of the average accuracy of the best available measurements of structure factors for monocomponent fluids. In the small angle (low k) region, the poorer statistics and the difficult exclusion of the main beam contributions imply larger error bars and it is very difficult to get accurate results below 1 \AA^{-1} of transferred momentum.

In the case of multicomponent systems, the additional data reduction to separate the measurements into the partial structure factors propagates asymmetrically giving rise to an increasing of uncertainty on the numerical values up to one order of magnitude over the precision of the rough original data [17].

Finally we shall comment briefly on the differences between the solid and liquid structure factors. In the case of the harmonic solid it is easy to compute (for a given lattice) the structure factor [28]: it is simply a sum of delta functions (Bragg peaks) centered on the reciprocal lattice vectors of the given structure with a strength modulated by the Debye-Waller factor $\exp(-2W)$ with added a continuous contribution from the multiphonon processes. Increasing the temperature the induced disorder eventually destroys the sharp Bragg's spots leaving out the continuous contributions which depends only from the module of the wavevector k for symmetry reasons. However in the liquid the shape of the structure factor is strongly reminiscent of the solid reciprocal lattice structure at the extent that it is

possible to give a semiquantitative description of the properties of the solid by using perturbations on the corresponding liquid as reference system [151].

For sufficiently complex systems the "projected" 3-D structural information contained in the structure factor is not sufficient to give an unambiguous description of the local order in the system. In this cases additional informations could be obtained from other new techniques like EXAFS, XANES, and related methods [29] which more carefully probe the short range order.

1.2 The static correlation functions of liquids.

1.2.1 Main concepts.

In this section we sketch the formal introduction of the n-body correlation functions for liquids, their formal properties and some of the (few) known exact relations.

We are interested in the equilibrium properties of a macroscopic system. It turns out that a good simplification is to approximate its behavior with the so called thermodynamic limit of that system (volume and number of particles diverging with keeping constant the number density): in this way we get rid of the particular boundary conditions and we are able to characterize sharply some behaviors like phase transitions. However we should not forget that the thermodynamic limit is merely an approximation and hence in some cases its usefulness could have to be checked [30].

The systems we study are such that the quantum behavior can always be confined to the choice of some effective pair interactions (molten salts) or it can be reported

to the properties of the homogeneous electron gas (liquid metals). In particular in the following we shall use classical statistical mechanics without any care of quantum corrections [31].

We deal with a system of N particles in a volume V (both eventually diverging) whose dynamics is ruled by the hamiltonian $H(p, q)$. At the equilibrium it will induce a probability density $\rho(H(p, q))$ in the phase space which satisfies the Liouville equation

$$\left\{ \rho, H \right\}_{\text{Poisson Brackett}} = 0 \quad 1.6$$

Defining the n -body density function as the reduced probability density:

$$\rho^{(n)}(r_1, \dots, r_n) = \int \rho(H(\underline{r}, \underline{p})) d\underline{r}_{n+1} \dots d\underline{r}_N d\underline{p}_1 \dots d\underline{p}_N \quad 1.7$$

we can derive from 1.6 an infinite sequence of coupled integral equations called the Yvon-Born-Green (YBG) hierarchy.

To evaluate the s lowest n -body density functions we need a decoupling scheme which allows to write ρ^{s+1} as functional of ρ^n ($n=1, \dots, s$).

One of the simplest decoupling schemes is the superposition approximation (SA) [32]. It is a factorization of ρ^{s+1} into lower order functions. Despite its appealing simplicity, the SA for the three-body density function gives very poor results for liquid regime [33] when inserted into the YGB equation.

Besides the Kirkwood-Salzburg approach [34], whose usefulness up to now has been confined to the theory, the most useful approaches for the practical evaluation of correlation functions in liquids are the integral equation methods and the perturbations.

Let us summarize, in the case of pair distribution

functions, the main ideas behind the so called integral equation approach (see later for a more formal introduction).

From the pair density function $\rho^{(2)}$ we can define the pair distribution function $g(\underline{r}_1, \underline{r}_2) = \rho^{(2)}(\underline{r}_1, \underline{r}_2) / \rho^{(1)}(\underline{r}_1)$ as the conditional probability of finding a particle {2} in the neighborhood of \underline{r}_2 when we have fixed one other particle {1} at \underline{r}_1 .

The function $g(\underline{r}_1, \underline{r}_2)$ will be 1 at large separations or for uncorrelated particles (ideal case). The pair correlation function $h(\underline{r}_1, \underline{r}_2) = g(\underline{r}_1, \underline{r}_2) - 1$ gives the deviations at \underline{r}_2 respect the average density by having fixed {1} at \underline{r}_1 . This deviation is due partly to the influence of the center of force in \underline{r}_1 and partly to the indirect effect induced by the changes of the density in the other positions. Ornstein and Zernike [35] introduced a new function $c(\underline{r}_1, \underline{r}_2)$, the direct correlation function, which contains only the "direct" effect of {1} on {2}, by "freezing" the density of the system in the other positions $\{\underline{r}\}$ at its average value $\rho^{(1)}(\underline{r})$ in absence of {1}. In other words if we imagine that we put a particle in \underline{r}_1 , $c(\underline{r}_1, \underline{r}_2)$ describes the subsequent variation of density at \underline{r}_2 having inhibited the relaxation elsewhere. A careful analysis of the definitions shows that the relation between $h(\underline{r}_1, \underline{r}_2)$ and $c(\underline{r}_1, \underline{r}_2)$ is: (Ornstein-Zernike (OZ) relation)

$$h(\underline{r}_1, \underline{r}_2) = c(\underline{r}_1, \underline{r}_2) + \int d\underline{r}_3 h(\underline{r}_1, \underline{r}_3) \rho(\underline{r}_3) c(\underline{r}_3, \underline{r}_2) \quad 1.8$$

By using the OZ equation as definition of $c(\underline{r}_1, \underline{r}_2)$, if we have an other relation between h, c and the pair potential we get a close set of equations. The main advantage of this approach is that in a homogeneous fluid the direct correlation function has a simpler

spatial structure than $h(\underline{r}_1, \underline{r}_2)$, it is more directly connected to the pair potential and finally, like $h(\underline{r}_1, \underline{r}_2)$, it has a straight relation to the measured structure factor.

Indeed, recalling the discussion of previous section, we can define $h(\underline{r}_1, \underline{r}_2)$ as correlation between density fluctuations:

$$\begin{aligned} \rho h(\underline{r}_1, \underline{r}_2) &= \rho h(|\underline{r}_1 - \underline{r}_2|) = \\ &= \frac{1}{N} \left\langle \sum_{i \neq j} \delta(\underline{r}_1 - \underline{r}_i) \delta(\underline{r}_2 - \underline{r}_j) \right\rangle - \rho \end{aligned} \quad 1.9$$

If we define the Fourier components of the density fluctuation as

$$\rho(\underline{k}) = \sum_j e^{i\underline{k} \cdot \underline{r}_j}$$

the measurable structure factor $S(\underline{k})$ is related to the density correlations at \underline{k} wavevectors and then to the Fourier transform $\hat{h}(\underline{k})$ of $h(\underline{r})$ or finally, through OZ, to the Fourier transform of the $c(\underline{r})$:

$$S(\underline{k}) = \frac{1}{N} \left\langle \rho(\underline{k}) \rho(-\underline{k}) \right\rangle = 1 + \rho \hat{h}(\underline{k}) = \frac{1}{1 - \rho \hat{c}(\underline{k})} \quad 1.10$$

The connection between the correlation functions of the homogeneous system and the thermodynamics is straightforward starting from 1.9. Let us assume that the N-body hamiltonian of the system is written as

$$H_N = T_N + U_N = \sum_i \frac{p_i^2}{2m} + \sum_{i=1}^N \sum_{i_1, \dots, i_m}^N U^{(m)}(\underline{r}_i, \dots, \underline{r}_{i_m}) \quad 1.11$$

i. e. we have written the potential energy as a summation of 1-body, 2-body, ..., N-body contributions; for homogeneous systems $U^{(1)}(\underline{r}_1) = 0$.

The partition function is

$$Z_N = \frac{\Lambda^{-3N}}{N!} Q_N = \frac{\Lambda^{-3N}}{N!} \int d\mathbf{r}_1 \dots d\mathbf{r}_N e^{-\beta U_N} \quad 1.12$$

(Q_N : configurational partition function) and the free energy per particle is:

$$f = \lim_{\substack{N \rightarrow \infty \\ V \rightarrow \infty \\ N/V \rightarrow \text{const}}} \frac{F_N}{N} = T \cdot \lim (-k_B T \log Z_N)$$

The s-body correlation functions are defined by:

$$g^{(s)}(r_1, \dots, r_s) = T \cdot \lim \frac{1}{Z_N} \int e^{-\beta U_N} d\mathbf{r}_{s+1} \dots d\mathbf{r}_N \quad 1.13$$

The internal energy per particle is

$$\begin{aligned} u &= T \cdot \lim \frac{\langle U_N \rangle}{N} = \\ &= \frac{\rho}{2} \int g^{(1)} \beta U^{(2)}(r) d\mathbf{r} + \frac{\rho^2}{6} \int g^{(3)}(r_1, r_2, r_3) \beta U^{(3)}(r_1, r_2, r_3) d\mathbf{r}_1 d\mathbf{r}_2 d\mathbf{r}_3 + \\ &+ \dots \end{aligned} \quad 1.14$$

An other connection between thermodynamics and correlation functions is given by the virial theorem [36].

$$\begin{aligned} \frac{\beta P}{\rho} &= 1 - \frac{\beta}{3N} \left\langle \sum_{i=1}^N \mathbf{r}_i \cdot \nabla_i U_N(\mathbf{r}) \right\rangle = \\ &= 1 - \frac{\rho}{6} \int g^{(1)} r \frac{\partial \beta U^{(2)}(r)}{\partial r} d\mathbf{r} + \dots \end{aligned} \quad 1.15$$

Finally from the normalization of the pair distribution function and from the thermodynamic relation $(\langle N^2 \rangle - \langle N \rangle^2) / \langle N \rangle = k_B T \chi_T$ (χ_T = isothermal compressibility) we get $\lim_{k \rightarrow 0} S(k) = nk_B T \chi_T$ whatever is the potential.

All the previous formulas can be extended to the case of multicomponent fluids by putting the species indices on the correlation functions and adding to each integration on the coordinates of a particle a summation over the possible species.

In particular the energy and the virial expression for a pair interacting system become:

$$U^{exc} = \frac{1}{2} \rho \sum_{\alpha, \beta} x_{\alpha} x_{\beta} \int d\vec{r} \beta U_{\alpha\beta}(r) g_{\alpha\beta}(r) \quad 1.16$$

$$\frac{\beta P}{\rho} = 1 - \frac{\rho}{6} \sum_{\alpha, \beta} x_{\alpha} x_{\beta} \int r g_{\alpha\beta}(r) \frac{\partial \beta U_{\alpha\beta}(r)}{\partial r} d\vec{r} \quad 1.17$$

(the concentrations x_{α} are defined by $\rho_{\alpha} = x_{\alpha} \rho$)

To discuss the long-wavelength behavior of the structure factors in a binary system is more useful to introduce the Bathia-Thornton [37] structure factors: from the correlations between density fluctuations of each species we can build the structure factors based on the charge (Q), density (N) and concentration (c) fluctuations [38]:

$$\delta N(k) = \delta n_1(k) + \delta n_2(k)$$

$$\delta c(k) = \delta n_1(k) - \delta n_2(k) \quad 1.18$$

$$\delta Q(k) = z_1 \delta n_1(k) + z_2 \delta n_2(k) \quad (\text{for charged systems})$$

$$S_{NN} = \frac{k_B T}{\rho} \langle \delta N(k) \delta N(-k) \rangle = x_1 S_{11}(k) + 2(x_1 x_2)^{1/2} S_{12}(k) + x_2 S_{22}(k)$$

$$S_{NC} = \frac{k_B T}{\rho} \langle \delta N(k) \delta c(-k) \rangle = x_1 x_2 [S_{11}(k) - S_{22}(k) + (x_2 - x_1)(x_1 x_2)^{1/2} S_{12}(k)]$$

$$S_{CC} = \frac{k_B T}{\rho} \langle \delta c(k) \delta c(-k) \rangle = x_1 x_2 [x_2 S_{11}(k) + x_1 S_{22}(k) - 2(x_1 x_2)^{1/2} S_{12}(k)]$$

$$S_{NQ} = \frac{k_B T}{P} \langle \delta N(k) \delta Q(-k) \rangle = x_1 z_1 S_{11}(k) + (z_1 + z_2) (x_1 x_2)^{1/2} S_{12}(k) + x_2 z_2 S_{22}(k)$$

1.19

$$S_{QQ} = \frac{k_B T}{P} \langle \delta Q(k) \delta Q(-k) \rangle = x_1 z_1^2 S_{11}(k) + 2z_1 z_2 (x_1 x_2)^{1/2} S_{12}(k) + x_2 z_2^2 S_{22}(k)$$

$$S_{QC} = \frac{k_B T}{P} \langle \delta Q(k) \delta C(-k) \rangle = z_1 x_1 S_{11}(k) + (z_2 - z_1) (x_1 x_2)^{1/2} S_{12}(k) + x_2 z_2 S_{22}(k)$$

The analysis of the long-wavelength limit yields

$$\lim_{k \rightarrow 0} c_{\alpha\beta}(k) (P_\alpha P_\beta)^{1/2} = \delta_{\alpha\beta} - \frac{(x_\alpha x_\beta)^{1/2} P}{k_B T} \left(\frac{4n e^2 t_\alpha z_\beta}{k^2} + \mu_{\alpha\beta} \right) \quad 1.20$$

where $\mu_{\alpha\beta} = \left. \frac{\partial \mu_\alpha}{\partial P_\beta} \right|_{T, P, V}$

which implies:

$$\lim_{k \rightarrow 0} S_{NN}(k) = P k_B T \chi_T + \delta^2 S_{CC}(k=0)$$

$$\lim_{k \rightarrow 0} S_{NC}(k) = -\delta S_{CC}(k=0)$$

$$\lim_{k \rightarrow 0} S_{CC}(k) = N k_B T \left[\frac{\partial^2 G}{\partial x_1^2} \right]_{T, P, N}^{-1} \quad 1.21$$

$$\left(\delta = \frac{1}{V} \left(\frac{\partial V}{\partial x_1} \right)_{P, T, N} = \frac{\sigma_1 - \sigma_2}{x_1 \sigma_1 + x_2 \sigma_2} \right)$$

and, for charged systems ($z_i \neq 0$)

$$\lim_{k \rightarrow 0} S_{QQ}(k) = \lim_{k \rightarrow 0} S_{NQ}(k) = 0 \quad 1.22$$

we stress that the exact correlation functions do satisfy the thermodynamic consistency requirements i. e., starting from each of the formulas connecting the structure to thermodynamics the same value for the

thermodynamic quantities will be obtained. In general approximate theories break the consistency and different routes to the same quantity will give different results. The extent of the inconsistency gives a partial measure of the goodness of the theory. Notwithstanding the consistency requirements are not sufficient from themselves alone to fix the form of any approximation [39], the forcing of their fulfilment to fix free parameters in approximate theories usually induces significant improvements.

In the case of charged fluids some care has to be put in dealing with the previous relations. Due to the long range of the Coulomb potential some of the integrals involved can be divergent. In these cases a careful exploiting of the overall neutrality of the system allows a reordering of terms in such a way that similarly diverging terms erase exactly between themselves leaving out the physically meaningful finite contributions.

For Coulomb systems the energetic gain induced by a good screening of the bare long-range interaction is at the origin of some additional sum rules: the so-called Stillinger and Lovett (SL) conditions [40].

The first SL condition is simply a local restatement of the neutrality of the system (the total amount of average charge around a given ion exactly counterbalances the central charge q_i).

$$\sum_j q_j \rho_j \int g_{ij}(r) dr = -q_i \quad i=1, \dots, n \quad 1.23$$

The second condition can be written as

$$\sum_{i,j} q_i q_j \rho_i \rho_j \int r^2 g_{ij}(r) dr = - \frac{3 \epsilon k_B T}{2 \pi} \quad 1.24$$

where q_i and ρ_i are the charge and the density of the

species i and ϵ the dielectric constant.

The existence of SL conditions, which is consequence of the non integrable $1/r$ tail of the potential, is directly reflected in the small k behavior of the charge-charge structure factor:

$$\lim_{k \rightarrow 0} S_{qq}(k) = \frac{k^2}{k_D^2} \quad 1.25$$

$$\text{where } k_D^2 = \frac{4\pi e^2 \rho}{k_B T}$$

It is possible to show [41] that the validity of the OZ equation and the asymptotic behavior

$$c_{ij}(r) \xrightarrow{r \rightarrow \infty} - \frac{\beta q_i q_j}{\epsilon r} \quad 1.26$$

imply the SL conditions.

The condition 1.26 is the particular case of the general asymptotic behavior of c :

$$c_{ij}(r) \sim -\beta \phi_{ij}(r) \quad 1.27$$

which is believed to hold for almost all thermodynamic states and for almost every simple fluid system. Notwithstanding many reasonable a priori arguments, indirect evidence and formal results [42] supporting the validity of the 1.27 there is no rigorous proof of its validity [43]. In any case in the following we shall assume that 1.27 holds for the systems we are interested.

1.2.2 Formal developments.

Many exact and approximate relations between the correlation functions were derived originally through cumbersome diagrammatic techniques applied to the virial expansions of the free energy and pair correlation functions. For instance, one of the more satisfying approximate theories, the so called hypernetted-chain (HNC) theory [44], was found in an attempt to include in the $g(r)$ the largest set of computable terms from the virial expansion [45].

A more physically controllable and mathematically sound basis for developing and interpreting approximations is given by the functional theory of correlations. In the following we shall collect some of the results for classical fluids derived using this approach.

We can recognise [46] the correlation function of an equilibrium system as the functional derivative of some suitable generating functional which turns out to be connected to thermodynamic quantities.

Let us consider a liquid one-component system whose hamiltonian is

$$H = \sum_i \frac{p_i^2}{2m} + \sum_{i < j} \phi_{ij} + \sum_i \psi(r_i) = \sum_i \frac{p_i^2}{2m} + U_N + \sum_i \psi_i \quad 1.28$$

where ψ is some external field. The gran partition function Ξ is given by

$$\Xi = \sum_{N=0}^{\infty} \frac{1}{N!} \int e^{-\beta U_N} \prod_{i=1}^N z(r_i) d\{r_i\} \quad 1.29$$

where $z(r_i) = \exp(\beta\mu - \beta\psi(r_i))$. The n-body density functions $\rho^{(n)}(r_1, \dots, r_n; \psi)$ in presence of the external field are defined as

$$\rho^{(n)}(r_1, \dots, r_n) = \frac{1}{\Xi} \sum_{N=2^m}^{\infty} \frac{1}{(N-n)!} \int e^{-\beta U_N} \prod_{i=1}^N z(r_i) d r_{n+1} \dots d r_N \quad 1.30$$

If we consider Ξ as functional of $z(\underline{r})$ it is easy to show that

$$\frac{\delta \Xi}{\delta z(\underline{r})} = \Xi z^{-1}(\underline{r}) \rho^{(1)}(\underline{r}, \psi) \quad 1.31$$

and for higher derivatives

$$1.32 \quad \frac{\delta^n \Xi}{\delta z(\underline{r}_1) \dots \delta z(\underline{r}_n)} = \Xi z^{-1}(\underline{r}_1) \dots z^{-1}(\underline{r}_n) \rho^{(n)}(\underline{r}_1, \dots, \underline{r}_n; \psi)$$

Similarly we can get the generalizations \mathcal{Y}_n of the pair correlation functions $h(\underline{r}_1, \underline{r}_2)$ (Ursell functions)

$$\begin{aligned} \mathcal{Y}_1(\underline{r}) &= \rho^{(1)}(\underline{r}) \quad ; \quad \mathcal{Y}_2(\underline{r}_1, \underline{r}_2) = \rho^{(2)}(\underline{r}_1, \underline{r}_2) - \rho^{(1)}(\underline{r}_1) \rho^{(1)}(\underline{r}_2) \\ \vdots \\ \mathcal{Y}_n(\underline{r}_1, \dots, \underline{r}_n) &= \rho^{(n)}(\underline{r}_1, \dots, \underline{r}_n) - \sum_{t=1}^{n-1} \binom{n-1}{t} \left\{ \rho^{(t)}(\underline{r}_1, \dots, \underline{r}_t) \mathcal{Y}_{n-t}(\underline{r}_{t+1}, \dots, \underline{r}_n) \right\}_{\text{Permutations}} \end{aligned} \quad 1.33$$

from the $\log \Xi$ considered as functional of the $z(\underline{r})$:

$$\frac{\delta^n \log \Xi}{\delta z(\underline{r}_1) \dots \delta z(\underline{r}_n)} = z^{-1}(\underline{r}_1) \dots z^{-1}(\underline{r}_n) \mathcal{Y}_n(\underline{r}_1, \dots, \underline{r}_n; \psi) \quad 1.34$$

By using the Gibbs result [47] that the grand partition function is minimum at the equilibrium density it is easy to prove that it is a unique functional of the one-body density function of the system (it is evident that we are dealing with the classical counterpart of the well known Hohenberg-Kohn theorem for the ground state energy of quantum systems). Moreover it is possible to show [48] that the free energy functional

$$\mathcal{R} = -\beta F_{\text{excess}} \quad 1.35$$

is the generating functional of the n-body direct correlation functions:

$$c^{(n)}(\underline{r}_1, \dots, \underline{r}_n; \psi) = \frac{\delta^n \mathcal{R}}{\delta \rho(\underline{r}_1) \dots \delta \rho(\underline{r}_n)} \quad 1.36$$

Finally if we regard $\log \Xi$ or \mathcal{R} as functionals of the pair interaction $\phi(\underline{r}_1, \underline{r}_2)$ we find [54 and appendix A] the result

$$\rho^{(2)}(\underline{r}_1, \underline{r}_2) = -2 \frac{\delta \log \Xi}{\delta \phi(\underline{r}_1, \underline{r}_2)} = -2 \frac{\delta \mathcal{R}}{\delta \phi(\underline{r}_1, \underline{r}_2)} \quad 1.37$$

The function $c^{(2)}$ defined by 1.36 coincides with the OZ direct correlation function (see appendix A).

Within the functional formalism it is possible to derive all the known relations between thermodynamic and structural quantities in a simple and straightforward way. Moreover, since the formalism is essentially the mathematical translation of the physical picture of the response of equilibrium quantities to external perturbations, the connection with the experimental viewpoint is particularly simple.

A useful and often used procedure for the determination of the distribution functions hinges on the fact that in a classical system at the equilibrium, the moments and the positions are completely decoupled. Thus it is possible to consider a $n+s$ distribution function of homogeneous liquids as the s particle function of an inhomogeneous system in the external field generated by n particles fixed at their positions [49].

Finally we shall sketch the derivation of an exact relation [50] for the correlation functions which will be extensively used in the following. Let us start with the free energy functional:

$$F[n(r)] = F_{id}[n(r)] + F_{exc}[n(r)] + \int \delta n(r) \phi(r_0, r) dr$$

$$(F_{id}[n(r)] = F_0 + k_B T \int dr' n(r') (\log n(r') - 1)) \quad 1.38$$

where F_{id} and F_{exc} are the ideal and the excess parts of the Helmholtz free energy of the inhomogeneous system at the density $n(r)$ and $\phi(r_0, r)$ is the external potential (which generates the inhomogeneity) due to an extra particle (equal to the constituent of the system) put at r_0 .

At the equilibrium density $\bar{n}(r)$ $F[n(r)]$ is stationary and the Euler equation is:

$$\frac{\delta F}{\delta u(\underline{r})} \Big|_{\bar{n}(r)} = \frac{\delta F_{id}[\bar{n}]}{\delta u(\underline{r})} \Big|_{\bar{n}} + \frac{\delta F_{exc}[\bar{n}]}{\delta u(\underline{r})} \Big|_{\bar{n}} + \phi(\underline{r}_0, \underline{r}) \quad 1.39$$

by using the previous formulas, the OZ equation and exploiting the mentioned equivalence between the homogeneous pair functions and the inhomogeneous 1-particle functions in an external field due to one extra particle at \underline{r}_0 , we find the exact relation:

$$g(r) = \exp[-\beta \phi(r) + h(r) - c(r) - b(r)] \quad 1.40$$

where $b(r)$, called for historical reasons bridge diagram function or elementary diagram function, is defined as

$$b(r) = - \sum_{n \geq 3} \frac{\rho^{n+1}}{(n-1)!} \int d\underline{r}_1 \dots d\underline{r}_{n-1} c^{(n)}(\underline{r}_1, \dots, \underline{r}_{n-1}, \underline{r}) h(\underline{r}_1) \dots h(\underline{r}_{n-1}) \quad 1.41$$

To aid for the reader the diagrammatic definitions [51] which correspond to the eqn. 1.40 and 1.41 are reported in appendix B.

1.3 Approximate theories.

The actual calculation of structural and thermodynamic quantities requires a careful usage of approximations in the general scheme. One of the methods with the broadest spectrum of possible applications is the computer simulation using the two main routes of Molecular Dynamics (MD) and Monte Carlo (MC). Very detailed descriptions of the methods can be found in the literature [52].

The well known limitations of computer simulation come from the relatively small number of particles ($\sim 10^2 \div 10^4$) which is practically possible to use in computations. Moreover the time consuming calculations necessary to include many-body interactions put a further limit to the present days performances.

Within these limits the computer simulation is able to give almost exact results i.e. thermodynamic properties and pair correlation functions are evaluated with a probable error of few percents and its help in understanding the physics of the many-body systems can not be overestimated.

However the existence of computer simulation possibility does not exclude the relevance of different approximate methods which can offer the advantage of a simpler implementation, smaller calculation times and, in some cases, more insight in the physics of the system at the price of a reduced control on the accuracy.

One of the main achievements of the work presented in the next chapters is the conclusion that approximate theories for charged liquids can be cast at a quantitative level comparable with the computer simulation.

In the following pages we shall briefly illustrate some of the most important approximate theories for classical fluids.

1.3.1 Perturbative theories and the Optimized Random Phase Approximation.

The most important characteristic of a liquid is the presence of an excluded volume effect due to the harsh short-range repulsion. This feature appears to be the main responsible of the high density regime liquid structure, the attractive part of the potential providing the "glue" for the cohesion of the system. This picture of the liquid dates back to the van der Waals investigations on the equation of state [53].

More specifically, it has been shown [54,55] that the hard sphere structure factor fits well the experimental data for many liquids [56]. Taking into account this observation, the perturbative theory proceeds in three steps: firstly the original pair interaction is splitted into the reference and perturbation part, next the reference part is approximate with some suitable well known repulsive system (in most cases hard spheres) and finally the effects of the perturbation on the structure and thermodynamics are evaluated.

The crucial step is the first one: a bad choice of the division gives poor results whereas a judicious choice of the separation can improve in a substantial way the convergence of the perturbative expansion. Good general choices were found by Barker and Henderson [57] and by Weeks, Chandler and Andersen [58] (WAC). We shall describe the WAC approach, referring to the literature for an account of different methods [59].

In the WAC theory [60-70] we can imagine an ideal

process in which we change continuously the pair potential from the hard sphere interaction into the actual repulsion. Since the potential enters in the partition function through the Mayer's function $f(r) = \exp(-\beta\phi(r)) - 1$, we can use the change of these functions as expansion parameter.

The difference $B_d = f - f_d$ (blip function) is different from zero only in a very thin region. The effect of switching on the true potential from the hard sphere one is reflected in a change of the free energy and of the correlation functions.

If we choose d in such a way that the first order variation of the free energy is zero i. e. if we take the hard sphere system whose thermodynamics is closest to that of the real one, we have an equation for d at each density and temperature:

$$\int d\mathbf{r} B_d(r) = 0 \quad 1.42$$

If the pair potential w has an attractive part, we can always separate it into a purely repulsive reference interaction (u_0) and a perturbation $u(r) = w(r) - u_0(r)$ containing the remaining part.

Approximating the repulsive part by using the relation

$$g_0(r) = y_d(r) \exp(-\beta u_0(r)) \quad 1.43$$

(where $y_d(r) = g_d(r) \exp(\beta\phi_d(r))$ is the so-called cavity distribution function of the hard sphere liquid whose diameter d has been defined by 1.42) we have to take into account systematically the effects of the attractive part.

By introducing the collective variables $q(\mathbf{k}) = \sum_j^N \exp(-i\mathbf{k} \cdot \mathbf{r}_j)$ and the Fourier transform of the perturbation $\hat{u}(\mathbf{k}) = \int (w - u_0) e^{i\mathbf{k} \cdot \mathbf{r}}$ we can write the partition function as

$$Q = Q_0 \left\{ e^{-\frac{1}{2} \beta N \rho \left(1 - \frac{1}{N}\right) \hat{u}(0)} \right\} \prod_{\underline{k}}' \exp[\beta \rho \hat{u}(\underline{k})] \left\langle \prod_{\underline{k}}' S(\underline{k}) \right\rangle \quad 1.44$$

where $s(\underline{k}) = \exp\left[-\beta \frac{\hat{u}(\underline{k})}{V} q(\underline{k}) q(-\underline{k})\right]$ is called the \underline{k} -th mode and $\rho = N/V$, Q_0 is the reference partition function and the prime (') indicates the exclusion of the $\underline{k}=0$ value. The first bracketed term is the mean-field contribution of the attractive part (van der Waals) while the remaining terms contain the effects of the density fluctuations and can be introduced in the theory in a systematic way.

In particular we can write ($s_i = s(\underline{k}_i)$)

$$\left\langle \prod_{\underline{k}}' S(\underline{k}) \right\rangle = \prod_{\underline{k}}' \langle S(\underline{k}) \rangle \cdot \left[\prod_{\substack{\underline{k}_1 \neq \underline{k}_2 \\ \underline{k}_1, \underline{k}_2}}' \frac{\langle s_1 s_2 \rangle}{\langle s_1 \rangle \langle s_2 \rangle} \right]^{1/2} \cdot \left[\prod_{\substack{\underline{k}_1, \underline{k}_2, \underline{k}_3 \\ \underline{k}_1, \underline{k}_2, \underline{k}_3}}' \frac{\langle s_1 s_2 s_3 \rangle \langle s_1 \rangle \langle s_2 \rangle \langle s_3 \rangle}{\langle s_1 s_2 \rangle \langle s_2 s_3 \rangle \langle s_3 s_1 \rangle} \right]^{1/3} \cdot \dots \quad 1.45$$

where the first product treats each mode as independent (Random Phase Approximation (RPA)), the second introduces the correlation between two modes, the third between three and so on.

Taking the logarithm of 1.45 we get

$$-\frac{\beta \Delta F}{V} = F_0 - \frac{1}{2} \beta \rho^2 \left(1 - \frac{1}{N}\right) \hat{u}(0) + \sum_{n=1}^{\infty} a_n \quad 1.46$$

where

$$a_1 = \frac{1}{V} \sum_{\underline{k}}' \left[\rho \beta \hat{u}(\underline{k}) + \log B_1(\underline{k}) \right]$$

$$a_n = \frac{1}{V n!} \sum_{\underline{k}_1}^{\dots} \log B_n(\underline{k}_1^{-1}) \quad n \geq 2 \quad 1.47$$

and

$$B_1(\underline{k}) = \langle S(\underline{k}) \rangle$$

$$B_2(\underline{k}) = \frac{\langle s_1 s_2 \rangle}{\langle s_1 \rangle \langle s_2 \rangle} \dots \quad 1.48$$

The explicit evaluation of B_1 gives [71]:

$$F = F_{RPA} + \text{higher order terms}$$

$$F_{RPA} = F_0 - \frac{1}{2} \beta \rho^2 \int u(r) g_0(r) dr + \frac{1}{2} \frac{1}{(2\pi)^3} \int d\underline{k} \cdot \left\{ \beta \rho \hat{u}(\underline{k}) S_0(\underline{k}) - \log [1 + \beta \rho \hat{u}(\underline{k}) S_0(\underline{k})] \right\} \quad 1.49$$

At the level of direct correlation function the RPA assumes the simplest form:

$$c_{RPA}(r) = c_0 - \beta u(r) \quad 1.50$$

which implies

$$S_{RPA}(k) = \frac{S_0(k)}{1 + \beta \rho \hat{u}(k) S_0(k)} \quad 1.51$$

The main limit of the RPA is that if $\beta \rho \hat{u}(k) S_0(k) < -1$ the $S_{RPA}(k)$ becomes negative i.e. physically meaningless.

More in general $g(r)$ is different from zero inside the excluded volume.

In order to improve the RPA results without going to higher orders in the expansion it is possible to exploit the freedom in the choice of the potential inside the hard core ($\phi_{HS}(r) = \phi_{HS}(r) + \phi(r) \theta(\sigma - r)$). If we expand the correction $\phi^c(r) = \phi^c(r) \theta(\sigma - r)$ into orthogonal functions we can use the condition of minimum on the (approximate) free energy 1.49 to get

$$\frac{\delta \mathcal{A}}{\delta \phi^c(r)} = g(r) = 0 \quad r < \sigma$$

The resulting approximation $c(r) = c_{RPA}(r) + \phi^c(r)$ is called Optimized RPA (ORPA) [79].

The previous optimization condition is equivalent to a resummation of the mean force potential in such a way that the new optimized potential becomes weaker than the original bare potential having included part of the screening effects. Here we note that the essential feature of the optimization condition is the reintroduction of the physically excluded volume effect on the $g(r)$ by changing the form of the RPA direct correlation function at small distances. This would suggest a more general extension of the optimization procedure also in the case of continuous potentials in the same spirit of the MSA integral equation for such potentials (see later). We shall go back to this point in the ch.3 when we shall discuss the application of the ORPA to a coulombic reference system.

As illustration of the quality of the approximation for neutral one-component fluids in fig.2 we show the results of the standard ORPA for a Lennard-Jones liquid in the strongly coupled regime.

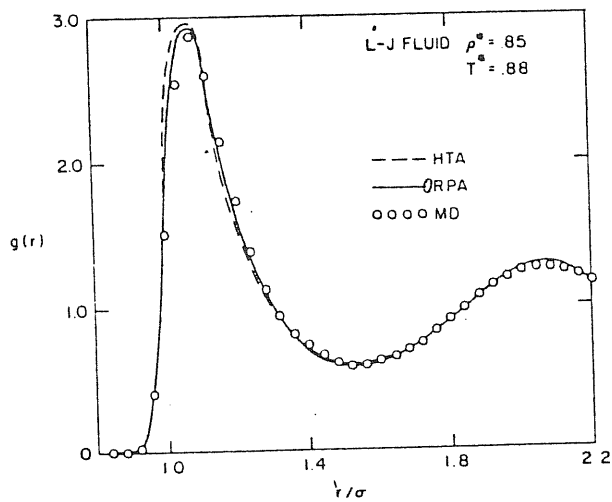


fig. 2. Radial distribution function for a Lennard-Jones fluid near the triple point (ORPA and simulation). The HTA curve neglects the attractive part of the potential. From ref. [62].

1.3.2 Integral equations and the Modified Hypernetted Chain approximation.

The integral equation approach to the liquid structure is just the introduction of suitable approximations in the exact formal relations between different correlation functions (see sections 1.2.1, 1.2.2). Many equivalent routes exist to derive the same equations [71].

A particular transparent way of deriving integral equations is the Percus method [49] which is based on the truncation at some order of the functional expansion in powers of the "external potential" originated by a fixed particle. The idea is that if we are able to find a combination of density distributions and external field which is sufficiently slowly varying with the chosen parameter of expansion, we can approximate it with the few first terms. If we have a slowly varying potential we can expand the induced density:

$$\begin{aligned} \delta\rho(\underline{r}) &= \rho(\underline{r}, \psi) - \rho(\underline{r}, 0) = \rho [g(\underline{r}) - 1] = \rho h(\underline{r}) = \\ &= \int d\underline{r}' \frac{\delta\rho(\underline{r})}{\delta[-\beta\phi(\underline{r}')] } \beta\phi(\underline{r}') = -\rho\beta\phi(\underline{r}) + \rho^2 \int h(\underline{r}_{12}) [-\beta\phi(\underline{r}_{23})] d\underline{r}_2 \end{aligned} \quad 1.53$$

or

$$h(\underline{r}_{13}) = -\beta\phi(\underline{r}_{13}) + \rho \int h(\underline{r}_{12}) [-\beta\phi(\underline{r}_{23})] d\underline{r}_2 \quad 1.54$$

and comparing with OZ we get

$$c(\underline{r}) = -\beta\phi(\underline{r}) \quad 1.55$$

which is equivalent to the RPA or, for charged systems, to the Debye-Hueckel approximation.

The problems of the RPA, as already discussed, come in the short range distances where the potential varies abruptly. If we repeat the same expansion having ϕ_0 as reference interaction (instead $\phi_0 = 0$), we shall derive $c(\underline{r}) = c_0(\underline{r}) - \beta\phi(\underline{r})$, where $c_0(\underline{r})$ is the direct correlation function of the reference potential, recovering the form of RPA discussed in the WCA approach.

We can improve the results by choosing the density as variable since it is more smoothly varying with the position. If we recall that for non-interacting particles $\rho^{(1)}(r, \psi) = z(r) = e^{\mu - \beta\psi}$, we can try to expand $\rho^{(1)}(r, \psi)/z(r)$ in powers of $\delta\rho(r)$ up to the first order

$$\begin{aligned} \frac{\rho(r, \psi)}{z(r)} &= \frac{\rho(r, 0)}{z(r)} + \int \left[\frac{\delta}{\delta\rho^{(1)}(z|\phi)} \frac{\rho(1|\phi)}{z(1)} \right]_{\phi=0} \delta\rho(z) d\{z\} = \\ &= \frac{\rho}{z} + \frac{\rho^2}{z} \int c(1,2) h(2,0) d\{z\} \end{aligned} \quad 1.56$$

and using OZ we get

$$g(r) = \exp(-\beta\phi(r)) [g(r) - c(r)] \quad 1.57$$

which is the Percus-Yevick equation [72] which has to be coupled to the OZ equation to get a closed set of equations.

Since the logarithm usually "damps" the variations we can suppose that $\log \rho(r, \psi)/z(r)$ is also better approximated by the linear term in $\delta\rho$. In this way we derive the hypernetted chain equation (HNC) [44]:

$$g(r) = \exp[-\beta\phi(r) + h(r) - c(r)] \quad 1.58$$

Going back to 1.40 we see that HNC is equivalent to set $b(r) = 0$. Exactly as in the case of the RPA we can expand the functionals around some reference density different from the ideal one [73]. Taking the hard sphere liquid as reference system we have a "reference PY" [74], a "reference HNC" [75] etc. The problem is, of course, the choice of a suitable reference. The crucial importance of this choice was not fully appreciated until the paper by Rosenfeld and Ashcroft we shall discuss thoroughly later on.

Finally we introduce the mean spherical approximation (MSA) [76]. It can be regarded as a sort of interpolation between the exact behaviors: $g(r=0) = 0$ and $\lim_{r \rightarrow \infty} c(r) = -\beta\phi(r)$:

$$\begin{cases} g(r) = 0 & r < \sigma \\ c(r) = -\beta \phi(r) & r \geq \sigma \end{cases} \quad 1.59$$

where σ is a distance to be fixed. It can also be interpreted as a non-standard ORPA where the distance σ is not given by some hard core reference (see pag 22).

The quality of the results of PY, HNC and MSA is not too much different. In some cases one approximation can be better than the others or it can be solved in a simpler way but as far as we look at the resulting structures we have no fundamental reason to prefer one of them systematically.

For a general potential these closures have to be coupled to the OZ equation and solved numerically [77]. However the PY equation for hard spheres and the MSA for potentials of the form

$$\phi(r) = \sum_i A_i \frac{e^{-\alpha_i r}}{r} \quad 1.60$$

can be solved analytically [78].

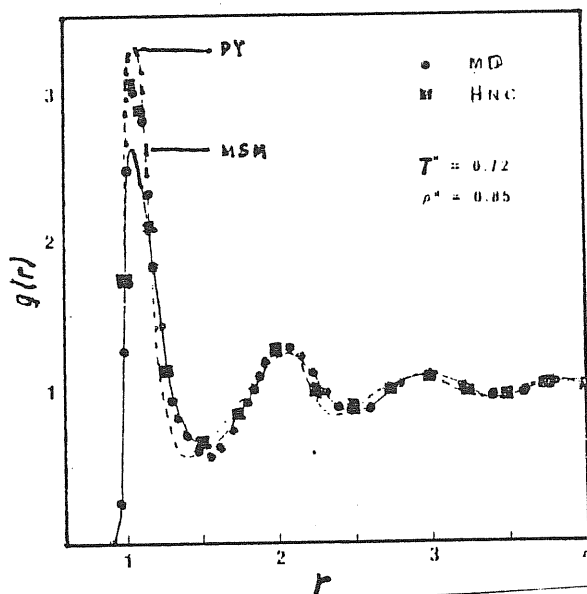


fig. 3. Radial distribution function for the Lennard-Jones fluid near the triple point calculated using several approximate integral equations. From ref [71].

All these equations can be derived from a variational principle on some approximate functional expression of the free energy [79]. This opportunity allows a careful control of the thermodynamics (free energy). It is possible to show that the HNC has an automatic consistency between the "energy" and the "virial" routes to the thermodynamics.

In fig. 3 a comparison is shown for the thermodynamic and the structural results of these theories for a simple one component Lennard-Jones liquid.

In order to improve the results of these approximate theories many different modifications have been tried in the past [80]. One firm conclusion obtained in that studies is that the best improvements come from the introduction of physically motivated parametrized corrections and fixing the parameters by requiring the fulfilment of some thermodynamic consistency.

In this way the Generalized Mean Spherical Approximation (GMSA), the Modified Hypernetted Chain (MHNC) or the Thermodynamically Consistent equations (TC) of Rogers and Young [81] have been developed in the recent years.

The GMSA [82] is based on the observation that a closure like

$$\begin{cases} g(r) = 0 & r < \sigma \\ c(r) = -\beta\phi(r) + A \frac{e^{-dr}}{r} & r \geq \sigma \end{cases} \quad 1.61$$

introduces two free parameters A and d which change the MSA closure where it appears to give the worst results and at the same time the asymptotic behavior is not affected. Moreover in the cases in which analytical solutions of the MSA have been worked out it is also possible to find analytical solutions of GMSA [83].

The values of the parameters can be fixed by imposing that different routes to the thermodynamics give the same results (internal consistency) or by requiring that "exact" computer simulation results are reproduced by the theory. This second alternative is more simple to be implemented but it requires a good previous knowledge of the thermodynamic properties and, for some states it can fail to give solutions at all if the GMSA structure is not compatible with that constraint.

The original form of the MHNC for one-component fluids is a reference HNC (see p. 26) where the choice of the hard sphere diameter is made in such a way that the thermodynamic consistency is improved. In particular the work of Rosenfeld and Ashcroft [B1] showed that:

a) the bridge functions behave as a repulsive short-range potential;

b) the insertion in the formula 1.40 of the Verlet-Weis Grundke-Henderson [B4] parametrization or the analytical solutions of the PY equation for hard spheres are sufficient to give essentially the same one-parameter family of functions $b(r; \eta)$ ($\eta = \frac{\pi}{6} \rho \sigma^3$) the differences being usually negligible at first approximation (see fig. 4);

c) the important region where we have to know the bridges is below and rather close to the first peak of $g(r)$ (approximately the interval (r_1, r_2) where $g(r_1) \sim 10^{-3}$ and $g(r_2) \sim \text{peak}$)

d) the determination of σ by requiring that $\chi_T^{\text{vir.}} = \chi_T^{\text{fluct.}}$ or, in a simpler way, that $\chi^{\text{fluct.}} = \chi^{\text{simul.}}$ or $U_{\text{MHNC}} = U_{\text{Simulation}}$ is sufficient to give the other thermodynamic

quantities and the structural functions well inside the precision of the existing simulation data.

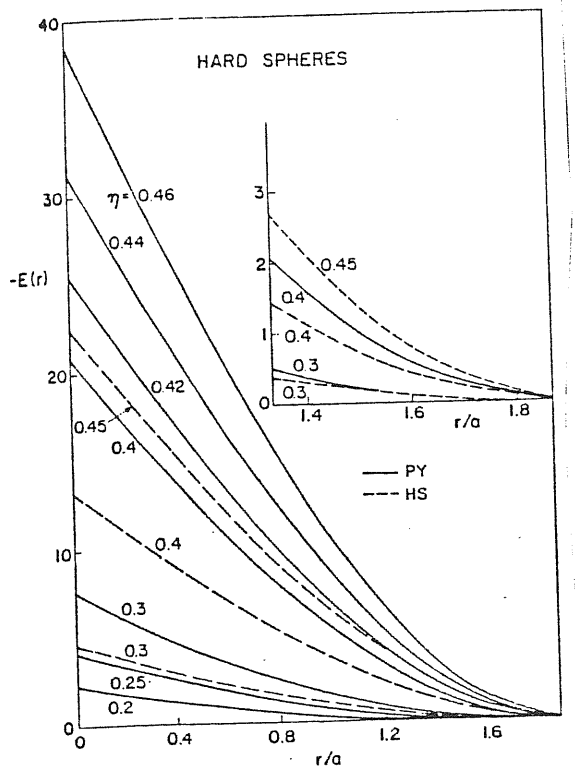


fig. 4. Bridge functions ($b(r) = -E(r)$) for hard spheres from the Percus-Yevick (PY) approximation and for the Verlet-Weiss (HS) parametrization of MC data ($a = (3/4\eta\rho)^{1/3}$). From ref. [81].

The set of equations to be solved is:

$$g(r) = \exp[-\beta\phi(r) + h(r) - c(r) - b_0(r; \eta)] \quad 1.62.1$$

$$h(r) = c(r) + \rho \int d\mathbf{r}' h(|\mathbf{r} - \mathbf{r}'|) c(r') \quad 1.62.2$$

$$b_0(r; \eta) = h_\sigma(r) - c_\sigma(r) - \log y_\sigma(r) \quad 1.62.3$$

where $y_\sigma(r) = \exp(\beta\phi_\sigma(r))g_\sigma(r)$ for hard spheres of diameter σ is obtained either from VWGH or from PY. The diameter σ is fixed by some consistency requirement. In fig. 5 we report the result for the Lennard-Jones liquid from the original paper.

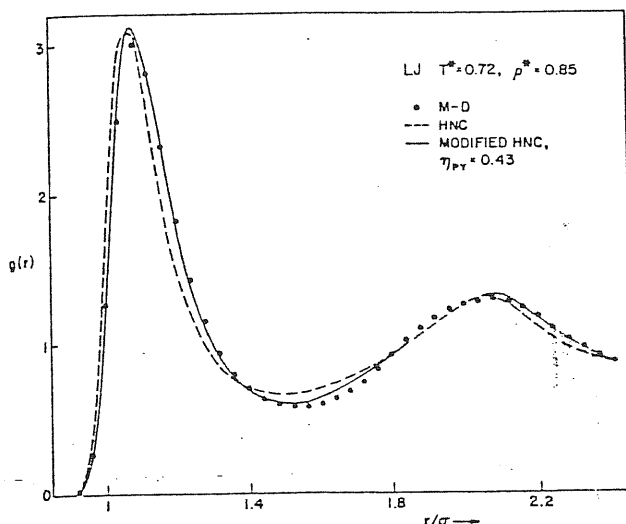


fig. 5. Radial distribution function for the Lennard-Jones liquid near the triple point. The dots are Molecular Dynamics results from Verlet. From [81].

We note here that the two main elements of the theory, the particular form of the bridge functions and the thermodynamic consistency requirements vary in the recent applications of the MHNC depending on the simplicity of calculations or on the accuracy of thermodynamic and structural properties required or on what consistency is improved.

All these factors are not uniquely fixed also because the variations of the results are usually inside the error bars of the simulated "exact" results used as gauge of the theory.

An improved recipe for the bridge functions of monocomponent fluids has been done by Foiles, Ashcroft and Reatto [85]: the bridges as defined by 1.62.3 go asymptotically as h_0^2 . This implies that if the $h(r)$ for the actual system is significantly different from that for the hard spheres (phase and amplitude of the oscillations) the usage of the hard sphere bridge functions will give a wrong contribution to the long distance correlations. For some systems near the triple point this region reaches the second peak of the $g(r)$. In these cases strange unphysical deformations of this peak are the signal of some inadequacy of the theory.

The empirical modification proposed by the previous authors is a kind of interpolation between the universal hard sphere behavior at short distance and some more specific information at large distance. In particular they show that it is sufficient to build the bridge function as

$$b(r) = f(r) b_0(r, \sigma) + (1 - f(r)) b_{\text{HSA}}(r) \quad 1.63$$

where

$$f(r) = \begin{cases} 1 & r \rightarrow 0 \\ 0 & r \rightarrow \infty \end{cases} \quad 1.64$$

and its specific choice is not crucial while b_{NSA} denotes the result of the formula $b = -\beta\phi + h - c - \log(g)$ when evaluated for $g = g_{NSA}$.

The results show a small but definite improvement on the original theory for one-component fluids.

Finally, it has been shown by Lado [86] that it is possible to derive both the MHNC equation and the choice of the diameter σ from a condition of minimum on some approximate form for the free energy. Starting from the formula

$$\frac{\beta F(\lambda)}{N} = \frac{\beta F(0)}{N} + \int_0^\lambda d\lambda \frac{1}{2} \rho \int dr g(r; \lambda) \Delta \phi(r) \quad 1.65$$

where $\lambda=0$ means a reference system in which the perturbation $\lambda \Delta \phi$ is suitably switched on and by making the approximation $b(r, \lambda) = b_0(r)$ we get, using the formula 1.40,

$$\begin{aligned} \beta \frac{\Delta F(\lambda)}{N} = & -\frac{1}{2} \rho \int dr \left\{ \frac{1}{2} h^2 + h - g \log g e^{\beta \phi} \right\} - \frac{1}{2\rho} \int \frac{dk}{(2\pi)^3} \left\{ \log [1 + \rho \hat{h}(k)] - \rho \hat{h}(k) \right\} + \\ & - \frac{1}{2} \rho \int dr b_0(r) [g(r) - g_0(r)] \end{aligned} \quad 1.66$$

Since the equation MHNC is satisfied, the condition of minimum respect the variations of $b_0(r)$ becomes:

$$\int dr [g(r) - g_0(r)] \delta b_0(r) = 0 \quad 1.67$$

This is an alternative equation to fix the hard sphere diameter of the reference or as many parameters as one has introduced in the bridge functions.

Notwithstanding the theoretical appeal of a minimization of the free energy, looking at the published results, it seems that the possibility of a definite judgement between different alternative ways of fixing the bridge parameters depends on the simultaneous improvement of the accuracy of the parametrizations and of the precision of the computer results. The existing spread of results is well inside the uncertainty of nowadays simulations.

A recently developed theory which follows the same philosophy of the MHNC is the Thermodynamically Consistent theory of Rogers and Young. According to an older idea of Hutchinson and Conkie [B1] they write the closure as

$$g(r) = \exp(-\beta\phi(r)) \left[1 + \frac{\exp[(h(r)-c(r))f(r)] - 1}{f(r)} \right] \quad 1.68$$

where $0 \leq f \leq 1$, $f(0)=0$ and $f(\infty)=1$ and i is parametrized in such a way that we can find the value of the parameters by imposing some thermodynamic consistency requirement. The closure 1.68 is equivalent to a mixing of PY and HNC by weighting more the PY at small r and more the HNC at large distances.

The results for one-component repulsive systems are good. It would be interesting to check the quality of the results for more complex systems like molten salts.

Much less calculations have been carried out for multicomponent systems. As we shall discuss in the Ch.4 this systems seem to be more stringent tests for any integral equation theory. In particular our extension of the MHNC techniques to the molten salts has been the first successful attempt to go beyond the HNC or PY theory for mixtures.

Recently, motivated by the increasing interest on alloys, molten salts and mixing properties of two or three component fluids, some more works on this line have appeared [B7].

Chapter 2. MODEL SYSTEMS FOR COULOMB LIQUIDS.

2.0 Why model systems?

In the study of the statistical mechanics of liquids we have no exactly solvable systems [88] like the harmonic solid or the Ising model (with the only exception of few particular cases at low dimensionality [89]).

The method of computer simulation is a way to by-pass this difficulty by giving detailed numerical description of many model systems.

The most extensively studied is the hard spheres liquid that is a model system in which only the excluded volume effects of a real liquid have been kept: the pair interaction $\phi(r)$ is

$$\phi(r) = \begin{cases} +\infty & r < \sigma \\ 0 & r > \sigma \end{cases} \quad 2.1$$

The thermodynamics of such a model is a very crude simplification of a real system: no dependence of the interaction effects from the temperature and no phase transition between a liquid and gaseous behaviour. Nevertheless the hard sphere structures model very well the scattering data and their usage as reference in perturbative calculations for simple liquids is extremely useful as already discussed in the chapter 1.

In the study of coulomb systems, in which the effects of coulomb interaction are dominant, we need some more specialized reference system: for example the usual blip function expansion breaks due to the non integrable long range tail of the potential. Classical charged liquids of two oppositely charged components like molten salts or electrolytic solutions can be modelled, at zeroth level of approximation, by a system

of charged hard spheres. Partly quantum systems like liquid metals and their alloys are better approximated by a liquid of point-like ions embedded in a uniform neutralizing background of opposite charge.

In this way we have two new model systems: the charged hard spheres (CHS) with interaction

$$\phi_{ij}(r) = \begin{cases} \frac{e^2 z_i z_j}{r} & r > \sigma_{ij} \\ +\infty & r < \sigma_{ij} \end{cases} \quad 2.2$$

(e : electronic charge; z_i : positive or negative valences; σ_{ij} : minimum approach distances) and the classical multicomponent plasmas (MCP) with potential

$$\phi_{ij}(r) = \frac{e^2 z_i z_j}{r} \quad r > 0 \quad 2.3$$

where the z_i have the same sign.

The CHS system can be considered as a primitive model of a real ionic system in which all the electronic effects (polarization, core deformation etc.) are neglected leaving out only the essential short range hard repulsion and the long range coulomb tail.

The MCP instead can be looked as the limit case of a metallic alloy at very large pressure (infinite) when the conduction electrons have lost their screening ability.

In particular, the astrophysical conditions, at the inner of a giant planet [89], a white dwarf [90] or at the surface of a neutron star [91] or some fusion plasmas should be reasonably approximated by the limiting behaviour of the model.

Finally we note that, despite its apparently exotic definition, the two dimensional one component plasma (interaction $\propto 1/r$) has a physically faithful representation in the monolayers of electrons at the

surface of liquid helium as we shall discuss thoroughly later on.

2.1 The Three Dimensional One Component Plasma.

The 3-D One Component Plasma (OCP) is probably the most extensively studied and the best known liquid together the hard spheres.

Its excess thermodynamic properties can be completely characterized by only one coupling parameter

$$\Gamma = \frac{e^2 z^2}{k_B T a} = \beta \frac{e^2 z^2}{a} \quad 2.4$$

where e is the electronic charge, k_B the Boltzmann constant, T the absolute temperature, z the valence of ions, and a , the ion sphere radius, is defined in term of the number density as

$$\frac{4\pi a^3}{3} = \frac{1}{\rho} \quad 2.5$$

In other words a is the radius of the sphere whose volume is equal to the average volume per particle.

The main theoretical result for the OCP are very well discussed in the review paper by Baus and Hansen [92].

In the following we shall report only part of the known results to facilitate the discussion of the theory of the structure for such systems.

The problems connected to the existence and to the peculiarities of the thermodynamic limit (TL) have been solved in recent years [93]. The main results are:

1. the TL of the internal energy per particle and of the free energy per particle do exist.

2. the free energy per particle (f) is not a convex function of the density and hence the pressure as defined by $p = - \left. \frac{\partial f}{\partial \rho} \right|_T$ and the isothermal compressibility

are not positive definite;

3. however the mechanical stability of the system is ensured by taking into account the effects of the microscopic electric field [94]. The relation between thermodynamics and correlation functions is given by the relations 1.16, 1.17 which can be specialized as:

$$\beta u_{exc} = \frac{\beta U^{exc}}{N} = \frac{3}{2} \Gamma \int_0^{\infty} r k(r) dr = \frac{\Gamma}{\pi} \int_0^{\infty} [S(k) - 1] dk \quad 2.6$$

$$\frac{\beta P_{exc}}{\rho} = \frac{\beta u_{exc}}{3} \quad (\text{virial theor.}) \quad 2.7$$

Because the singular behavior of $c(k)$, the compressibility sum rule has to be modified and it becomes:

$$\lim_{k \rightarrow 0} S(k) = \frac{k^2}{k_D^2 + \frac{\chi_0}{\chi_T} k^2} \quad 2.8$$

where $k_D^2 = \frac{4\pi n^2 e^2 \rho}{k_B T}$ and $\chi_0 = \frac{1}{\rho k_B T}$ and χ_T are the ideal gas and the interacting system isothermal compressibilities. The 2.8 can be rewritten as

$$\frac{\chi_T}{\chi_0} = (1 - \rho c^R(k=0))^{-1} \quad 2.9$$

where the function $c^R(k)$ is the Fourier transform of the regular part of the direct correlation function:

$$c^R(r) = c(r) + \frac{\Gamma}{r} \quad 2.10$$

The Debye Huckel approximation:

$$g_{DH}(r) = 1 - \frac{\Gamma}{r} \exp(-\sqrt{3T} r) \quad 2.11$$

$$\beta u_{DH}^{exc} = -\sqrt{\frac{3}{2}} \Gamma^{1/2} \quad ; \quad \beta f^{exc} = -\sqrt{\frac{\Gamma^3}{3}}$$

becomes exact at the $\Gamma \rightarrow 0$ limit and gives useful values for the thermodynamic quantities up to $\Gamma \sim 10^2$.

For a long time the computer simulation data of Hansen and De Witt [95] have been the only reliable source of informations on higher coupled systems. Approximate theories suitable for these systems, like

HNC or MSA, give only semiquantitative informations with errors larger than the 10% or more on thermodynamic and structural properties.

The solution of HNC equation has to be done numerically [96,97] and it requires a careful treatment of the long range tails of the correlation functions [97,98].

The solution of MSA is analytical [99] but we need some criterium to fix the matching parameter σ or, looking things in another way, we have to choose the best charged hard spheres system embedded in a background by which we approximate the DCP. The choice is not unique [100]. Probably the best from a theoretical point of view is that of Gillan [101]: we fix σ as the value for which

$$\lim_{r \rightarrow \sigma^+} g(r) = 0 \quad 2.12$$

which is equivalent to make continuous simultaneously the $g(r)$ and the $c(r)$. Moreover the previous choice (in the next we shall refer to it as the Gillan's choice) is also equivalent to extremize the approximate MSA functional for the free energy and the internal energy per particle [101].

In the last 5 years some new simulations data have appeared and some improved theories have filled the gap between integral equations and computer experiments.

The simulation results for the correlation functions are available as tabulations of the smoothed data from the Monte Carlo runs [102]. The thermodynamics can be summarized by the fitting formula [103] for the liquid free energy per particle:

$$\beta f^{excess}(T) = aT + k(bT^{1/4} - cT^{-1/4}) + (d+3) \log T + \\ - [a + k(b-c) + 1.1516] \quad 2.13$$

where

$$\begin{aligned}
 a &= -0.897744 \\
 b &= 0.95043 \\
 c &= 0.18956 \\
 d &= -0.81487
 \end{aligned}$$

from which the internal energy and the compressibility can be obtained:

$$u^{exc} = \beta \frac{\partial t_{exc}}{\partial \beta} = \Gamma \frac{\partial f_{exc}}{\partial \Gamma} \quad 2.14$$

$$\frac{\chi_0}{\chi_T} = \frac{\partial \beta P}{\partial n} = 1 + \frac{u^{exc}(\Gamma)}{3} + \frac{\Gamma}{9} \frac{\partial}{\partial \Gamma} u^{exc}(\Gamma) \quad 2.15$$

From a comparison of the evaluated free energy for the liquid and for the solid, the current estimate of the coupling at which the DCP freezes (melts) is [103]

$$\Gamma_N = 178 \pm 1$$

We have to make two comments about this value. The first is that the error bar is only the propagated effect of the statistical uncertainty due to the Monte Carlo method in the determination of the liquid and solid state thermodynamic quantities [104]; it cannot take into account systematic errors due to the periodic boundary conditions used in the simulation work. At present there is no way to check their influence on the melting point but we note that if the periodic boundary condition would have a stability effect on the solid configuration the DCP should have an higher Γ of freezing.

The second observation is that some indications do exist [105] about the possibility of supercooled metastable states above the freezing point up to values of Γ around 500 \sim 1000.

From the available data it appears quite safe to extrapolate the fitting formula 2.13 to the range 178 \sim 250 in order to describe the supercooled liquid branch [106].

While in their original form integral equation theories give poor (PY)[97] or semiquantitative (HNC,MSA) results, the modified closures which improve the thermodynamic consistency reach an excellent agreement with the simulation data.

The first developed between this "second generation" theories for the OCP was the GMSA of Chaturvedi, Senatore and Tosi [107].

The equations of GMSA: $h = c + \rho \int h + c$

$$\begin{cases} g(r) = 0 & r < \sigma \\ c(r) = -\frac{\rho}{r} - \frac{A}{r} \exp(-dr) & r \geq \sigma \end{cases} \quad 2.16$$

are solved analytically in terms of the external parameters A , d , σ and ρ . For fixed ρ , A , d , and σ are evaluated by imposing the continuity condition on $g(r)$ (eqn. 2.12) and by requiring the fitting of the Monte Carlo thermal equation of state and compressibility ($U_{GMSA} = U_{MC}$, $\chi_T^{GMSA} = \chi_T^{MC}$).

These last two conditions force some thermodynamic consistency in the theory. Notwithstanding the problems at small coupling, mainly due to the crude MSA-like closure for the $g(r)$ [108], the theory is very successful as parametrization of the OCP structure factor at intermediate and high couplings. As it has been shown in fig. 6 the main differences between computer simulation and GMSA are confined near the contact distance σ in real space and at large wavevectors in reciprocal space. The non analytical behavior of $g(r)$ near σ is reflected into a slight phase shift of the maxima and minima after the first peak of $S(k)$. Some dependency of the structural results on the exact parameters of the fitting formulas has been detected as shown in fig. 6.

Already in the paper of Rosenfeld and Ashcroft it was shown that the MHNC gives good results for the OCP.

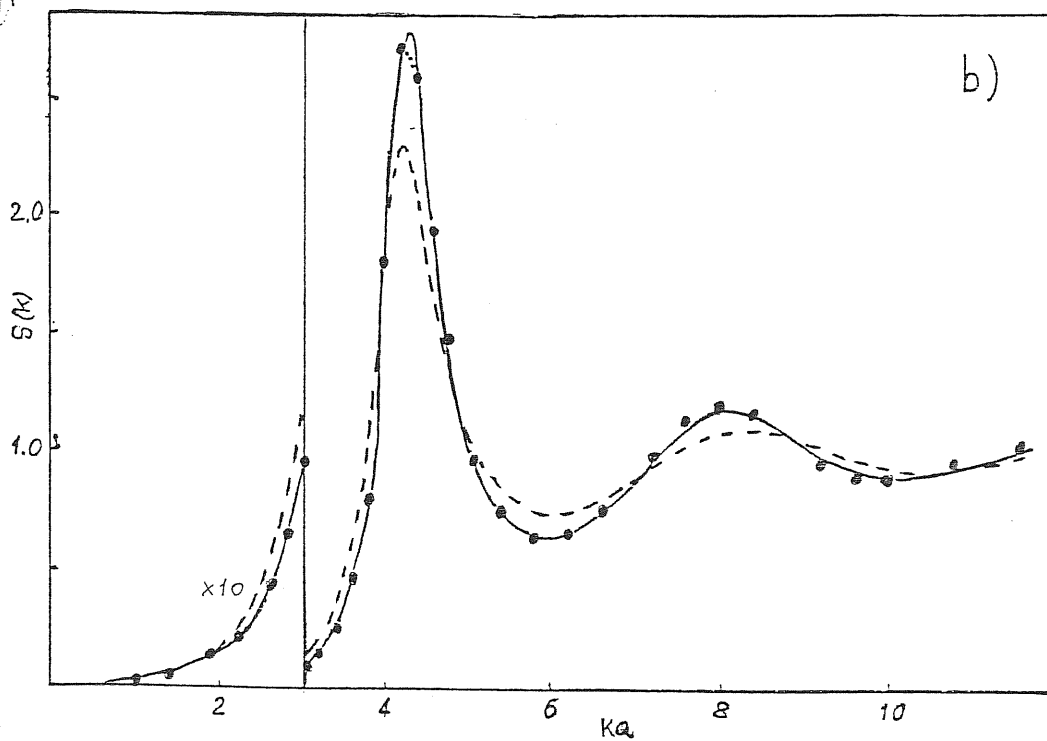
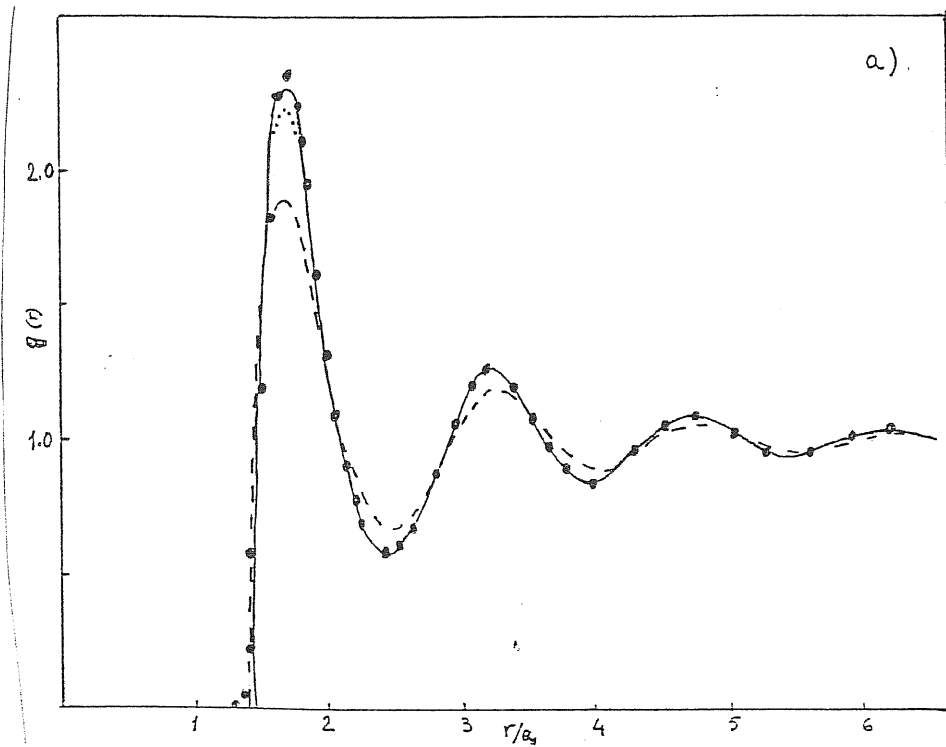


fig. 6. OCP 3-D at $\Gamma = 160$. Pair distribution function (a) and structure factor (b). Black circles: MC [102]; dashed line : MSA; full line : GMSA in connection with the most recent equation of state; points : original GMSA [107] in which an older, less accurate equation of state was used.

Now more precise computer simulation data [109] have been compared with the outcome of MHNC in which the bridge functions are taken from the Percus-Yevick solution of hard spheres and the diameter σ is fixed by requiring that the numerical derivative of the pressure respect the density is equal to the isothermal compressibility evaluated from formula 2.9. The thermodynamic results are shown in tab. 2. I

tab. 2. I. From Rogers et al. [109].

Γ	U/NkT			η
	HNC	MC	HNC bridge	
2	-1.315	-1.320±0.000	-1.323	0.095
5	-3.732	-3.757±0.000	-3.762	0.158
10	-7.935	-7.998±0.001	-8.004	0.215
20	-16.538	-16.673±0.001	-16.677	0.278
50	-42.788	-43.102±0.001	-43.103	0.364
100	-86.974	-87.522±0.001	-87.525	0.435
150	-131.364	-132.110±0.002	-132.106	0.466
170	-149.152	-149.970±0.001	-149.975	0.480

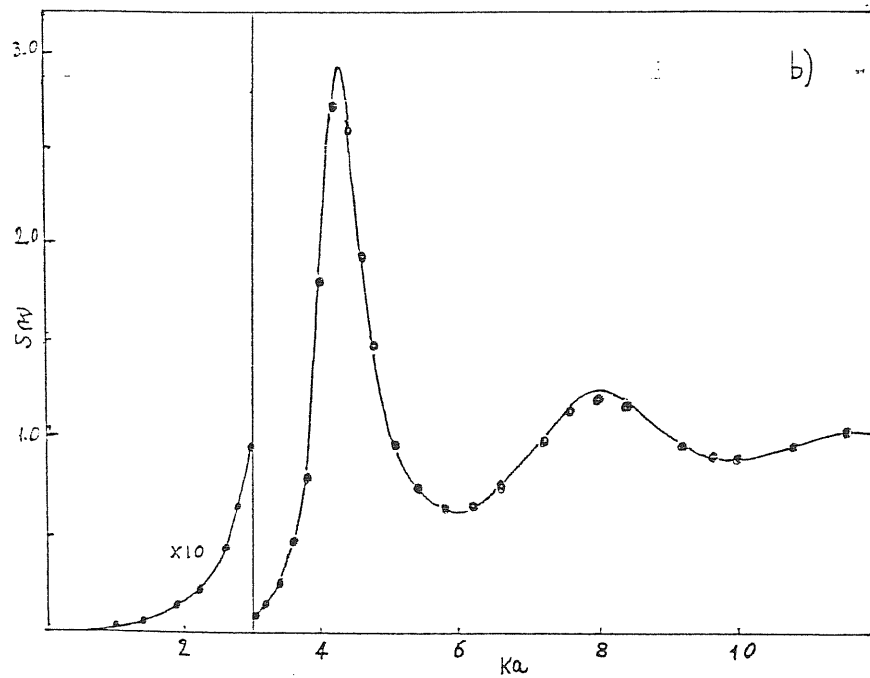
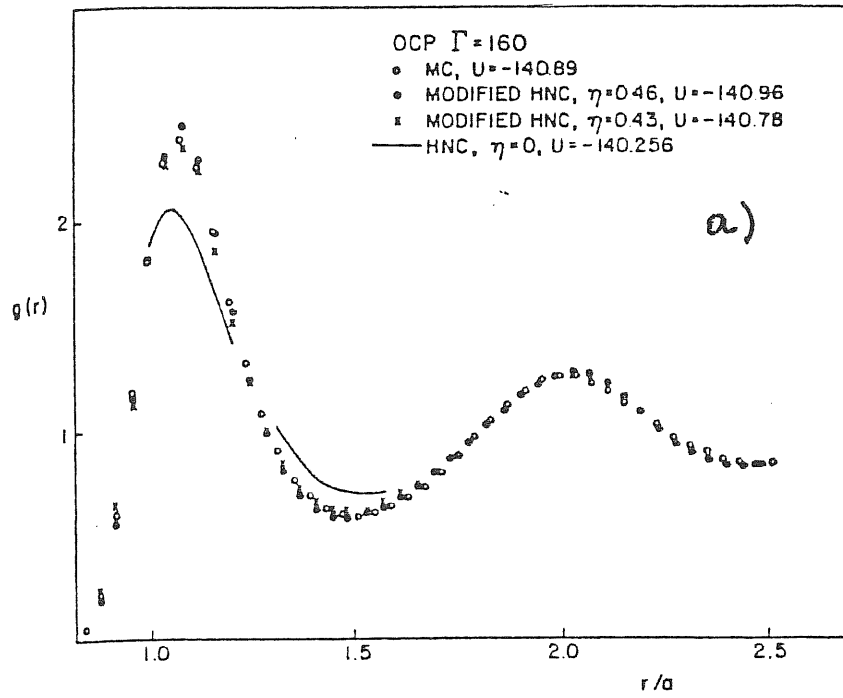


fig. 7. OCP 3-D at $\Gamma = 160$. Pair distribution function (a) from Rosenfeld and Ashcroft [81]. (b): structure factor. Black circles: MC; full line: MHNC.

The correlation functions $(g(r), S(k))$ are indistinguishable from the simulation data inside the error bar (fig.7). The very good agreement between computer simulation internal energy and that from the MHNC suggests that a simpler practical recipe to get the structure factors is just to fit the simulated equation of state. Some variations on this MHNC scheme have been exploited in the literature (see ch.1). The overall agreement with the simulation is in any case very satisfying and to assess the exact degree of accuracy of these schemes will require to go beyond the present precision of the computer simulation.

We are already able to make some comments on the side of the theoretical results:

1. The calculation of the virial compressibility by deriving the virial pressure respect the density at fixed σ is not completely self-consistent: the dependence of σ from the density has been neglected. The completely consistent calculation should evaluate the full dependence of η from Γ ($\eta(\Gamma)$) by solving the implicit differential equation for $\eta(\Gamma)$ implied by the consistency requirement ($\chi_r^{flatt} \rightarrow \chi_r^{vir}$). We do not expect large differences on the structural properties but, as far as we know this route has not been explored up today probably due to the computational problems;

2. the evaluation of the hard sphere diameter by fitting the MC equation of state gives results very close ($\sim 1\%$) to that obtained from the self-consistent equation

3. the usage of more "refined" bridge functions, like that obtained from the VWGH [84] parametrization of

the simulation results, does improve the consistency with the MC thermodynamics especially at the larger couplings but the corresponding structures do not differ appreciably from that obtained with the PY bridges;

4. however, since the hard sphere bridges have peaks whose positions are mismatched respect the OCP $g(r)$, some unphysical deformations of the second peak of the $g(r)$ can appear at the largest couplings and especially with the VWQH bridges which have a higher peak than PY when evaluated at the different diameters corresponding to the same β (see fig. 8);

5. it is possible to improve thermodynamics and structure respect the problems of the previous point 4 by using the cross-over 1.63 between hard sphere bridges at short distances and some more specific information about the coulombic correlations at larger distances [85] but, within the present days computer simulations the improvement is just a minor one;

6. the usage of the extremum criterium 1.67 to fix the hard sphere diameter gives poor results when PY bridges are used [110], while with the VWQH bridges the resulting diameters are very close to that obtained in the other way.

7. the TC theory gives results of slightly poorer quality than MHNC. The claim of the authors about faster performances than the Ashcroft and Rosenfeld recipe seems strongly dependent on the numerical algorithm used to solve the integral equations.

A different approach to MHNC has been developed by Iyetomi and Ichimaru [111]. They start from the diagrammatic expansion of the higher order correlation functions in term of h bonds (see appendix B). The

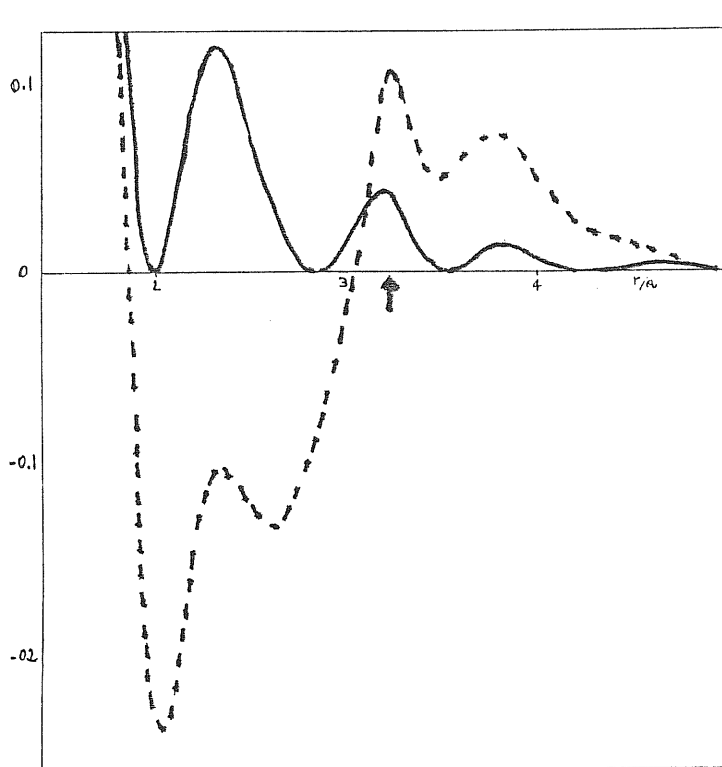


fig. 8. Bridge functions from the PY equation at $\mu = 0.468$ (full curve) and from the VWHG parametrization at $\mu = 0.500$ (dashed curve). These bridges ensure the fitting of the 3D OCP Monte Carlo internal energy at $\Gamma = 160$. The arrow marks the position of the second peak of $g_{OCP}(r)$.

simplest approximation to $h^{(3)}$ which does not involve unphysical divergencies is equivalent to express the 3-body direct correlation function as

$$c^{(3)}(r_1, r_2, r_3) = h(r_{12}) h(r_{23}) h(r_{31}) \quad 2.17$$

which implies

$$b(r) = - \frac{\rho^2}{2} \iint d\underline{r}' d\underline{r}'' h(|\underline{r} - \underline{r}'|) h(|\underline{r} - \underline{r}''|) h(|\underline{r}' - \underline{r}''|) h(r') h(r'') \quad 2.18$$

or, in diagrammatic notation,

$$b(r) = B_4(r) = \text{Diagram} \quad 2.19$$

Which is the lowest contribution to the h-bond expansion of the bridge functions. This term should give the long-range behavior of the bridges since it contains the minimum number of bonds [112]. At short and intermediate distances, with large couplings, it is necessary to take into account more contributions whose evaluation is more and more complicated. Their global effect can be reintroduced in $b(r)$ by a suitable renormalization at short distances.

Iyetomi and Ichimaru propose bridge functions of the form:

$$b(r) = f(r) B_4(r) \quad 2.20$$

where $f(r)$ goes to 1 for large r and it is such that $b(0)$ gives the ion sphere [113] value for the function $H(r) = h(r) - c(r) - b(r)$ at $r=0$. It turns out that the precise form of $f(r)$ does not matter and a form like

$$f(r) = (C-1) \exp[-(r/\xi)^2] + 1 \quad 2.21$$

where C is the ratio $b(0)/B_4(0) = \frac{h(0) - c(0) - H(0)}{B_4(0)}$ and ξ is the distance at which $B_4 \sim 0$ is sufficient to give a good agreement with simulation results. It is evident that this scheme of MHNC hinges on the heavy calculation of the five-fold integral which is about 10^4 times slower than the direct evaluation of a PY bridge. For this reason the practical usage of this scheme is not

convenient for one-component systems. We reported quite in details this MHNC scheme because in our extension of the MHNC for molten salts we found important to use the structural information contained in $b(\tau)$.

Strictly related to the OCP is the two-component plasma (TCP): a system of two charged species with different valences but of equal sign embedded in a suitable neutralizing background.

Besides the astrophysical relevance of this model, it would be a very interesting reference to deal with metallic alloys.

The theoretical and computational works on this system have received much less attention than for OCP. Some simulation data are available for some choices of charges and concentrations [114]. HNC results have been reported [114,115] and also solutions of the MSA with an approximate Gillan's condition [116] has been published.

In the preliminar investigation on the possibility of extending the Rosenfeld and Ashcroft ideas to liquid mixtures we have evaluated the MHNC results for the TCP with charges 2:1 for which there are comparison data from HNC, MSA and computer simulation.

We approximated the bridge functions b_{11}, b_{12}, b_{22} with three PY bridges for one-component systems of hard spheres. Each of them with its own diameter. In principle we could exploit the richer thermodynamics of the two component system to fix the parameters by forcing a complete consistency but the computational problems of such strategy are not trivial. To reduce the computational effort we fix the ratio between the like diameters and the unlike one: $\sigma_{11} / \sigma_{12}$ and $\sigma_{22} / \sigma_{12}$ are taken from the ratio between the peak

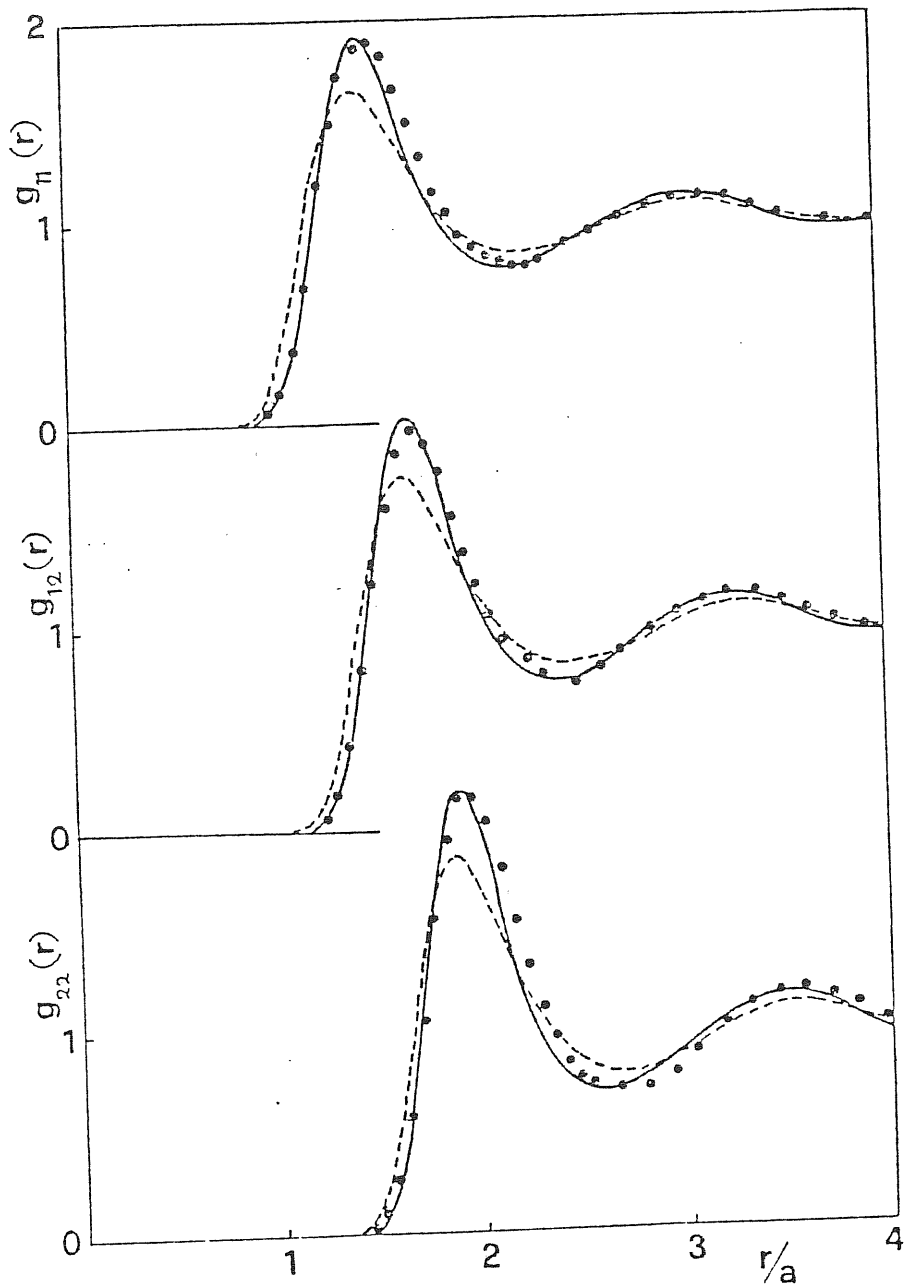


fig. 9. Radial distribution functions for the 2:1 TCP at $r=40$. Full curve: MHNC; dashed curve: HNC; dots: Monte Carlo results [114].

positions of the $g_{jj}(r)$ at the HNC level. The remaining parameter σ_{12} is fixed by some consistency requirement. In particular, taking into account the discussion about the OCP, we have chosen to fit the MC thermal equation of state. Obviously more self-contained routes could be explored.

The results are shown in fig. 9. They clearly indicate that for this kind of two-component systems, in which the excluded volume effects are nearly additive and the concentration ordering is close to be completely random, the simplest extension of the original recipe is working with sufficient precision to significantly improve on the MSA and HNC results.

We look at these results as preliminar. A more careful investigation of the thermodynamic implications of our choice of the diameters and more extensive simulation data are necessary to completely assess the performances of the MHNC for this system [117].

2.2 The two-dimensional one-component plasma.

One of the most powerful tools of the nowadays statistical mechanics is the systematic study of the influence of the dimensionality on the statistical behavior of the system. In the case of Coulomb systems the passage from the real-life 3-D space to lower (or higher) dimensional spaces is not uniquely defined: we can assume the particles to interact with the pair potential $z^2 e^2 / r$ or we can use the D-dimensional Poisson equation to define the D-dimensional Coulomb interaction. In two dimensions this is proportional to $\log(r)$.

Despite the theoretical interest for this "log(r)" plasma, its properties for example are relevant to the solutions of the Sine-Gordon equation [118] or to the

description of the quantum Hall effect [119], we are more interested to the $1/r$ interaction.

For this system an arbitrarily close physical realization is represented by the layer of electrons trapped at the surface of liquid helium. More in general the 2-D DCP solutions could be useful in the study of the liquid-like behavior of alkali metals intercalated in graphite planes [120].

2.2.1 The physical system.

An electron approaching the surface of the liquid helium from the vapor side experiences a repulsive surface barrier of about 1 eV which prevents its penetration inside the bulk. Moreover, near the surface, it feels also an attractive image potential [121].

The resulting effect gives the possibility of trapping suitable deposited electrons in a potential well at the surface [122].

The electrostatic potential of a positively biased metal plate located in the liquid below the surface is sufficient to confine the electrons inside a limited area [123] (see fig. 10).

It is an interesting experimental possibility that by changing the thickness of the helium layer between the electrons and the plate, we can change continuously the electron-electron effective interaction going from the coulombic to the dipolar [124] potential.

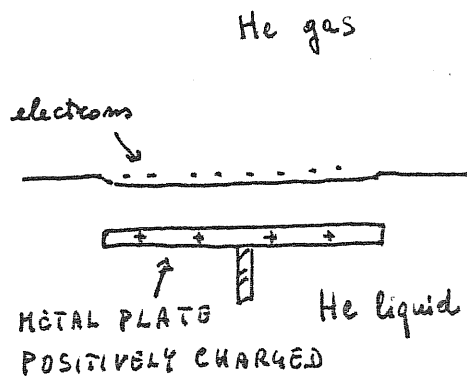


fig. 10

By confining ourselves to thick layers (l/r interaction) we can change the density between $10^5 - 10^9$ e/cm^2 . The densities are such that the interelectronic spacing ($\sim 10^4 \text{ \AA}$) is much larger than the spread of the charge density in the direction perpendicular to the surface ($\sim 10^{20} \text{ \AA}$), so the system can be considered as two dimensional in first approximation. At the experimental temperature of $\sim 0.5^\circ K$ the coupling strengths $\Gamma = \frac{e^2}{k_B T} (n \lambda)^{1/2}$ are between 2 and 200. Moreover the Fermi energy, also at $n=10^9 e/cm^2$, is $0.03^\circ K$ so the system is well described within the classical statistics.

Since we can reach very high couplings, we can expect to find some kind of classical Wigner crystallization by decreasing the temperature [125]. Actually experimental evidence for a liquid-solid transition has been found by Grimes and Adams [126]. They observed the sudden appearance of resonances in the real part of the electromagnetic impedance at radio-frequency when the temperature was decreased below $0.457^\circ K$. The analysis of such result [127] implies the presence of a triangular lattice of electrons on the helium surface. The experimental parameters correspond to a Γ of 137 ± 15 for the melting transition.

2.2.2 The model system.

The coupling in this system is given by the dimensionless parameter $\Gamma = \frac{e^2}{k_B T a}$ where a is defined as $\pi a^2 = 1/m$. The Debye wavenumber is $k_D = 2 n \beta e^2$ and in dimensionless units $a k_D = 2 \Gamma$; the Fourier transform of the interaction is $2 n e^2 / k$. Just as in 3-D, the long range Coulomb interaction manifests in a typical long-wavelength behavior of $S(k)$:

2.22

This form for $S(k)$ can be derived by using standard arguments of linear response theory and taking into account the dimensionality of the space ([128] and see appendix C).

One consequence of the form 2.22 is that while the first SL condition holds (neutrality), the third moment of the $h(r)$ does not exist. In this case, since the potential does not satisfy the Poisson equation, the $h(r)$ has an algebraic long distance behavior. This introduces some difficulty in the derivation of the right Debye-Hueckel limit [129] and also in the numerical solution of the integral equations [130].

Many computer simulations for dense systems are available [131-140]. We note that the effects of correlations are generally increased on the 3-D case. In this respect a theory for 2-D liquids is more demanding than in 3-D.

The MC thermodynamics can be summarized by the fitting formula for the internal energy [92]:

$$\beta u_{int} = a\Gamma + b\Gamma^{1/4} + c$$

where $a = -1.107763$, $b = 0.76373$, $c = -0.4419$. We note that in the 2-D computer simulation it is possible to use a larger number of particles as compared with the 3-D simulations before we reach the practical limitations of storage and computer time. As consequence of this fact the results have generally a smaller error bar. Different simulations [135, 136] give values of Γ_n , at which the liquid-solid transition occurs, in the range $120 \div 140$. The situation about the order of the observed transition is much less clear.

An explicit comment on the 2-D solid OCP is necessary. A well known argument due to Peierls [141]

and generalized by Mermin [142] forbids the characterization of the 2-D solid phase through a periodic one-particle density. The theorem shows that the Fourier components of the (supposed) periodic density ($\rho_{\mathbf{q}}$ where $\mathbf{q} \neq 0$ is some reciprocal lattice vector) satisfy an inequality which, at the thermodynamic limit, implies their vanishing. The physical mechanism responsible of this behavior is related to the presence, in harmonic approximation, of long-wavelength transverse phonons which destroy the long range translational order. The argument can be applied to the 2-D OCP too [143]. However the solid as dense phase characterized by elastic constants and low mobility of particles is not forbidden by the theory. For this kind of 2-D infinite solids a theory of melting [144] based on the Kosterlitz and Thouless [146] ideas has been developed. It requires a two-step melting: firstly the weak quasi-long-range order as characterized by algebraically diverging Bragg peaks is suppressed and the system goes into a new phase in which long range orientational order is present like in a liquid crystal. In a second transition the system loses also this kind of order and we have the usual liquid.

The question of what is the physical characterization of the observed transition is not an assessed point of the theory [145] and some care has to be put in the use of the thermodynamic limit results to interpretate the observed systems. Indeed the disruption of the usual translational long range order approaching the thermodynamic limit is a very slow process [147] (the rms deviation from the periodic equilibrium positions increases as $\log(N)$ where N is the number of particles). From this viewpoint, when we use statistical mechanics theories which embody the

thermodynamic limit, we should take them as simplifications to avoid the finite size corrections and boundary conditions complications but we should not put too much emphasize on some pathological behaviors at this limit.

2.2.3 Theory of the structure.

To evaluate the static structure of the 2D OCP we have applied the MHNC scheme as proposed by Rosenfeld and Ashcroft. We have used the same numerical scheme as developed by Lado [130] and we used the accelerating procedure of Ng [98] to improve the velocity of convergency. Taking $b(r)$ from the PY equation for the hard disk system [148] we choose the diameter by fitting the simulated value for the internal energy per particle.

As in the 3D case this method improves enough on the MSA or HNC [132,133] results but the increased role played by correlations makes more important the mismatch between the structures in the hard disk bridge functions and the OCP correlation functions.

In particular already at $\Gamma = 90$ the wrong position of the peak of the hard disk $g(r)$ induces an unphysical deformation of the second peak of $g_{OCP}(r)$ making explicit the non universal behaviour of the bridges beyond their first zero. To improve the results we have found necessary to use the same cross-over approach proposed by Ashcroft, Foiles, Reatto [85] for the 3D liquids: the bridges are written as

$$b(r) = f(r) b_{PY}(r) \sigma + (1 - f(r)) b_{MSA}(r) \quad 2.24$$

where

$$f(r) = \frac{1}{2} \left[1 - \frac{1}{2} \left(\frac{r-R}{W} \right)^2 \right]$$

b_{PY} and b_{MSA} are obtained from 1.40 by using for

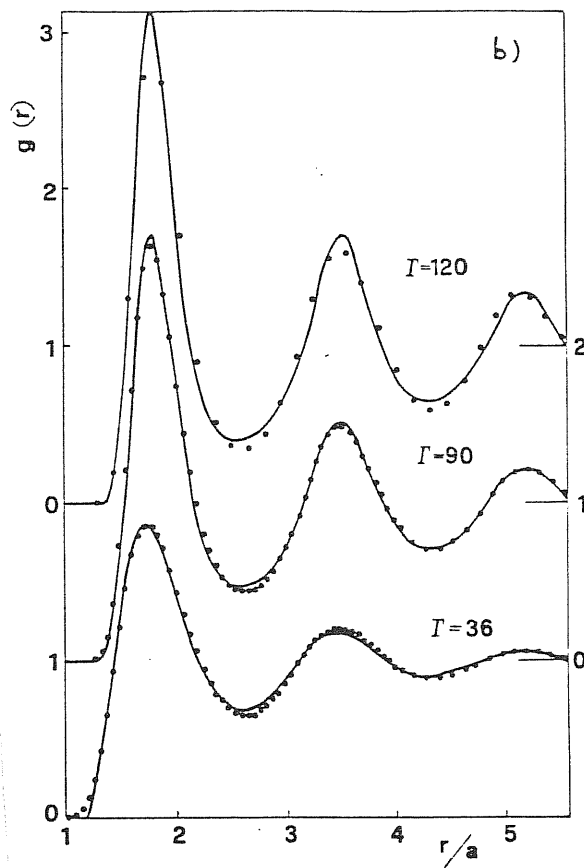
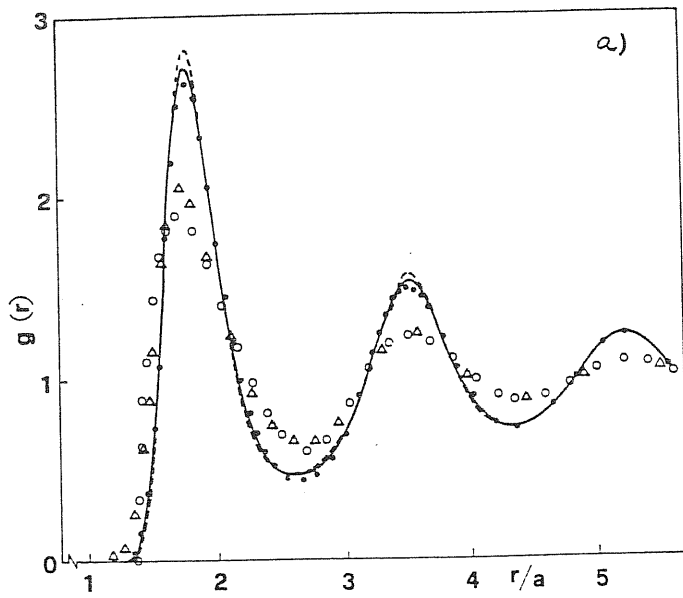


fig. 11. a): Radial distribution function $g(r)$ of the 2-D OCP at $\Gamma = 90$. HNC: triangles; MSA: circles; MC: full curve: MHNC; dashed curve: MHNC with only PY bridges.

$g(r)$ and $c(r)$ the corresponding PY and MSA (with the Gillan's condition) functions [149]. R and W are fixed from the positions of the first peak and the second zero in the HNC $g(r)$.

The MSA results used to generate the bridges are new. A comparison of the results as presented in fig. 11 and tab. 2.11. 2.11 shows the following points:

Tab. 2.11 Excess internal energy and isothermal compressibility of the 2D plasma†.

	$\Gamma = 36$		$\Gamma = 90$		$\Gamma = 120$	
	$U_{ex}/Nk_B T$	$(nk_B T K_T)^{-1}$	$U_{ex}/Nk_B T$	$(nk_B T K_T)^{-1}$	$U_{ex}/Nk_B T$	$(nk_B T K_T)^{-1}$
HNC	-38.466	-35.46	-97.683	-93.74	-130.67	-126.5
MSA	-38.539	-34.41	-97.695	-91.88	-130.65	-124.2
MHNC-PY	—	—	(-98.262)	-69.52	—	—
MHNC	(-38.758)	-28.79	(-98.262)	-71.36	(-131.38)	-94.11
Monte Carlo	-38.758	-28.27	-98.262	-72.96	-131.38	-97.83

† The Monte Carlo results are from a fit by Baus and Hansen (1980) to data of Gann *et al* (1979). Values in parentheses have been fitted to these data.

1) The MSA results with the Gillan's choice of are of the same quality than HNC results.

2) The MHNC results are a significant improvement on HNC or MSA.

3) The degree of agreement with computer simulation, although very satisfying, is not as excellent as that achieved for the 3D DCP.

2.2.4 Freezing

The density wave theory of freezing started with the pioneering work of Kirkwood and Monroe [150]. In its modern version, as developed by Ramakrishnan and Youssuf [151] and others, the theory is able to give meaningful and quantitative predictions on the localization and characterization of the phase transition in terms of the

liquid structure.

The theory uses the HNC-like equation for the one particle density in term of the pair correlation function of the fluid, which has always the fluid solution $\rho(r) = \text{const.}$, and it looks for the appearance of inhomogeneous solution with some specified periodicity. In general, due to the highly non linear behavior of such equations, the bifurcation is not continuous.

Moreover the thermodynamic transition is localized as the state at which the difference of the evaluated free energy between liquid and the solid phase vanishes.

If we express the one particle density

$$n(\underline{r}) = n \left[1 + \sum_{\underline{G} \neq 0} \rho_{\underline{G}} \exp(i \underline{G} \cdot \underline{r}) \right] \quad 2.25$$

where \underline{G} are the reciprocal lattice vectors fixed in such a way that the volume per particle in the perfect solid is equal to the volume per particle in the liquid. The equations to be solved, stopping the expansion at the level of two body correlations, are:

$$\rho_{\underline{G}} = \psi_0^{-1} \int d\underline{r} \exp[i \underline{G} \cdot \underline{r} + \sum_{\underline{G}' \neq 0} \tilde{c}(\underline{G}') \rho_{\underline{G}'} \exp(i \underline{G}' \cdot \underline{r})] \quad 2.26$$

$$\frac{\Delta F}{N} = k_B T \left[-\log \psi_0 + \frac{1}{2} \sum_{\underline{G} \neq 0} \tilde{c}(\underline{G}) |\rho_{\underline{G}}|^2 \right] = 0 \quad 2.27$$

where

$$\psi_0 = \int d\underline{r} \exp \left[\sum_{\underline{G} \neq 0} \tilde{c}(\underline{G}) \rho_{\underline{G}} \exp(i \underline{G} \cdot \underline{r}) \right] \quad 2.28$$

and it is related to the change in chemical potential between the two phases:

$$\Delta \mu = k_B T \left[-\log \psi_0 - \frac{1}{2} \sum_{\underline{G} \neq 0} c^{(3)}(\underline{G}, 0) |\rho_{\underline{G}}|^2 \right] \quad 2.29$$

$$\text{and } c^{(3)}(\underline{G}, 0) = -\tilde{c}(\underline{G}) + \frac{1}{2} T \frac{\partial \tilde{c}(\underline{G})}{\partial T} \quad 2.30$$

The difference of entropy $\Delta S = S_s - S_l$ is

obtained from:

$$\Delta S = k_B T \left. \frac{\partial}{\partial T} \left(\frac{\Delta F}{k_B T} \right) \right|_{T=T_h} \quad 2.31$$

Looking at fig.12 we can note that there is a very strong correlation between the first three stars of reciprocal lattice vectors and the two main peaks of $\rho^{\hat{c}}(k)$: the liquid is structurally predisposed to crystallize into a triangular lattice.

The subsequent stars fall where the $\rho^{\hat{c}}(k)$ is zero or close to zero indicating a small relevance of that order parameters to the freezing (this do not imply that they are zero!).

If we use the MHNC structure, including up to the first 10 reciprocal lattice stars, we find freezing at $T_h = 149$ (against the value of Kalia et al. [136] 118 ~ 130 and the experimental of 137 ± 15 [126]) with a change of μ $\Delta\mu = -0.6 k_B T$ against the experimental $\Delta\mu = -0.14 k_B T$ and $\Delta S = -1.2 k_B$ against $\Delta S = -0.3 k_B$ (expt.).

We have also verified that the 2-D Hansen-Verlet criterium [152] for the freezing is fulfilled: we found a value of the structure factor at the first peak of 4.73 against a "universal" value of $4.4 \pm 10\%$.

These results should be contrasted with a less specific and more qualitative analysis of the 2-D freezing by Ramakrishnan [153] who finds a less pronounced first order character of the transition at the simple one-order-parameter level of approximation.

We have checked the stability of the triangular lattice against small deformations which tend to transform it into a body-centered rectangular lattice:

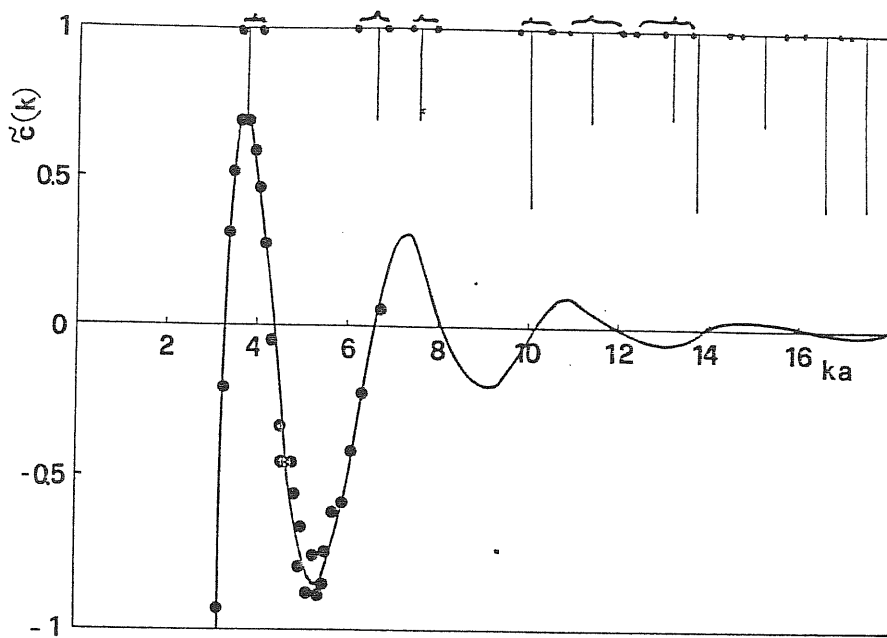


fig. 12. Direct correlation function $z_c(k)$ at $\Gamma=90$ in MHNC (full curve) compared with MC [133] (full circles). The bars at the top of the figure show the positions of the reciprocal lattice stars of the perfect triangular lattice, with lengths proportional to their multiplicity. Dots at the top indicate the relative splitting of these stars when the lattice is distorted into a body-centered rectangular.

as soon we vary the angle between two basis vectors of the lattice, the reciprocal space stars will be splitted into different substars. In particular the star corresponding to the driving first peak of $c(k)$ will be splitted into one star of four vectors which goes closer to the first peak and another of two vectors moving far away from the peak (see fig.12). Due to the asymmetry of the peak the resulting effect is an increasing of ΔF at fixed μ which implies an increasing of ρ_n . Thus we have proven the stability of the triangular lattice against this kind of deformation.

In principle we could not exclude the transition from the liquid to a triangular solid with vacancies [154] such that the unitary cell contains a fractional number of particles. This would imply to vary the scaling factor of the star position until a minimum of the free energy is reached. We have not allowed for this possibility. We know from other calculations (3D) that the expected change in the result is a minor one [155] and the theory tends to give poor estimate of the defect concentration.

The discrepancies on the variation of μ and S at the freezing may be due to the crude approximations involved by the equations 2.26-28 which neglect all the many body correlations. The results are inside the usual quantitative limitations of the density wave theory of the freezing in the present form.

More detailed simulation results for the highest coupling liquid structures and the related thermodynamics as compared with our MHNC results could make clearer the origin of the observed discrepancies.

In conclusion we would like to stress that we have

presented a quantitative treatment of the 2D freezing looked as the onset of a thermodynamically stable density wave.

The fact that we do find a periodic one-particle density in 2-D is not astonishing in an approximate (mean-field like) theory [156].

The question of alternative freezing-melting mechanisms can not be answered within the nowadays formulation of the theory. Our results reasonably agree with some of the simulation studies [136] but we have no control on the orientational order parameters to exclude the relevance of the Halperin and Nelson's picture.

Finally we would like to stress that our treatment of the structure and of the freezing of the 2-D OCP is applicable with few modifications to different physically interesting related situations like the adsorbed rare gas monolayers on the surface of the graphite [157] or alkali metals intercalated in graphite [158].

2.3 Charged hard spheres.

Ionic systems like electrolytic solutions or molten salts require complex interaction potentials to be described in a quantitative way. However the main qualitative behaviours of these systems are reproducible with a very idealized model interaction: the charged hard spheres (CHS) potential:

$$\phi_{ij}(r) = \begin{cases} +\infty & r < \sigma_{ij} \\ \frac{q_i q_j e^2}{\epsilon r} & r > \sigma_{ij} \end{cases} \quad 2.32$$

where ϵ is some (high frequency) dielectric constant.

The statistical mechanics of the CHS has been extensively studied in recent years but usually under the restriction $\sigma_{12} = \frac{\sigma_{11} + \sigma_{22}}{2}$ (additivity) [159].

The hypothesis of additivity is not necessary and in some cases unphysical. Usually the excluded volume effects for oppositely charged ions as measured by the radii of the exclusion holes are not additive.

Particularly in the case of electrolytic solutions the Coulomb couplings are not too strong but the multiple ionic hydration possibility enhances the relevance of non additivity effects.

In the case of negative non additivity ($\sigma_{12} < \frac{\sigma_{11} + \sigma_{22}}{2}$) the gain in the electrostatic energy due to the smaller minimum approach distance between anion and cation could increase the average time of pairing between unlike ions and. This effect offers the possibility of modelling compound forming electrolytic solutions like cadmium and nickel phosphate [160] or cadmium sulphate [161]. Moreover it would allow more freedom to describe liquid alloys and molten salts as well as concentrated solutions of alkali metals in molten alkali halides.

In the opposite case of positive non additivity ($\sigma_{12} > \frac{\sigma_{11} + \sigma_{22}}{2}$) the neutral system shows a tendency to demix [162]. The charged system has not been numerically investigated up to now in the literature but, as we shall show in the next part, it has a very rich and subtle behavior which can be summarized as a tendency to loose pairing between like ions.

Beside its intrinsic interest and the possibility of using it as a reference system for non completely miscible alloys (by taking equal sign or zero valences [163]), this model could directly be used to describe alkali iodide-iodine solutions [163], molten alkali hyperoxides [164] or the observed phase separation in electrolytic solutions at supercritical conditions

[165].

2.3.2 The model

The neutral case i.e. hard sphere with diameters σ_i such that $\sigma_{12} = \frac{\sigma_{11} + \sigma_{22}}{2}$ have been already studied in the literature. Some computer simulation results for the negative [167] and positive [168] deviations from the additivity have been confined almost completely to the thermodynamic properties.

Between the approximate integral equations only the PY has been exploited particularly in many attempts of finding an analytical solution for this system [169].

Only in the work of Nixon et al. [170] extensive numerical calculations for the PY equation in the negative non additivity case (for the symmetric model ($\sigma_{11} = \sigma_{22}$)) have been carried out.

The known results can be summarized in the following way:

1. The non additivity always implies a trivial effect of variation of the volume available to the system. If we define an effective packing fraction $\eta_{eff} = \eta_0 \sigma^3 [1 + (1+\alpha)^3]$ where α is such that $\sigma_{12} = (1+\alpha) \left(\frac{\sigma_{11} + \sigma_{22}}{2} \right)$ we have a rough indication of this effect on the properties of the system.

2. If $\alpha < 0$ the subsequent gain in entropy favours an enhancement of the mixing between the two species (a good mixing maximizes the available volume of the configuration space); in the opposite case the same mechanism favours the segregation of the two components [171].

3. The previous behaviours are obviously reflected

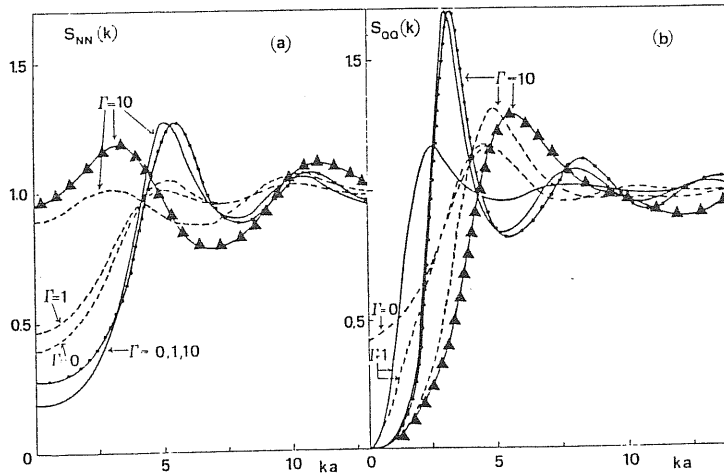


fig. 13. Charged hard spheres. $S_{NN}(k)$ (a) and $S_{oo}(k)$ (b) for $\sigma = 1.2a$ ($4\pi\epsilon_0/3 = 4/9$). Full lines: MSA for $\alpha = 0$ dashed: MSA for $\alpha = -0.5$ at $\Gamma = 0, 1$ and 10 . Dots and triangles are HNC results at $\Gamma = 10$ for $\alpha = 0$ and $\alpha = -0.5$.

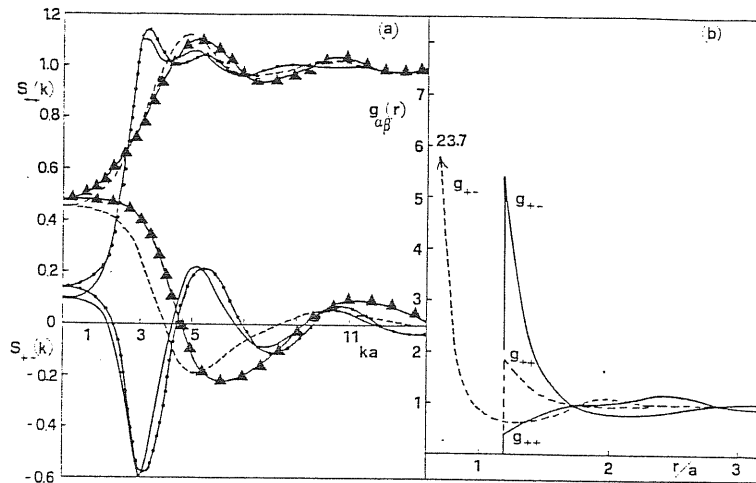


fig. 14. (a): partial structure factors $S_{++}(k)$ and $S_{+-}(k)$ at $\Gamma = 10$ and $\sigma = 1.2a$. Full line: MSA; dots: HNC at $\alpha = 0$; broken line: MSA; triangles: HNC at $\alpha = -0.5$. (b): HNC pair distribution functions $g_{++}(r)$ and $g_{+-}(r)$ at $\Gamma = 10$ and $\sigma = 1.2a$ for $\alpha = 0$ (full line) and $\alpha = -0.5$ (broken line).

in an enhancement ($\alpha > 0$) or a decrease ($\alpha < 0$) of the long wavelength limit of the concentration-concentration structure factor.

For what concerns the additive mixtures of charged hard spheres they have been studied extensively with computer simulation or integral equation methods (we recall that the MSA for such systems is analytically solvable [78]) and we refer to the literature for the description of this system [172].

2.3.3 Results for the model system

We have studied the non additive symmetric system of charged hard spheres ($\sigma_{++} = \sigma_{--} = \sigma$, $\tau_{\pm} = -\tau_{\mp} = 1$) in both cases: positive and negative deviations from additivity.

Since we were interested more in the qualitative trends than in accurated quantitative predictions, we have used the MSA and the HNC closures without trying any further improvement.

We solved both numerically and we looked at the structural properties (correlation functions) and at the unlike coordination number as defined by

$$N_{+-} = 2\pi\rho \int_0^R r^2 g_{+-}(r) dr \quad 2.33$$

where R is the minimum of $g_{+-}(r)$.

Negative non additivity

Switching on the Coulomb interaction we further enhance the trends shown by the neutral system. In fig. 13 we show the variation from $\Gamma = 0$ to $\Gamma = 10$ of the S_{NN} and S_{QQ} (for this system $S_{QQ} = S_{CC}$).

In fig. 14 we show the partial structure factors and the $g_{ij}(r)$.

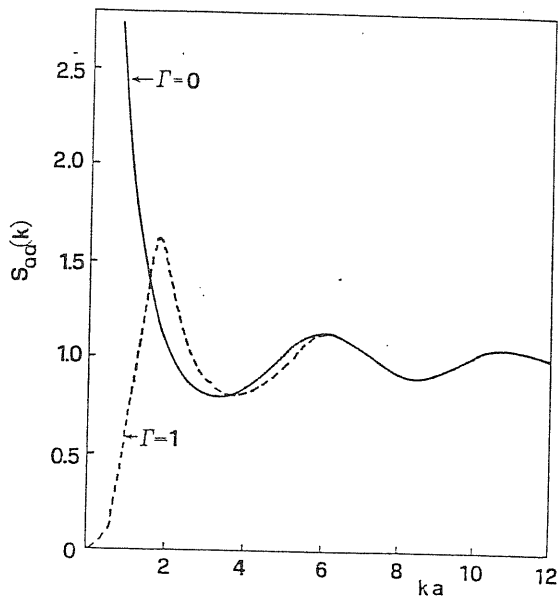


fig. 15. $S_{00}(k)$ in MSA for $\sigma = 1.2a$ and $\alpha = 1.67$ at $\Gamma = 0$ (full curve) and $\Gamma = 10$.

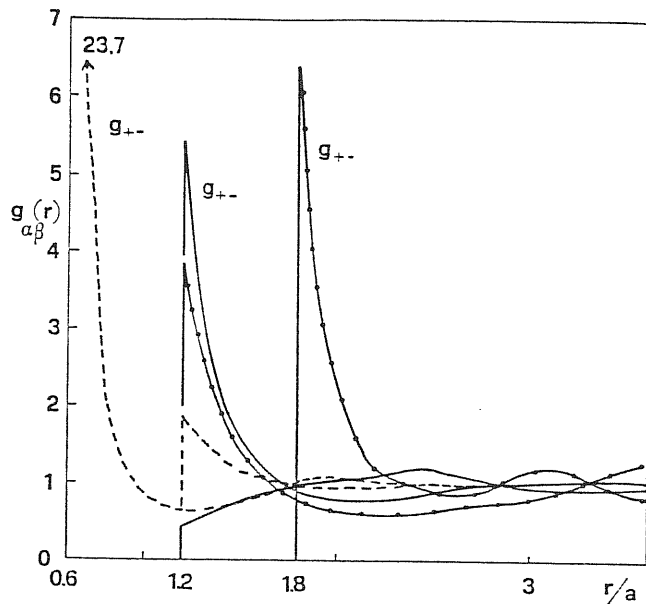


fig 16. HNC pair distribution functions $g_{++}(r)$ and $g_{+-}(r)$ at $\Gamma = 10$ and $\sigma = 1.2a$ for $\alpha = -0.5$ (broken curve), $\alpha = 0$ (full curve) and $\alpha = 0.5$ (dots).

The tendency towards unlike pairing is clearly shown by the coordination numbers as reported in tab. 2. III.

tab 2. III Unlike coordination numbers as function of the coupling and of the non-additivity .

α	Γ	0	1	10
0		4.5	5.5	5.5
- 0.5		2.4	2.5	1.6

Positive non additivity

Positive non additivity tends to increase the $S_{cc}(k=0)$ of the neutral system over the ideal value $x_1 x_2$ and eventually it can diverge (phase separation). The overall neutrality of a charged system must suppress completely this long wavelenght concentration fluctuations but since the system feels some entropic advantage in building medium scale inhomogeneities the resulting S_{qq} shows a well defined peak at finite k vectors (fig. 15).

This tendency to cluster like particles can be seen more clearly looking at the behaviour of the pair correlation functions (fig. 16).

Since in this case the "entropic" mechanism is in competition with the energetic one, we could expect a non trivial behaviour of the structural information. Indeed if we switch on the Coulomb interactions from 0 to high couplings for fixed non additivity ($\Gamma \sim 50$

would be appropriate for molten salts) we go from the phase separation tendency of the neutral system through a clustering tendency on a smaller scale to end with the usual ionic behavior (well defined alternation of charged shells) but in a strongly constrained system as revealed by the strong reduction of the compressibility.

The CdSO_4 electrolytic solution.

In order to check the relevance of the negative non additive model for the hydrated ions in aqueous solutions we have evaluated the structure for parameters suitable to represent a primitive model of the 2M CdSO_4 aqueous solution at 62 °C for which X-ray diffraction data [161] are available.

From the analysis of the data Caminiti [160] derives indications for the presence of an high average concentration of $[\text{Cd}(\text{H}_2\text{O})_{6-\frac{1}{2}}(\text{OSO}_3)_{\frac{1}{2}}]^{2-2+}$ groups.

We have taken the value of $\sigma_{++} = 4.6 \text{ \AA}$, $\sigma_{+-} = 3.5 \text{ \AA}$, $\sigma_{--} = 3.0 \text{ \AA}$ from the analysis of X-ray experiment [161]. The resulting MSA structure at $\Gamma = 6.53$ (experimental conditions taking into account the dielectric constant of water) is shown in fig.17.

Focusing on the S_{++} we notice that while the period of oscillations is directly connected to the preferred contact distance σ_{+-} between the cation and the anion inside the complex, the phase of oscillations carries informations on the long range correlations. This information is not contained in the quasi lattice model [173] used to interpretate the experimental data.

Unfortunately a quantitative comparison between our partial structure factors and the total X-ray diffraction

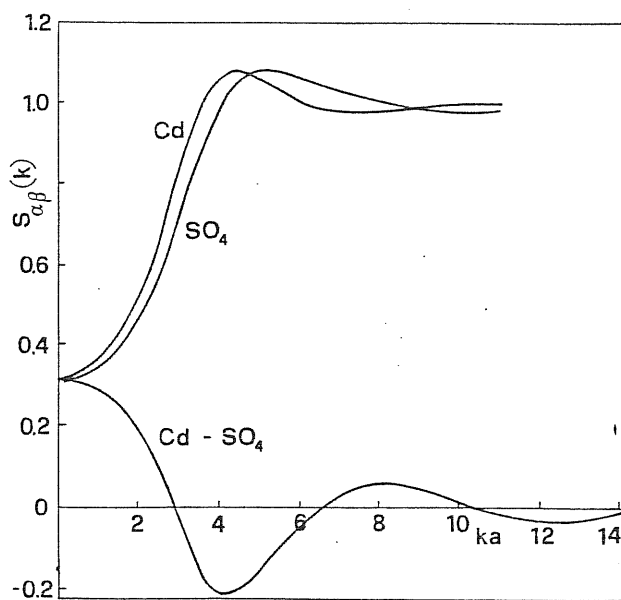


fig. 17. MSA partial structure factors for model of 2M CdSO_4 aqueous solution at 62 C.

pattern is presently impossible due to the dominant contribution from the free water structure factor which is obviously absent in our model.

When more specialized probes [174] than the usual X-ray scattering will give a better picture of the real structure of these electrolytic solutions, the non additive charged hard spheres could be a flexible and physical model to contrast with the experiments.

Chapter 3. LIQUID METALS.

3.0. Introduction.

For the majority of the metallic elements, many properties, included the electronic ones, do not change very much with the transition from the solid to the liquid [175]. Exactly as in the solids, the complexity of the electronic structure has a crucial role in the theoretical evaluation of the physical properties of the liquid.

The simplest metals are those for which the electronic structure is closest to the nearly-free electron model. This requirement automatically rules out the transition metals or more complex systems in which d or f states play a dominant role in the determination of the scattering properties of the ions.

There is also an other possible meaning for "simple" metals. If we look at the experimental structures of many liquid metals near the freezing, we can separate the metals whose $S(k)$ shows a strong similarity with the rare gas structure and those which have shoulders or other structures superposed on a simple profile. The alkali metals are simple for both these definitions. In recent years the interest on the thermophysical properties of the liquid alkali metals has increased as motivated by technological application possibilities (like their use as refrigerators in the nuclear power plants).

Liquid alloys have maybe a larger technological interest than the pure liquid metals. Moreover the compositional degrees of freedom make their physical behavior more complicated but also theoretically more interesting.

3.1 Physics of the liquid alkali metals and their alloys.

From a physical viewpoint the alkali metals are interesting for many reasons. The relative simplicity of their electronic structure, by allowing a reasonable estimation of the effective ion-ion interaction, makes them the best candidates as test systems for statistical theories. The very large compressibility allows experimental investigations of the effects of very high compressions and very high expansions. A 5 kbar pressure changes the volume of rubidium by about the same amount than 30 kbar changes the volume of iron. At the melting point they have the lowest density among the liquid metals thus providing a more severe test for exchange and correlation corrections of the electron gas theories. Furthermore the melting point is easily accessible up to large pressures. Despite the relative simplicity of their constituents, the alkali alloys show a series of different behaviors going from the quasi-ideal mixing of the K-Rb or Na-K to the strong tendency to demix of the Na-Cs at 80% of sodium concentration.

In tab. 3.1 we have collected some of the main thermophysical properties of the alkali metals.

All the alkalis freeze into a bcc crystalline structure at 1 atm pressure but under high pressure the solids undergo structural phase transitions. The liquid structures at the melting point scale very well with the density as shown in fig. 18.

We observe that the parameters \bar{T} and r_s at the melting point are characteristic of a strongly coupled ionic system and an intermediate coupled electronic component. If we could regard the ionic component as a

tab 3. I Thermophysical properties of the alkali metals.

Metal	Atomic number	Atomic weight	Density g/cm	r_s	melting temp. (C)	$\bar{r}_H = \frac{e^2}{k_B T_A} \chi_T \cdot 10^{12} \frac{\text{dynes}}{\text{cm}^2}$		$2k_F (\text{\AA}^{-1})$
Li	3	6.94	0.525	3.28	180.5	212.1	11.	1.03
Na	11	22.99	0.927	4.05	97.8	210.7	19.	0.83
K	19	39.10	0.827	5.02	63.5	186.9	38.	0.67
Rb	37	85.47	1.437	5.42	39.9	186.7	49.	0.62
Cs	55	132.91	1.854	5.77	28.6	181.2	64.	0.58

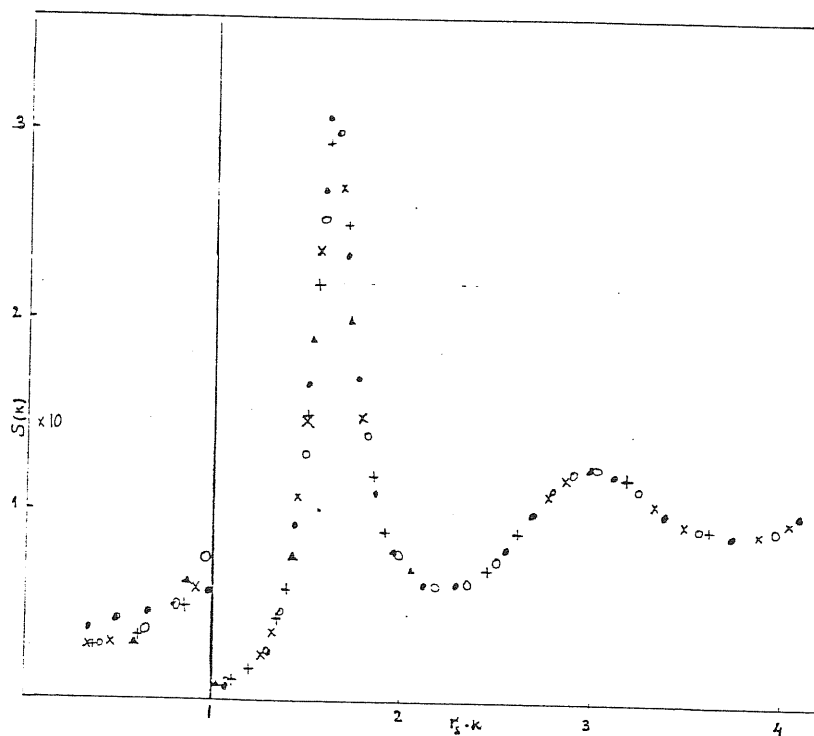


Fig. 18. Experimental structure factors of the alkali metals just above the melting point versus the scaled wavenumbers $r_s k$. ● : Li, ○ : Na, + : K, ▲ : Rb, × : Cs. Data from Ruppertsberg, Hujiben, Copley.

pure OCP it should have to be freezed (or in a metastable state) at these values of Γ . The presence of a polarizable background reduces the effective inter-ionic coupling making the system liquid.

This effective potential can be obtained using the usual perturbative approach [176] on the homogeneous electron gas and the weakness of the electron-ion scattering [177] effects makes reasonable to stop the expansion at the second order of the pseudopotential. At this level, with local pseudopotentials, the thermodynamics and the structure can be obtained starting from the following expression for the energy of a given ionic configuration $\{R_i\}$:

$$U = NU_0 + U_{BS}\{R\} + U_M\{R\} + O(v_{ps}^3) \quad 3.1$$

where U_0 is independent on the ionic positions but depends on the pseudopotential and the properties of the uniform electron gas. The "band structure" (U_{BS}) and the Madelung (U_M) terms can be expressed in terms of the Fourier components of the density as

$$U_{BS} = \frac{1}{2V} \sum_{q \neq 0} \chi_c(q) |\sigma_{ps}|^2 \rho_q \rho_{-q} \quad ; \quad U_M = \frac{1}{2V} \sum_{q \neq 0} \frac{4\pi e^2 q^2}{q^2} (\rho_q \rho_{-q} - N)$$

The explicit presence of structure independent terms is related to the fundamental role of the valence electrons in the determination of the cohesive energy of the system. From the structural viewpoint the Madelung and the band structure terms are more interesting: they are equivalent to the presence of an effective pair potential

$$\phi(r) = \frac{3^2 e^2}{r} + \frac{1}{2\pi^2} \int_0^\infty \frac{4\pi e^2 k r}{k r} \hat{\phi}_{BS}(k) k^2 dk \quad 3.2$$

where

$$\hat{\phi}_{BS}(k) = \frac{1}{4\pi e^2} \left(\frac{1}{\epsilon(k)} - 1 \right) \sigma_{ps}^2(k) \quad 3.3$$

It is clear that in this potential we have assumed a

purely coulombic repulsion between the bare ions neglecting terms like Born-Mayer short-range repulsions, van der Waals interactions etc. As a first approximation we can exclude an important contribution from these terms on the argument that under normal pressure conditions the average minimum approach distance as measured by the exclusion hole in the pair distribution function is larger than the ionic core diameter; moreover the van der Waals terms should be efficiently screened by the valence electrons. Obviously the effective validity of this approximation hinges on careful and extensive comparisons between theory and experiments [178].

A more important comment about the pair interaction 3.2 is that, also in the alkalis, the higher order terms [179] could be not negligible and, besides to introduce many-body interactions, their presence modifies also the structure independent and the pair interaction terms in 3.1. A suitable adjustment of the parameters of the bare pseudopotential can take into account approximately this effect [180].

At the level of pair interaction, the main sources of uncertainty are the form of the model potential and the approximation used for the exchange and correlation effects in the electronic dielectric function. In the range of the local model potentials the empty-core Ashcroft's pseudopotential [181]

$$\phi(r) = \begin{cases} 0 & r < r_c \\ -\frac{ze^2}{r} & r > r_c \end{cases} \quad 3.4$$

despite its simplicity, appears quite satisfactory for the study of liquid structures.

For the local field corrections in the dielectric function it is important to have built-in the maximum number of consistency requirements. Within this

constraints, only few of the many proposed dielectric functions [182] are satisfying in the range of densities we are interested. One reasonable choice, also looking for a computationally simple function, is the Vashishta and Singwi [183] dielectric function which improves the Singwi Tosi Land Sjolander [184] theory by forcing the fulfilment of the compressibility sum rule. The resulting local field factor $G(k)$ is given by the authors in tabular form [183]. More recently Ichimaru and Utsumi [185] have published an analytical fitting formula for $G(k)$ which embodies the known results and the Monte Carlo and variational results for the electron gas [186].

The previous argument can be easily extended to the treatment of the ionic potentials in the alloys. The potential 3.2 will be replaced by a matrix

$$\phi_{\alpha\beta}(r) = \frac{1}{2n^2} \int_0^\infty \frac{w_{\alpha\beta}(kr)}{kr} \hat{\phi}_{\alpha\beta}(k) k^2 dk \quad 3.5$$

$$\hat{\phi}_{\alpha\beta}(k) = \frac{4\pi z_\alpha z_\beta}{k^2} e^2 \left[1 + \left(\frac{1}{\epsilon(k)} - 1 \right) \frac{V_\alpha(k) V_\beta(k)}{\left(\frac{4\pi e^2}{k^2} \right)^2 z_\alpha z_\beta} \right] \quad 3.6$$

where $\epsilon(k)$ depends on the concentration through the average density of the system.

The interplay between the electronic properties and the ionic structure in a metal is subtle: the electrons determine the structural arrangement of the ions but their transport properties are strongly affected by the structure. In particular the electric resistivity has a direct connection with the ionic structure factor [187].

A semiclassical treatment of the transport properties of the electrons gives the Ziman's formula [188]:

$$\rho_{el} = \frac{12\pi m^2}{h^3 \rho e^2 k_F^2} \int_0^1 |V_{ei}|^2 S(k) \left(\frac{k}{2k_F} \right)^3 d \left(\frac{k}{2k_F} \right) \quad 3.7$$

Many problems are related to the determination of the exact limits of validity of 3.7 [189], nevertheless, it allows a simple interpretation of the behavior of the resistivity of liquid metals and their alloys as consequence of changes in thermodynamic state.

3.2 Alkali metals and their alloys as Electron-Ion Plasmas.

Most of the work on the liquid metals has been done within the frame of the pseudoatom description based on the previously discussed effective potential approach. The introduction of an effective ion-ion potential allows to treat the metal as a monoatomic liquid, except for the attention one has to pay to take into account the density dependence of the effective pair potential.

A different approach goes back to the work of Bohm and Staver [190] in their evaluation of the speed of sound from the ionic plasma frequency screened by the electron gas. In this viewpoint the essential two components nature of the metal, ions and electrons, is explicitly preserved.

The system is treated as a two-fluids system, each of them with its own response properties. In the weak electron-ion coupling regime, it is possible to derive [191] a simple formula for the screened ionic response or, through the fluctuation and dissipation theorem, for the structure factor of the metal.

One obtains for the static structure factor $S(k)$ of the liquid metal the expression (see appendix E)

$$S(k) = \frac{S_0(k)}{1 + \beta \rho \tilde{v}(k) S_0(k)} \quad 3.8$$

where $S_0(k)$ is the structure factor of the bare ion subsystem neutralized by a suitable uniform background (DCP) and $\tilde{v}(k)$ is given by

$$\tilde{U}(k) = \frac{V_{ei}(k)^2}{\frac{4\pi e^2}{k^2}} \left(\frac{1}{\epsilon(k)} - 1 \right)$$

3.9

$V_{ei}(k)$ is the bare electron-ion pseudopotential and $\epsilon(k)$ the dielectric function of the homogeneous electron gas. In a similar way we can get the electron-ion and the electron-electron structure factors [192, 193].

By comparing the 3.8 with the formula 1.51 and $\tilde{V}(k) = W(k) - U_o(k)$ we immediately note that the result is formally equivalent to the RPA level of the usual pseudopotential method if we take the DCP as reference system.

It has been shown [194] that with some empirical adjustments the EIP treatment is suitable for the description of many structural and thermodynamic properties of the liquid alkali metals and their alloys.

The extension of the EIP model to polyvalent simple metals faces with the difficulty that the coupling between the electronic and ionic components is higher and the approximation involved in the 3.8 is expected to fail. The difficulty is better highlighted by considering the plasma coupling of the ionic component: for alkali metals near the triple point it is around 200 which corresponds to a near the freezing or metastable DCP but, since the valence appears in the coupling with the square, di- or tri-valent metals would have unphysical couplings for the bare ionic component.

For the alkalis we have not such difficulties and the EIP model can explain in an easy and natural way the striking regularities and the effects of varying the temperature, pressure, density and composition on the structure factors. Moreover it appears to be a simple conceptual frame for developing theoretical treatment for the inhomogeneous situations at the surfaces.

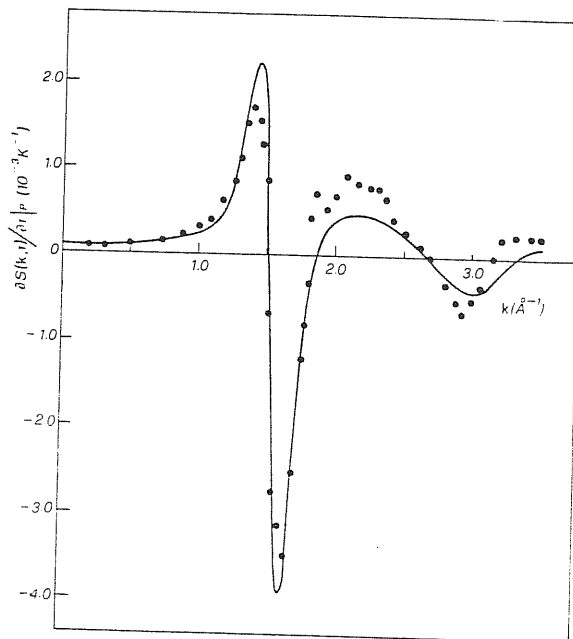
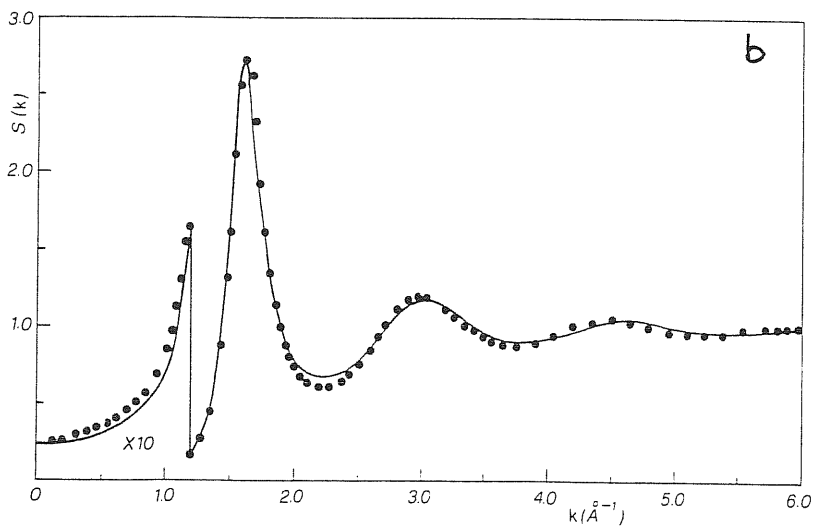
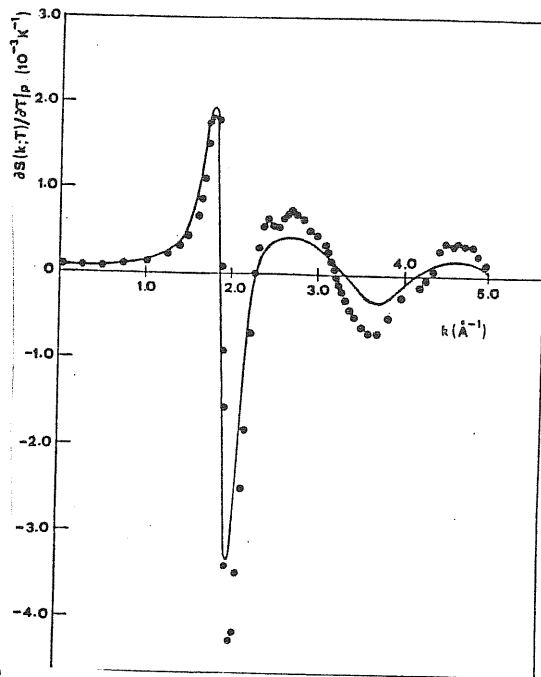
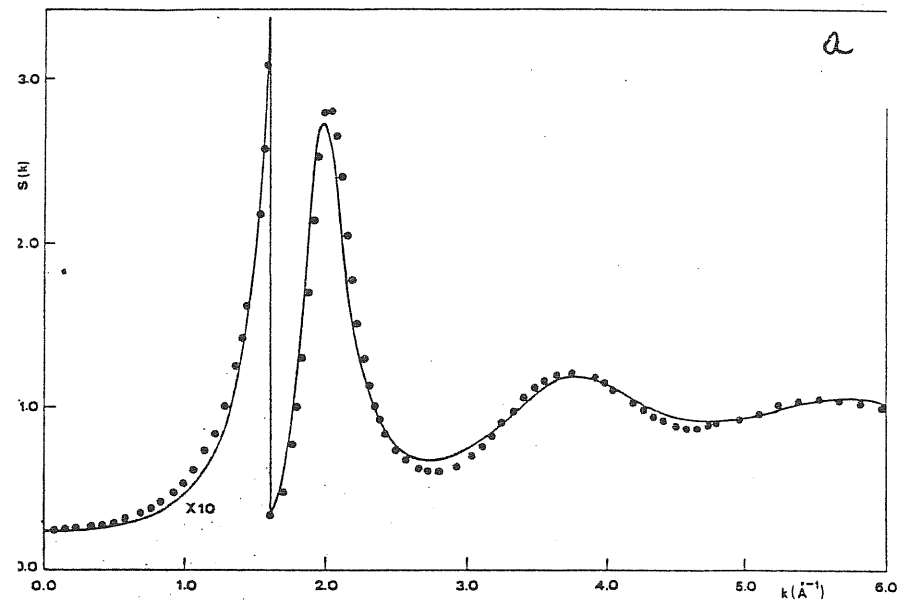


fig. 19. Electron-Ion Plasma model: RPA structure factors and their temperature derivatives for liquid sodium (a) and potassium (b) (full lines) compared with the data of Greenfield et al. [27] (dots).

3.3. Electric resistivity calculations.

As it has been shown in fig.19 the simple RPA formula 3.8 gives good results for the structural properties and their variations provided some empirical adjustment is made on the parameters:

1. the coupling of the ionic bare component is scaled in such a way as the triple point of each alkali corresponds to the Γ_N of freezing of the OCP as determined from the computer simulation ($\Gamma_N = 178$);

2. the bare pseudopotential is the empty-core model potential with the core radius r_c adjusted to fit the isothermal compressibility of the liquid metal through the long-wavelength limit of the $S(k)$:

$$\lim_{k \rightarrow 0} S(k) = \rho k_B T \chi_T$$

3. the Vashishta Singwi dielectric function has been used for the electron gas.

The points 1 and 2 are clearly empirical in nature. As it will be more clear when we shall discuss the ORPA treatment, they are related and they can be simultaneously released by improving the statistical mechanics treatment. For the present discussion 2 can be regarded as the adjustment to the liquid of a practice used in the solid state theory [177]. As consequence of the truncation of $\tilde{v}(k)$ at its first node, the first peak of the metal structure factor is exactly equal to the OCP one. This implies the necessity of the assumption 1: the actual ionic Γ for lithium and sodium would have too high first peaks in the structure factors as compared with the experimental ones.

An analysis of the long-wavelength limit for the alloys, focused on the Na-K and the Li-Na systems, showed that this simple model exaggerates the tendency

to segregation of the components of the alloy unless some account is taken of the electronic charge transfer between the components.

An analysis of the variations of the electric resistivity with the thermodynamic state according to the Ziman formula gives a detailed probe to check the quality of the theoretical structure in the wavelength region below, though rather close to, $2k_F$. Since the first node of the pseudopotential is located precisely in this region, the electronic resistivity calculations are a specific test for the bare ion (OCP) structure factor and hence for the EIP model in this wavenumber region.

To evaluate the electric resistivity, besides the metallic $S(k)$ we need the knowledge of the electron-ion scattering matrix elements V_{ei} . In principle they should be related, apart different screening corrections [195], to the same potential which enters in the evaluation of $S(k)$. Such a program would require a considerable higher degree of sophistication than what is involved in our choice for the structural parameters.

For simplicity, since we are more interested in the variations of the resistivity, we have used for V_{ei} the Ashcroft form screened by the electronic VS dielectric function but we have put in this term core radii fitted to the measured resistivity of the liquid at the freezing temperature at atmospheric pressure.

The degree of internal consistency of such a choice is shown in table 3. II where the values of r_c which enter in the $S(k)$ and in $V_{ei}(q)$ are shown.

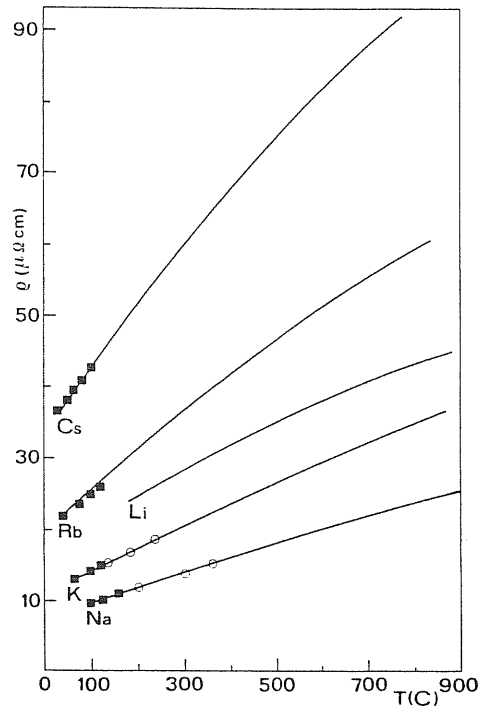


fig. 20. Electric resistivity of alkali metals versus temperature at constant density. Squares and circles: experimental results from Endo and Lien et al. [1961].

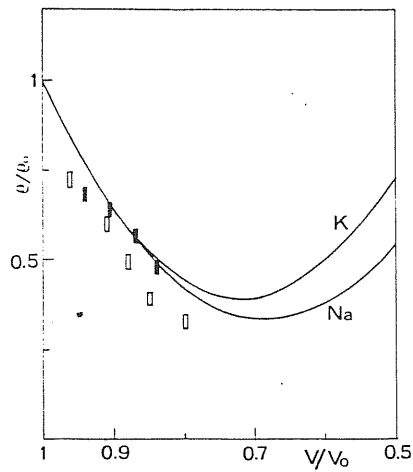


fig 21. Electric resistivity of liquid sodium and potassium versus volume at constant temperature of 220 $^{\circ}\text{C}$ (curves) compared with the experimental data \square (K) and \circ (Na).

\bar{r}_M in formula $\Gamma = \bar{r}_M \frac{\bar{r}_M}{T} \left(\frac{\rho}{\rho_M} \right)^{1/3}$ was fixed at 189 to have an overall fit of the experimental heights of the peaks near the freezing.

tab. 3. II Radii used in the Ashcroft's model potential. (Å)

	Li	Na	K	Rb	Cs
r_c (resistivity)	0.598	0.882	1.107	1.134	1.159
r_c (compressibility)	0.666	0.930	1.223	1.354	1.427

The obtained values for the linear temperature coefficients at constant pressure, temperature and volume are shown in table in comparison with the experimental data [196]. Particularly the values of $(\partial \log \rho_{ee} / \partial \log T)_V$ are significant as test for the structure factor since the only dependence on the temperature should come from $S(k)$. The variations of resistivity over wide ranges of temperature and densities are reported in fig. 20 and 21.

A careful analysis of the structural and thermodynamic properties of the liquid alloys of alkali metals [197] within the EIP model reveals that the structural model at this stage does not yield a quantitative account of the concentration fluctuations. For this reason we have focused ourselves on resistivity calculations for alloys which do not appear to be far from the ideal solution limit. These include the Na-K and other alloys in the middle of the alkali series.

We have used the Faber-Ziman [198] extension of formula 3.7 to the case of alloys; by rewriting it in terms of the Bathia-Thornton structure factors (see

p. 12) we have

$$\rho_{el} = \frac{12\pi m^2}{h^3 \rho c^2 k_F^2} \int_0^1 \left\{ |V_{NN}|^2 S_{NN} + 2|V_{NC}|^2 S_{NC} + |V_{CC}|^2 S_{CC} \right\} \left(\frac{k}{2k_F} \right)^3 d\left(\frac{k}{2k_F} \right) \quad 3.10$$

where the electron-ion scattering matrix elements are completely determined by those for the pure metals (τ_c from table 3. II) the only effect of the concentration being the obvious change of the electronic density.

Since the usage of the multicomponent extension of the RPA with this choice of parameters implies a divergency of the structure factors at small wavenumbers for many thermodynamic states, we have further approximate $S_{CC}(k)$ with its ideal value ($S_{CC}(k) = x_1 x_2$). In this way we have eliminated the spurious [199] RPA divergency by not changing too much the physical behavior of the system.

The isothermal dependence of on the concentration in the Na-K is shown in fig. 22 where also the building up of the final curve from S_{NN} and $S_{NN} + S_{NC}$ is shown. The crucial role played by the concentration fluctuations is evident. Hence it is not surprising that going to systems like Na-Rb, Rb-Cs, K-Rb, where the non-ideality is stronger, our results, based on the hypothesis $S_{CC} = S_{CC}^{id} = x_1 x_2$, give larger discrepancies with the experiments [200] (fig. 23).

The main conclusion for the alloys is that the simple RPA level treatment is not directly applicable and the apparently innocuous ansatz $S_{CC} = S_{CC}^{id}$ is a too drastic simplification but for the nearly ideal Na-K. Moreover an improvement of the model may require the introduction of different effective charges for the components of the alloy to allow for the possibility of modelling some electronic charge transfer.

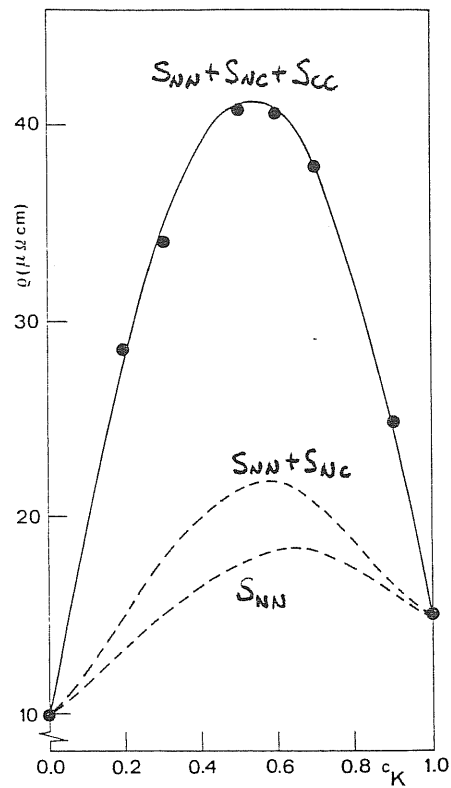


fig. 22. Electric resistivity of Na-K alloy at 100 C versus the concentration of potassium. Full curve: theory; dots: experiments. The progressive contributions from the Bathia-Thornton structure factors are shown.

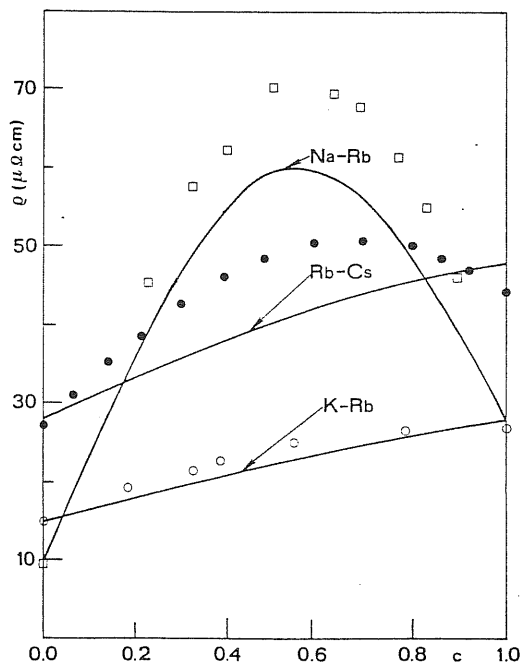


fig. 23. Electric resistivity of K-Rb, Na-Rb and Rb-Cs at 100 C versus the concentration of the second component. Full curves: theory; dots, circles and squares: experiment

3.4. Beyond the RPA treatment of the pure alkali metals.

As firstly suggested by Senatore and Tosi [2011], the truncation of the bare pseudopotential above its first zero in the k space is equivalent to a non standard ORPA (see p.21). Indeed, since the ions of the liquid metals do not penetrate into the excluded volume around each of them, we could modify the repulsive Coulomb potential well inside this hole, without changing the thermodynamic properties of the system. Changes at small r are obviously reflected in the short wavelength region. In this sense we could justify, more in the spirit of liquid state theories, the cut-off of $\tilde{V}(k)$ at its first node. As it is apparent in fig.24 the modification of the potential outside the correlation hole is very small.

The alternative we have followed was to implement the full ORPA treatment for the alkali metals.

Since the OCP structure factor is approximated very well by the GMSA of Chaturvedi et al., we have a well defined hard core inside which we can change the potential without modifying the physical properties of the system as in the original version of the WAC theory. Thus we modify the RPA relation 1.50 written for the direct correlation function into

$$c(r) = c_0(r) - \beta u(r) - \Theta(\sigma - r) \left[q - s \left(1 - \frac{r}{\sigma}\right) + \left(1 - \frac{r}{\sigma}\right)^2 \sum_{m=0}^{\infty} c_m P_m \left(\frac{2r}{\sigma} - 1\right) \right] = \\ = c_0(r) - \beta \tilde{u}(r) \quad 3.11$$

where $\Theta(x)$ is the Heaviside step function and $P_m(x)$ is a Legendre polynomial. The coefficients q, s, c_m are determined from the condition

$$\frac{\delta \text{trPA}}{\delta \tilde{u}(r)} = 0 \quad r < \sigma \quad 3.12$$

which is equivalent to say that the RPA pair

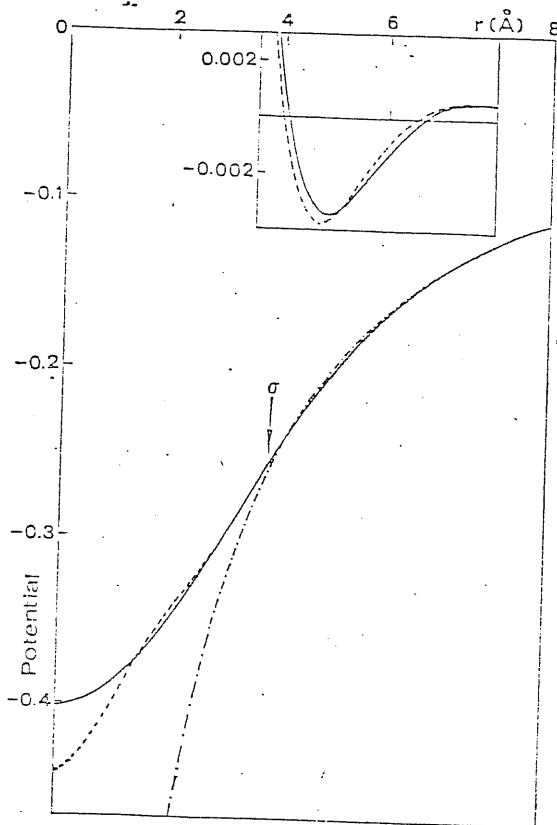


fig. 24. Potentials for liquid potassium at 65 C. Full curve: truncated potential $\tilde{v}_s(r)$ used in the RPA calculations within the EIP model; dashed curve: true $v_s(r)$ potential; dot-dashed: Coulomb potential (units of $e^2/\text{\AA}$). The arrow marks the diameter σ of the GMSA for the OCP component. The inset shows on an enlarged vertical scale the total ion-ion potential in the region of its main minimum

distribution function with the potential $\bar{U}(r)$

$$g(r) = g_0(r) - \frac{1}{(2\pi)^3} \frac{1}{\rho} \int dk \beta \rho \bar{u}(k) S_0^2(k) \left(1 + \beta \rho \bar{u}(k) S_0(k)\right)^{-1} \quad 3.13$$

must be zero inside the core. Technical details about the practical implementation of the calculation are given in Appendix F.

We have checked our ORPA procedure against the existing simulation data for liquid Rb [202] with the Price et al. [203] pair potential. Fig. 25 reports our results for $S(k)$ at 319°K while a comparison with data of Mountain [204] for the $g(r)$ at 350°K are given in fig. 26

We stress that our results for this system do not involve any adjustable parameter. The agreement between the simulation and the ORPA is extremely good; the remaining discrepancies in the $g(r)$ and in the phase shift at large wavenumbers are clearly related to inaccuracies of the GMSA theory for the OCP.

On comparing these theoretical results with those for the corresponding OCP, we can assess the effects of the electronic screening on the liquid structure factor. For $k \rightarrow 0$ $S_0(k)$ vanishes as k while the effect of the screening makes $S(k=0)$ finite. The position of the first peak is shifted by only about 0.02 \AA^{-1} to larger k and its height is little affected since $\bar{U}(k)$ tends to have a node in this region (see fig. 27). The comparison between $u(k)$ and $\bar{U}(k)$ shown in fig. 27). clearly indicate the reasons for the success of the empirical cut of the $u(k)$ at its first node. The optimized potential has been reduced over the original one by about one order of magnitude in the region of the first peak. This explains also the observed similarity [205] between the OCP and the alkali metal structure factors at intermediate and

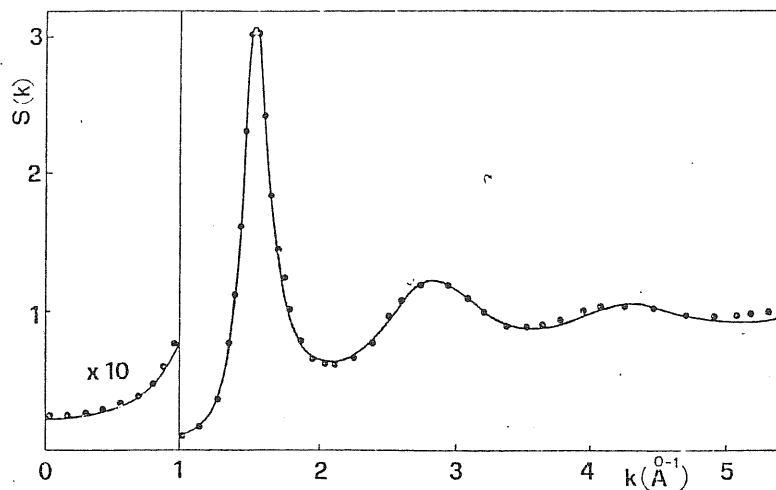


fig. 25. Structure factors of a model for Rb at 319 K. Full curve: ORPA. Dots: Molecular dynamics results of Rahman [202].

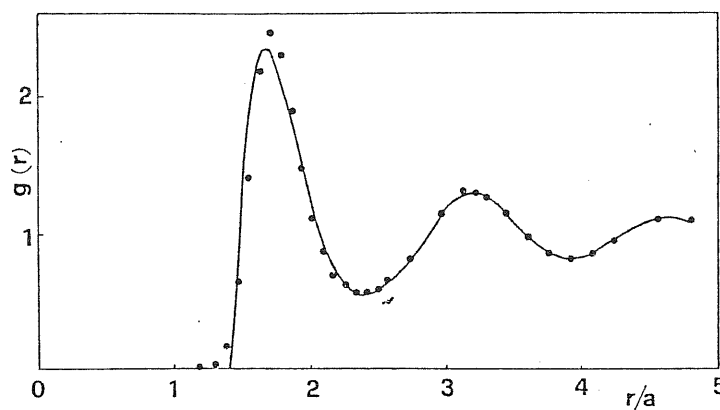


fig. 26. Pair distribution function of a model for liquid Rb at 350 K from ORPA (full curve) and Monte Carlo data of R. D. Mountain (dots) [204].

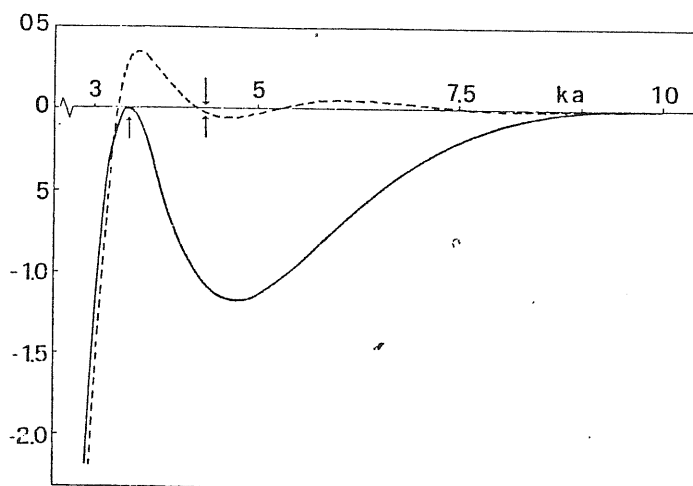


fig. 27. Comparison between the optimized potential $\beta u(k)$ (broken curve) and the true $\beta \phi(k)$ (full curve) for the model of liquid Rb shown in fig 25. The double arrow denotes the position of the main peak of $S(k)$ and the single arrow marks the first node in $\beta u(k)$.

large wavenumbers.

Having checked the statistical mechanics theory, we have calculated the $S(k)$ for the alkali metals at their freezing point to make connection with the experimental diffraction data. For the electron-ion potential we have used the Ashcroft's empty core pseudopotential with two different dielectric functions: the Vashishta Singwi (VS) and the Singwi Sjolander Tosi Land (SSTL) choice. With the latter we have used the core radii r_c determined by Price et al. by fitting the solid phonon spectrum [206], while in connection with the former we have adjusted r_c to fit the measured $S(0)$.

The results for the alkalis at their melting point are shown in fig.28 as compared with the best available experimental measurements [26,27]. The quality for the Rb can be judged from the comparison between the Rahman's results and the experiment (fig.29)

Besides the Lithium for which the worsening when we try to fit the compressibility can be reported to the strong scattering ability of this ion, the overall agreement is good providing an "a posteriori" justification for the chosen pseudopotential.

We can contrast our results with the more standard ORPA calculations within the pseudoatom approach, which employ the hard spheres as reference system. It is well known that a direct implementation of the original scheme does not give completely satisfying results [207] for the alkali metals. In particular the existing implementations of the ORPA with the hard sphere reference system look unable to avoid an unphysical bump at small k without releasing the excluded volume condition $g(r) \approx 0$ [208].

The more specific informations about the effective

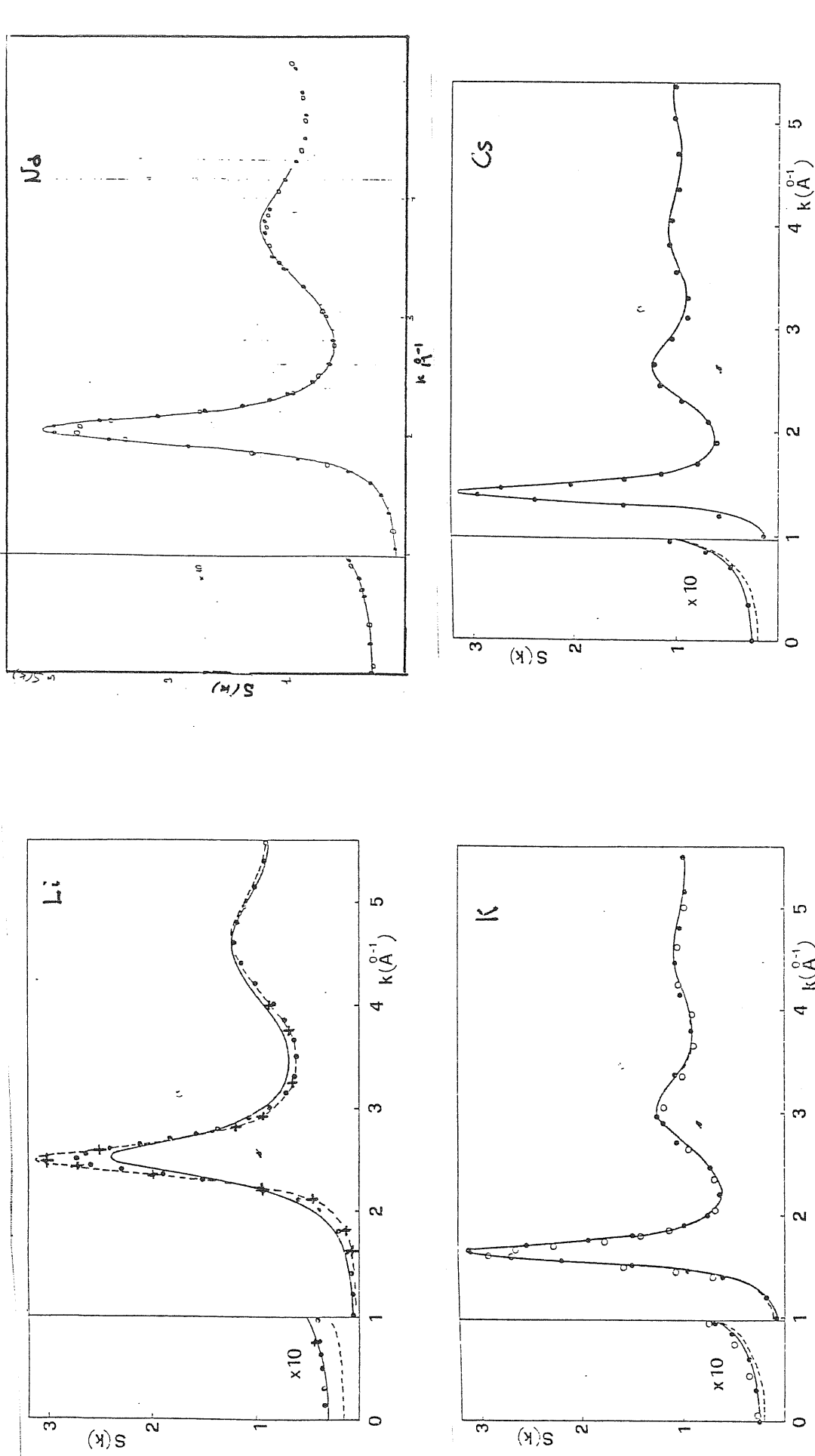


fig. 28. DRPA structure factors for the alkali metals (full curves) compared with the experimental data. Note that for Na an improved GMSA structure factor for the OCP has been used (see ref. [4]).

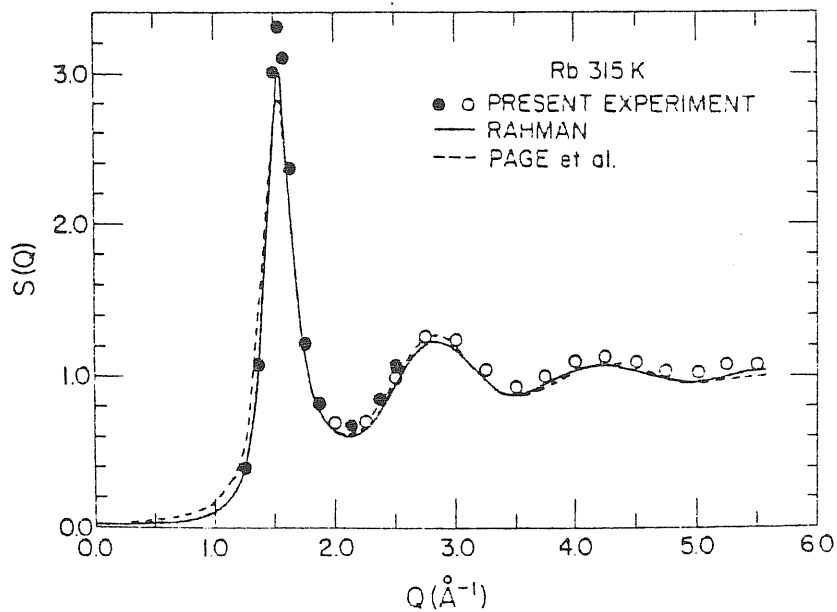


fig. 29. Comparison between the experimental and the simulated [202] $S(k)$ for Rb (from Copley and Rowe, Phys. Rev. A9, 1690 (1974)).

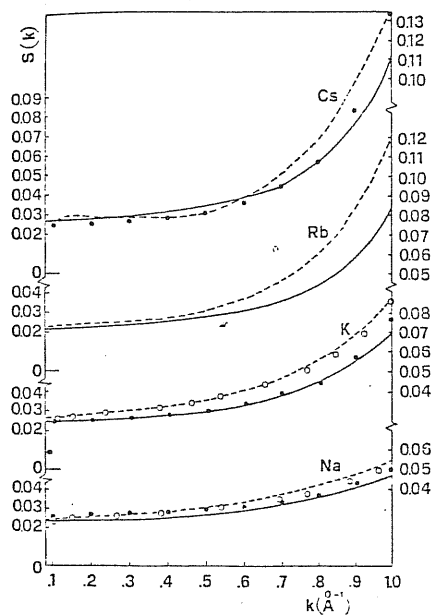


fig. 30. Structure factors of liquid Na, K, Rb and Cs in the small-angle region (0.08 \AA^{-1} , 1 \AA^{-1}). The experimental data are from Waseda (broken curve), Hujiben and van der Lugt (dots) and Greenfield et al. (circles). Full curve: ORPA results (with r adjusted to fit the experimental $S(0)$).

pair potential in the real systems are hidden in the region below the first peak and particularly below 1 \AA^{-1} [209]. A comparison of our results and the experiments in this small k region is shown in fig.30. It is apparent that besides the Na, some discrepancies exist between different measurements (see discussion in the section 1.1). The Waseda's [210] measurements should be more precise than the others in this region.

Some interest has been raised in recent years about the presence of a linear term in the small angle region as convincingly demonstrated by Waseda [210] and previously suggested by Matthai and March [211]. On this point we can only comment that no such term appears in our simple treatment of the electron-ion coupling [212].

Finally we would like to add something more about the theoretical determination of the structure from the viewpoint of the pseudoatom model. The recent developments of the modified integral equation methods have raised the possibility of an extensive study of the structural and thermodynamic implications of the many effective potentials proposed for liquid metals. Since these approaches are more efficient from the side of the computer time requirements (about one order of magnitude faster than the usual ORPA on the hard sphere reference) and more flexible about the systems they can manage, their usage for the liquid metals and alloys looks very promising.

We have done a trial run for the case of the simulated rubidium. The PY bridge functions have been fixed by requiring the fitting of $S_{HD}(0)$. The agreement is remarkable (fig.31) however an extensive and selfcontained application of the MHNC theory to the liquid metals needs a careful analysis of the

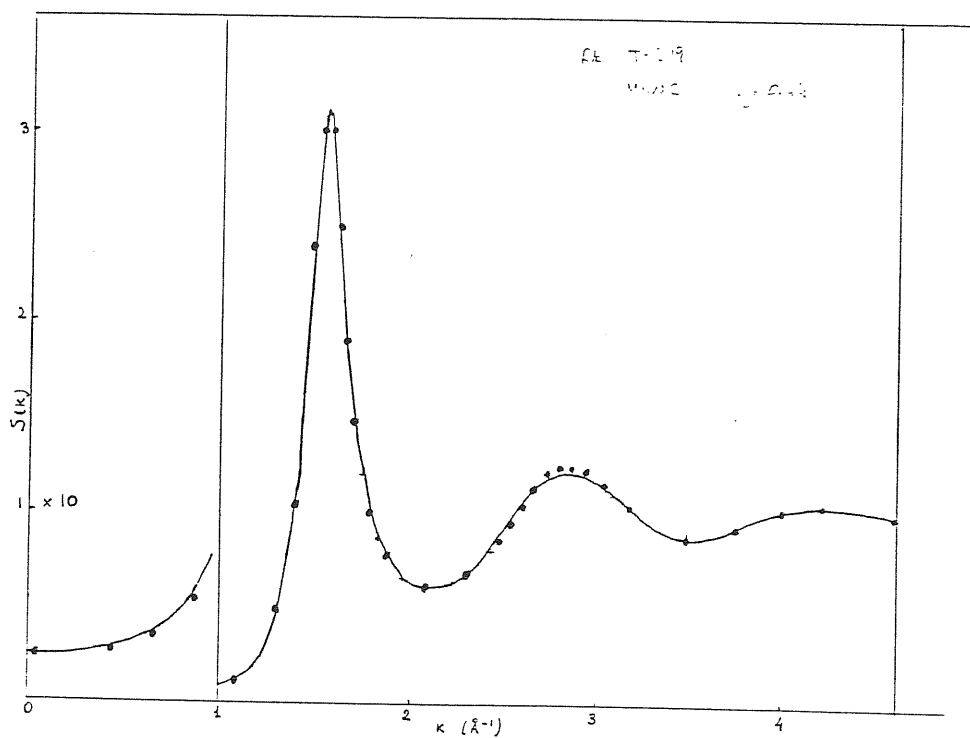


fig. 31. Structure factor for the same model for liquid Rb at 319 K shown in fig 25. Full curve: MHNC; dots: Molecular dynamics results of Rahaman [202].

thermodynamic consistency requirements within the pseudopotential based approach to the effective potentials [213].

CHAPTER 4. MOLTEN SALTS.

4.0 Introduction.

Molten salts are a very important subject for their technological relevance and for the richness of their physical-chemical behavior.

The thermodynamic properties of these compounds are dominated by the presence of the long range Coulomb interactions. A more subtle role is played by this interaction in the structural properties.

In the huge variety of molten salts, we shall focus our attention on the simplest: alkali halides and some alkaline-earth halides for which a simple ionic model is sufficiently reliable.

4.1 Experimental data, primitive model and refined potentials.

Typical structure factors are shown in fig. 32. They are compared with data for an alloy in which the unlike interaction is similar to the like ones.

The more striking difference is in the shape of the unlike structure factors: we can say that the $S_{+-}(k)$ has developed a strong negative peak while the positive has been reduced to a broad shoulder above the minimum. This qualitative behavior reflects the tendency to a stronger than random mixing. It is not exclusive of the Coulomb interaction [214] but its presence in our charged system and the strong correlation between the negative peak of S_{+-} and the positive of S_{++} and S_{--} has a simple physical consequence. If we construct the NN, NQ, QQ structure factors NaCl (cfr. p.12) we get the result shown in fig.33. It is evident that the main negative peak of S_{+-} has been combined with the positive ones of S_{++} and S_{--} to give the dominant peak in the S_{qq} .

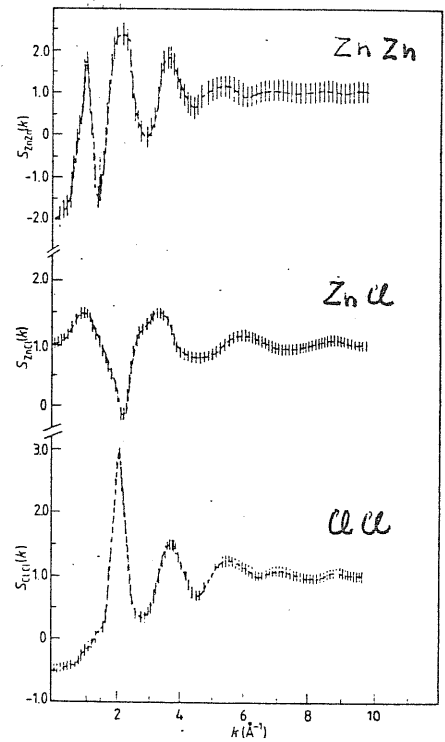
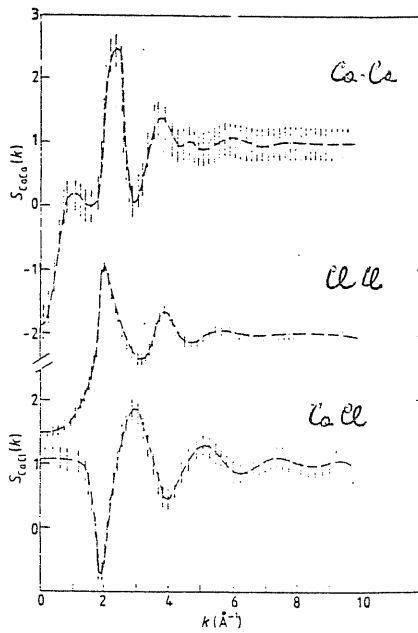
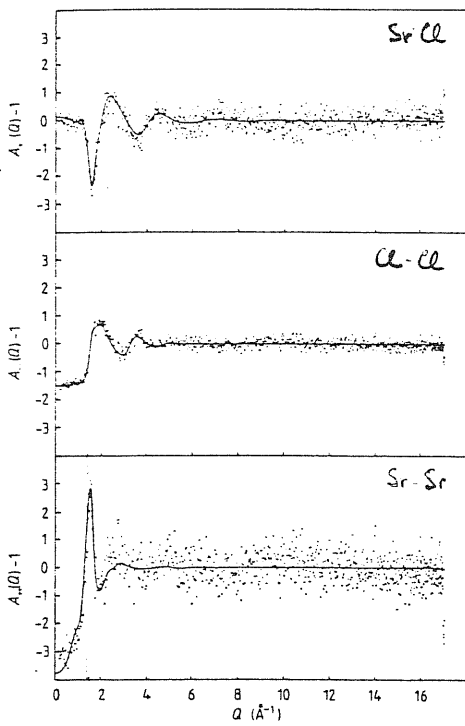
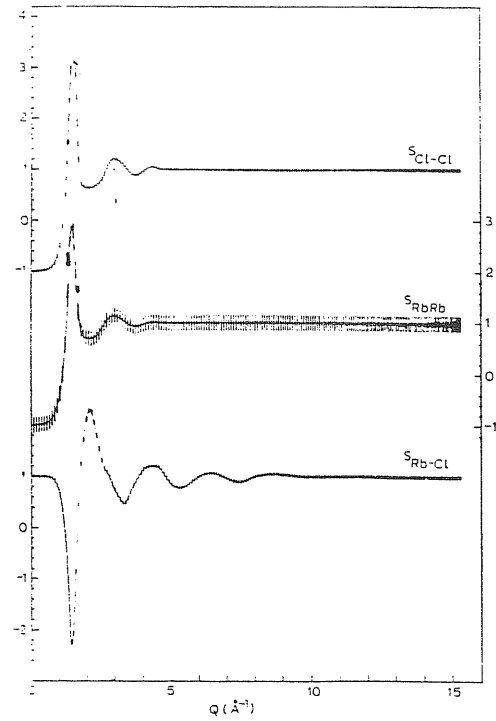
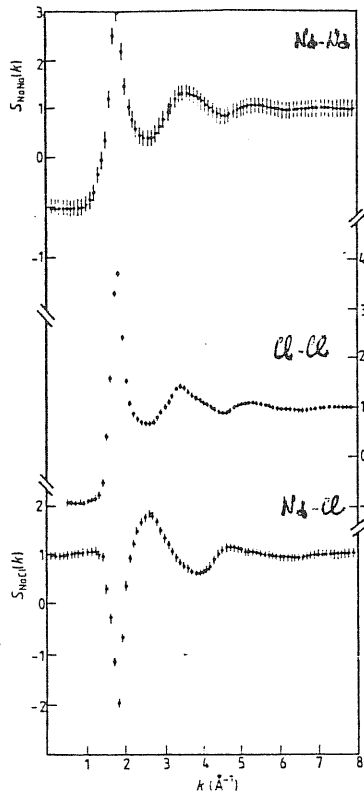
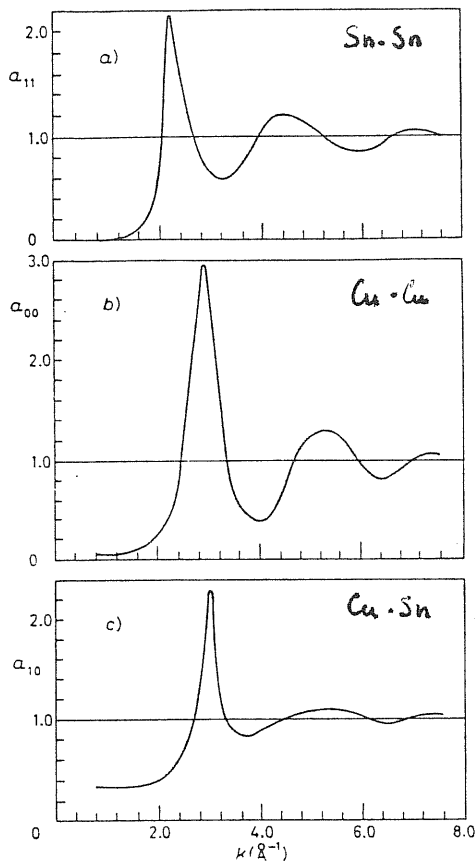


fig. 32. Experimental partial structure factors of: Cu₆Sn₅ alloy [16], NaCl [228], RbCl [17], SrCl₂ [228], CaCl₂ [239] and ZnCl₂ [240].

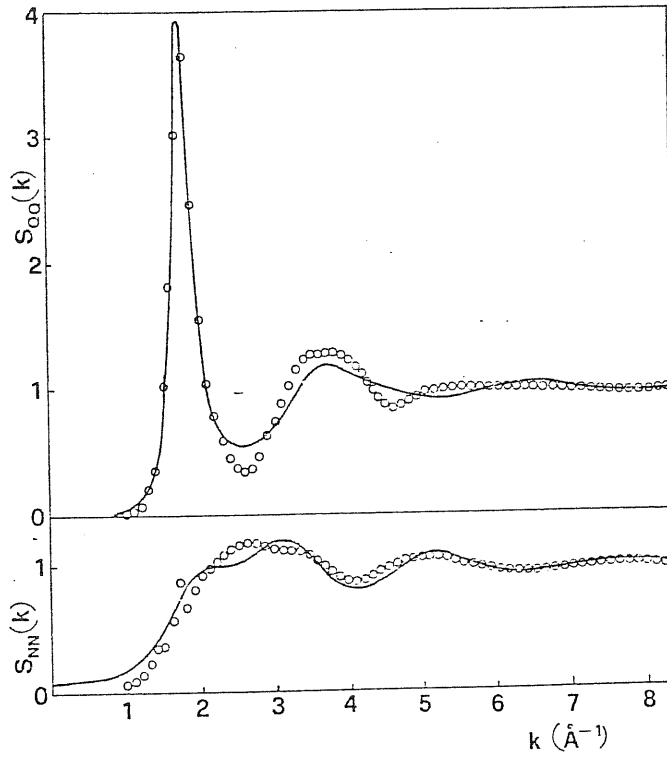


fig. 33. Number and charge structure factors in molten NaCl. Circles: from the experimental results [228]. Full curve: MHNC theory.

This implies the presence of a well defined charge periodicity in the real space which means that in the molten salt we have a spatial ordering strongly reminiscent of the solid state ordering: if we fix an ion we find very well defined shells of alternatively charged neighbours. Instead the NN ordering is much less important and the S_{NQ} is not very much different from zero. This indicates an almost complete decoupling between charge and density fluctuations.

In the case of the more asymmetric divalent chlorides the dominance of the charge ordering remains but there is no approximate NQ decoupling.

A crude "primitive model" for the molten salts is represented by the charged hard spheres already discussed in Chapter 2. The description of the alkali halides using the MSA analytical solutions for charged hard spheres has provided a first insight in the microscopic structure of these melts [215]. More detailed informations require a more refined modelling of the interactions.

Whithin the semiempirical pair potentials the Tosi Fumi [216] potentials give the best description of the properties of the solid alkali halides with the NaCl structure [217].

The functional form is of the Born Mayer Huggins Mayer type:

$$\phi_{ij}(r) = z_i z_j \frac{e^2}{r} + B_{ij} e^{-d_{ij} r} - \frac{C_{ij}}{r^6} - \frac{D_{ij}}{r^8} \quad 4.1$$

where the dipole-dipole and the dipole-quadrupole coefficients C_{ij} and D_{ij} were obtained by Mayer [218] from optical data in the crystals. A factor 4 of variation is within the present uncertainty of these coefficients, however we recall that the van der Waals interaction contributes only for few percents to the

cohesive energy of the solid.

More important is the determination of the repulsive term B_{ij} . Tosi and Fumi got their values by exploiting the requirements of portability of the potential from a salt to another and fitting the equation of state and the compressibility of the solid at room temperature.

The properties of the solid are quite well reproduced by the potential 4.1. Obviously, dealing with a rigid ion pair potential, the Lyddane-Sachs and Teller [219] relations for the phonon spectrum are violated and the optical branches are not well accounted for. Moreover the Chauchy relations between the elastic constants of the solid ($C_{12} = C_{44}$) are satisfied while in the real systems they are violated by the 10% about. This last drawback is a clear indication of the presence of many-body forces in the ion-ion interaction.

Computer simulation studies [220] have demonstrated the overall reliability of the Tosi Fumi potential also in the liquid state. The calculated thermodynamic quantities are compared with the experimental ones in tab. 4. I.

Taking into account the large sensitivity of the pressure to the details of the repulsive part of the potential, and recalling that the coefficients for the repulsive part come from a fit of properties of the solid, it is not difficult to understand the larger pressures found for the liquid. On the comparison between the theoretical and experimental structures we shall return later on.

4.2 Theory of the structural and thermodynamic properties of molten alkali chlorides and strontium chloride.

Until we remain at the primitive model level of description, we can expect only a semiquantitative connection with the experimental data. At this level the accuracy of the usual integral equation is not crucial and the practical advantages of the analytical solutions of the MSA for additive charged hard spheres put this theory in a particularly interesting position.

If we improve the model potential, since we lose any possibility of analytical solution, we also need an improved statistical theory. The HNC theory has been used successfully in the study of electrolytic solutions. It deals better with the softer repulsion of the realistic potentials. Moreover there is a strong theoretical evidence [50] that it is particularly suitable for the long tail coulomb potentials.

The study of the molten alkali halides, described by the Tosi Fumi potentials using the HNC equations [221], gives the results shown in tab.4.II and fig.34. The theory appears of semiquantitative validity, the main structural features are reproduced. However important flaws are the large penetration of the $g_{ij}(r)$, directly connected to the poor thermodynamic results, and the large underestimation of the secondary structure of the first peak of the like $g_{ii}(r)$. Moreover the usual thermodynamic inconsistency is clearly apparent in the values of the compressibility. Going to the reciprocal space, the smaller k region directly reflects the larger HNC fluctuation compressibility, while the remaining discrepancies are connected to the heights of the peaks.

tab 4. I From D. J. Adams, I. R. McDonald J. Phys. C 7, 2761 (1974)

Thermodynamic properties of alkali halides at zero pressure and temperature near the experimental melting points

Salt	$V(\text{cm}^3 \text{mol}^{-1})$												$-U(10^3 \text{J mol}^{-1})$			
	T(K)	expt	crystal			liquid			crystal			liquid				
			MC-HM	MC-P	expt	MC-HM	MC-P	expt	MC-HM	MC-P	expt	MC-HM	MC-P			
LiF	1120	11.1	—	12.02	14.3	—	17.18	990.2	—	1025.0	963.4	—	—	1008.9		
KF	1130	26.0	27.91	28.04	30.4	36.09	37.17	768.8	775.3	768.9	740.6	758.3	743.8	—		
CsF	976	31.8	—	38.90	41.6	—	51.04	701.6	—	692.1	679.8	—	—	668.9		
LiCl	883	22.4	22.78	†	28.2	30.35	35.89	814.9	819.0	†	795.0	801.1	820.3	—		
NaCl	1073	30.0	31.37	32.94	37.6	39.72	46.37	739.0	744.2	736.9	711.0	717.3	718.2	—		
KCl	1045	41.6	42.52	46.29	48.8	53.10	61.19	669.7	676.3	655.1	643.1	649.5	634.6	—		
RbCl	995	47.2	47.91	51.29	53.9	58.66	66.69	645.7	658.4	631.4	627.3	629.9	610.3	—		
KBr	1007	48.0	49.12	53.15	56.0	60.26	70.92	639.9	648.3	626.3	614.4	622.0	606.7	—		
RbBr	953	53.6	54.68	—	60.9	65.85	—	618.6	629.8	—	603.1	603.9	—	—		

expt = experimental results; MC-HM = results of Monte Carlo computations based on the Huggins-Mayer potential; MC-P = results of Monte Carlo computations based on the Pauling potential. †Spontaneous fusion occurred for LiCl.

Internal energy, pressure and compressibility for alkali chlorides. Values calculated from HNC theory compared with those of rigid-ion molecular dynamics simulation (experiment in the case of compressibility).

Salt	Molar volume (cm ³)	Temperature (K)	Internal energy (kJ mol ⁻¹)		Pressure (kbar)		Compressibility (10 ⁻¹² cm ² dyn ⁻¹)	
			HNC	MD	HNC	MD	HNC	Expt.
LiCl	29.60	1050	-766.5	-771.1	7.7	1.8	59.8	24.0
NaCl	37.51	1073	-684.3	-694.2	5.3	1.2	66.1	28.7
KCl	50.21	1043	-619.2	-626.4	5.3	1.4	89.3	36.2
RbCl	54.11	978	-602.6	-610.4	6.0	2.0	80.5	40.0
CsCl	61.09	973	-582.9	-590.5	4.7	1.0	101.3	42.9

tab 4. II From G. M. Abernethy, M. Dixon, M. J. Gillan, Phil. Mag. B43, 1113 (1981).

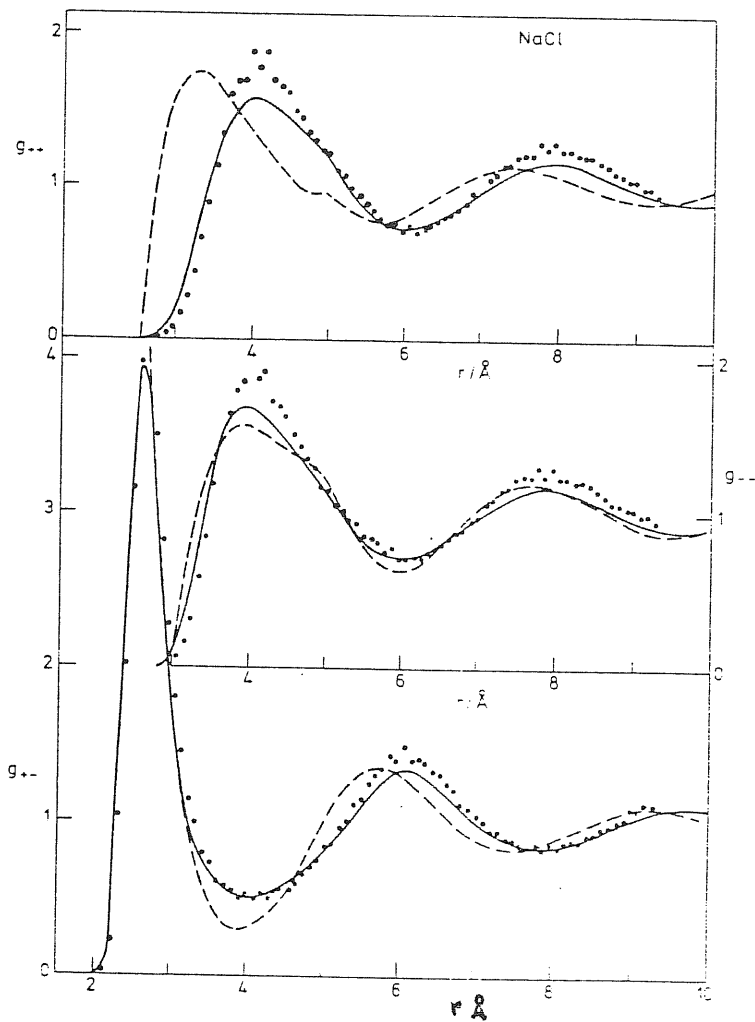


fig. 34. Radial distribution functions for NaCl at molar volume=37.51 cm³ T=1073°K. Dots: molecular dynamics, broken curve: MSA, full curve: HNC (from G.M. Abernethy et al.)

In extending the MHNC to molten salts we found that the bridge functions required to improve the HNC results have two main tasks:

1. they have to behave like a repulsive potential at the distances of the rising part of the $g_{ij}(r)$ to reduce the penetration of the particles and, consequently to improve the thermodynamics;

2. they have to provide the right intermediate range information on the effects of the higher order correlations [222] present in the system as reflected by the modulation of the peak of the $g_{ij}(r)$.

While for the first issue we can rely on a suitable parametrization of the hard sphere bridge functions as for the TCP (see p.47), for the second one we need some more appropriate information. Moreover the structural information contained in the MSA-like bridges, as used for the 2-D OCP, is clearly insufficient because we are not looking for the right periodicity only. We are also trying to put some averaged information on the correlations due to more than two particles (due to the strong coulomb attraction between unlike charges, the correlation between like ions always involves a third opposite charged ion). Following the work of Ichimaru [111], Pandharipande [112] and Bacquet and Rosky [223], we model our bridge functions as

$$b_{\alpha\beta}(r) = \exp(-r^2/5_{\alpha\beta}^2) b_{\alpha\beta}^{HS}(r) + (1 - \exp(-r^2/5_{\alpha\beta}^2)) B_{\alpha\beta}^{(4)}(r) \quad 4.2$$

Where the choice of a gaussian to interpolate between the short and the large distance behavior is particularly simple but in no way crucial. $B_{\alpha\beta}^{HS}(r)$ in the spirit of the Rosenfeld and Ashcroft should be the bridge functions for a two-component system of neutral non-additive hard spheres and $B_{\alpha\beta}^{(4)}(r)$ are the simplest

h-bonds bridge diagrams neglected in HNC and evaluated using the $h_{\alpha\beta}^{HNC}(r)$ functions (see appendix G):

$$B_{\alpha\beta}^{(4)}(r) = \text{triangle diagram} = -\frac{1}{2} \sum_{\gamma, \delta} \rho_{\gamma} \rho_{\delta} \int d\mathbf{r}' d\mathbf{r}'' h_{\alpha\gamma}^{HNC}(r') h_{\alpha\delta}^{HNC}(r'') h_{\gamma\beta}^{HNC}(|\mathbf{r}-\mathbf{r}'|) h_{\delta\beta}^{HNC}(|\mathbf{r}-\mathbf{r}''|) h_{\gamma\delta}^{HNC}(|\mathbf{r}'-\mathbf{r}''|) \quad 4.3$$

The $b_{\alpha\beta}^{(4)}$ should give the asymptotic behavior of $B_{\alpha\beta}(r)$ at large distances. The cross-over distances $\xi_{\alpha\beta}$ should be in between the position of the first and the second zero of $h_{\alpha\beta}^{HNC}(r)$. The hard sphere diameters $\sigma_{\alpha\beta}$ in the $b_{\alpha\beta}^{HS}(r)$ functions in principle should be determined by requiring the fulfilment of three independent consistency relations (or in an approximate way by minimizing an approximate formula for the free energy). The computational effort can be reduced by fixing in a reasonable way the ratios $\frac{\sigma_{++}}{\sigma_{+-}}$ and $\frac{\sigma_{--}}{\sigma_{+-}}$ and then fixing σ_{+-} by requiring the thermodynamic consistency between the compressibility from the fluctuation formula 1.21 and the derivative of the virial pressure respect the density.

We found that an optimal choice for the parameters $\xi_{\alpha\beta}$ and $\sigma_{\alpha\beta}^0$ is to take the positions of the first peaks of $h_{\alpha\beta}^{HNC}(r)$ and for $\frac{\sigma_{++}}{\sigma_{+-}}$ and $\frac{\sigma_{--}}{\sigma_{+-}}$ the ratios between these positions.

A final comment is necessary about the hard sphere bridges. Following Rosenfeld and Ashcroft we should use a parametrization of the pair functions for the non additive hard sphere system. However no such parametrization is available in the literature. The usage of the numerical solutions of the PY equations for the non additive mixture is possible and we have tried to use it but it seems that it does not improve sufficiently the thermodynamics. A careful analysis of the quality of the PY thermodynamics as contrasted with the computer simulation data points to a poorer performance of the PY when the negative non-additivity

is switched on.

For these reasons we have further modelled our $b_{\alpha\beta}^{HS}(r)$ by using the $b_{\alpha\beta}^{PY}(r; \mu_{\alpha\beta})$ functions from the analytical solutions of the PY equations for three one-component hard sphere systems.

We have compared our MHNC results for thermodynamic and structural properties of the alkali chlorides with the results of computer simulation reported by Dixon and Gillan and Lewis et al. [220].

The parameters of the interionic potential are from the Tosi and Fumi work for LiCl, NaCl, KCl and RbCl. The parameters for CsCl are from the work of Casanova et al. [224].

Temperature and densities are the same than in the simulation. In table 4.III we have given the thermodynamic parameters and the bridge parameters determined as previously discussed.

In table 4.IV we have the results for the thermodynamic properties of these molten salts compared with HNC, computer simulation and, whenever possible with the experimental data.

In fig. 35 we show the structural results. The agreement between our results and simulation is very satisfactory, although for the more asymmetric salts we get a decrease of accuracy.

In the calculations we have presented for the alkali chlorides we have assumed the same $b_{\alpha\beta}(r)$ for the density n of the calculation and for the nearby densities $n \pm \delta n$. This is not rigorously true and by taking into account the variation of $b_{\alpha\beta}(r)$ through its explicit dependence from the density (factor n^2 in front of $b_{\alpha\beta}^{(4)}(r)$ and factor n in the hard sphere packing fraction η) we can improve the results for the

TABLE 4.111

THERMODYNAMIC STATE, PACKING FRACTIONS AND CROSS-OVER PARAMETERS *)

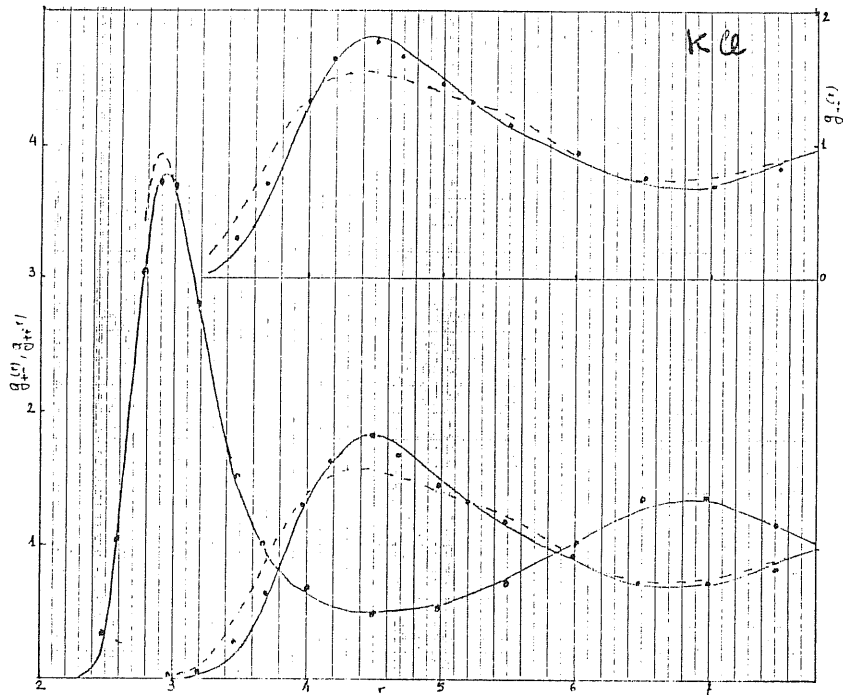
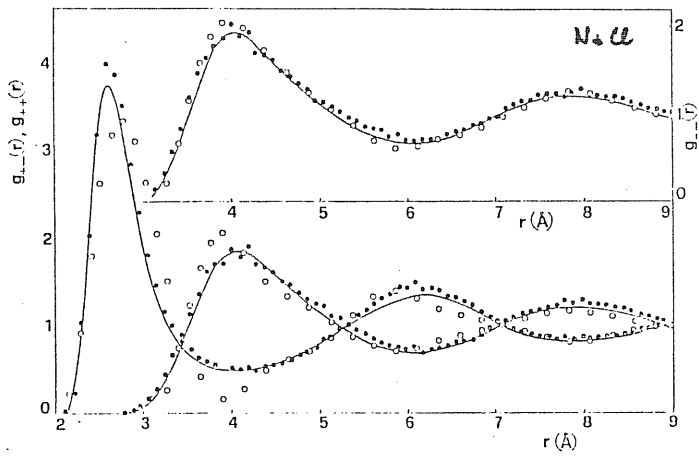
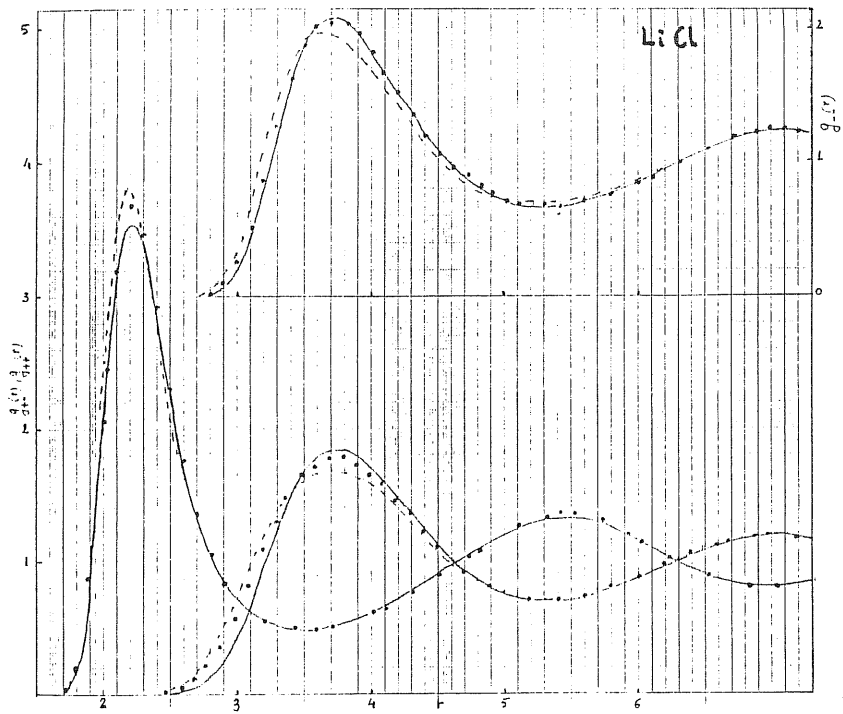
	T(K)	n (ion pairs/Å ³)	Γ	η ₊₋	η ₊₊	η ₋₋	ξ ₊₋ /a	ξ ₊₊ /a	ξ ₋₋ /a
LiCl	1050	0.02035	88.21	0.161	0.420	0.420	1.20	2.08	2.08
NaCl	1073	0.01606	79.77	0.295	0.543	0.543	1.34	2.07	2.07
KCl	1043	0.01199	74.46	0.239	0.437	0.437	1.35	2.08	2.08
RbCl	978	0.0111	77.45	0.313	0.502	0.502	1.41	2.08	2.08
CsCl	973	0.00986	74.76	0.258	0.417	0.435	1.40	2.07	2.10

*) The parameter $\Gamma = e^2 / (ak_B T)$ specifies the coupling strength for Coulombic interactions, with $a = (8\pi n/3)^{-1/3}$.

TABLE IV

THERMODYNAMIC PROPERTIES OF MOLTEN ALKALI CHLORIDES

		P (k bar)	βU_{exc}	βU_{Coul}	βU_{sr}	K_T^{virial} ($10^{-12} \text{ cm}^2/\text{dyn}$)	$K_T^{fluct.}$ ($10^{-12} \text{ cm}^2/\text{dyn}$)
LiCl	HNC	7.7	-45.38	-53.10	7.72	20	60
	Present	0.3	-45.58	-52.64	7.06	18.6	18.6
	Simulation	1.8	-45.65	-	-	-	-
NaCl	HNC	7.2	-39.95	-45.25	5.30	22	66
	Present	1.2	-40.28	-45.10	4.82	18.1	18.1
	Simulation	1.2	-40.40	-	-	-	-
KCl	HNC	5.3	-37.21	-41.70	4.49	31	90
	Present	1.4	-37.55	-41.65	4.10	26	26
	Simulation	1.4	-37.61	-	-	-	-
RbCl	HNC	6.0	-38.54	-42.44	3.90	27.6	80.5
	Present	2.0	-38.95	-42.45	3.50	25.1	25.1
	Simulation	2.0	-39.02	-	-	-	-
CsCl	HNC	4.7	-37.50	-41.04	3.54	32	101
	Present	1.5	-37.92	-41.12	3.19	27	27
	Simulation	1.0	-37.99	-	-	-	-



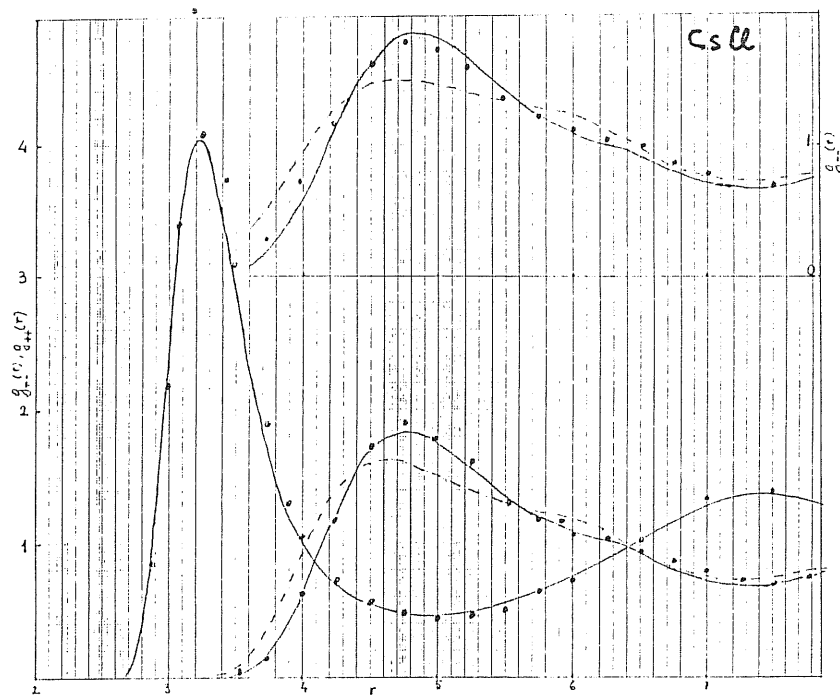
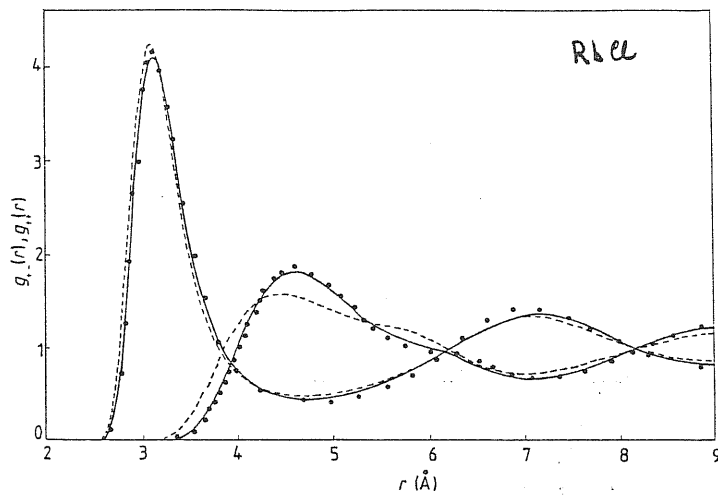


fig. 35. Pair distribution functions for the alkali chlorides
 Black dots: Molecular dynamics [220,221]; full curves: MHNC
 dashed curves: HNC.

compressibility slightly changing the other structural and thermodynamic properties (see [8]). We have strong indications that the remaining inconsistency (dependence of σ_{45} and of $b_{ij}^{(N)}/m^2$ from n) play a negligible role within the present level of accuracy.

A more severe test of the performance of the theory is the charge asymmetric case of the SrCl_2 . This system has a sufficiently ionic behavior to be reasonably approximate by a potential of the Born-Mayer-Huggins-Mayer kind:

$$\phi_{ij}(r) = \epsilon_{ij} \frac{e^2}{r} + B_{ij} e^{-\alpha_{ij} r} - C_{ij}/r^6 \quad 4.4$$

We have evaluated the MHNC structures with the same potential parameters [225] used by De Leeuw [226] in its simulation work.

The temperature was taken 1150°K and the molar volume $V = 61.94 \text{ cm}^3/\text{mole}$, which is the volume determined by the De Leeuw's Monte Carlo simulation at the same temperature and zero pressure.

Table 4.V gives our results for thermodynamic properties of the model, namely the pressure P (evaluated from the virial theorem) the excess internal energy per mole, separated into the Coulombic and short range contributions and the isothermal compressibility [227].

The comparison is with the De Leeuw's data and our simple HNC results. As in the case of alkali chlorides, a very good agreement with the simulation numbers is got with the MHNC.

The structural results are shown in fig. 36 as compared with the simulation and experimental results. Leaving apart the latter for the moment, we note that the agreement with the simulation is quite good. Some

7

tab 4. V SrCl₂ thermodynamic results.

Thermodynamic properties of molten strontium chloride near freezing (a)

	P(kbar)	U _{exc} (kJ)	U _{Coul} (kJ)	U _{sr} (kJ)	K _T (10 ⁻¹² cm ² /dyn)
HNC	9.5	-2062	-2237	175	8.6, 37.6 (b)
MHNC (c)	0.05	-2074	-2226	151	12
Simulation	0	-2078	-2228	150	11
Experiment (d)	0	-2044	-	-	13

(a) The first three rows refer to the liquid at 1150K and $V_M = 61.94 \text{ cm}^3/\text{mole}$, against $V_M = 58.16 \text{ cm}^3/\text{mole}$ from experiment.

(b) The two values for K_T in the HNC correspond to the use of the virial theorem and of thermodynamic fluctuation theory, respectively.

(c) The values of the parameters in the bridge function are $\sigma_{+-} = 2.72 \text{ \AA}$, $\sigma_{--} = 3.51 \text{ \AA}$, $\sigma_{++} = 4.69 \text{ \AA}$, $\xi_{+-} = 2.82 \text{ \AA}$, $\xi_{--} = 3.7 \text{ \AA}$ and $\xi_{++} = 4.9 \text{ \AA}$.

(d) The experimental value of U_{exc} is estimated from the crystal lattice energy at 298K reported by Busing (1970) on adding the measured enthalpy of the liquid at 1150K relative to the crystal at 298K. This enthalpy difference, as well as the compressibility of the liquid, are given by de Leeuw (1978a).

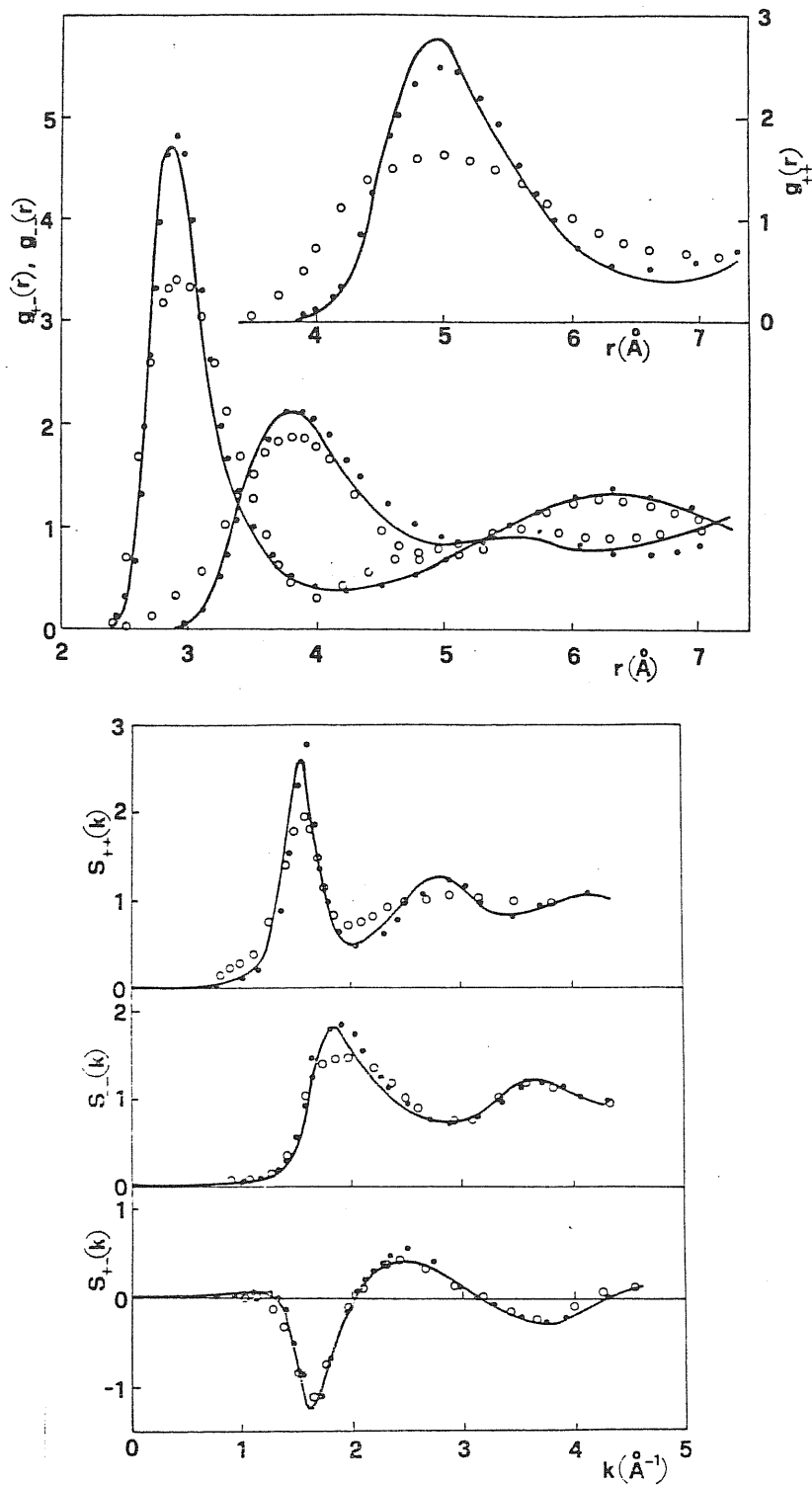


fig. 36. Pair distribution functions and structure factors of molten SrCl_2 near the freezing. Curves: MHNC at 1150 K; dots: MC of DeLeeuw [226] with the same pair potential; circles: experimental data [17].

discrepancies in the heights of the peaks of these functions are evident. This is in the same region where the cross-over between the hard sphere part and $b_{\nu}^{(4)}(r)$ is taking place.

In conclusion we claim that our approach to the estimation of the bridge diagrams is of rather general applicability to liquids where a strong degree of etherocoordination between the component species is induced, i.e. ionic liquids and presumably also "ordered" liquid alloys (like LiPb etc.)

4.3 Comparison with the experiments.

Having assessed the quality of our MHNC results against the computer simulation results, we have used the theory to get more insight in the real systems.

The comparison between the experimental [228] and the simulated thermodynamic data for the alkali chlorides, using the rigid ion Tosi-Fumi potential shows a remarkable degree of agreement.

Taking into account that the repulsive parameters of the potential have been fitted to data for the solid, this is a significant test of the correctness of the involved physics.

We have checked in the case of NaCl and KCl that a change of the repulsive parameter $\rho = \frac{1}{2}$ in the 4.1 by about 1% is sufficient to reduce the evaluated pressure to zero. On considering the effects of such uncertainty in the model parameters and of the residual discrepancies between calculated and observed liquid structure as shown in fig. 37 we estimate an uncertainty of roughly ± 10 KJ/mole in the internal energy as consequence of the uncertainty in the determination of the coefficients in the potential.

The calculated pair correlation functions for NaCl show a good agreement with the experimental. The main discrepancies are confined on the $g_{+-}(r)$ in the region immediately above the first peak: in the experiments the position of the peak is shifted to a somewhat larger interionic distance (2.78 instead 2.62 Å), it is somewhat wider and it shows a deeper minimum. This region, between 3 and 4 Å, corresponds to the region outside the minimum in the cation - anion potential.

The information contained in the shape of the first peak of $g_{+-}(r)$ points to an effective pair potential

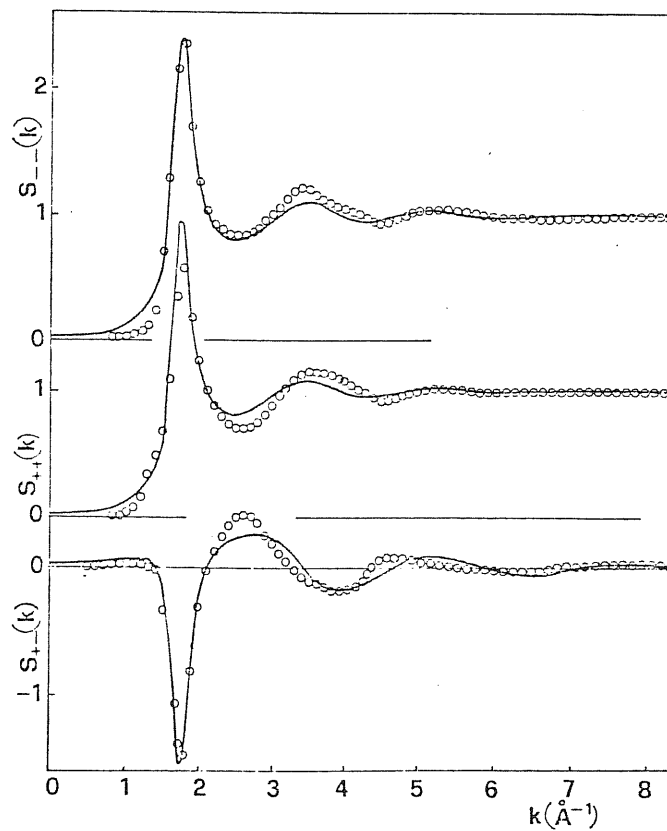


fig. 37. Partial structure factors in molten NaCl.
 full curves: MHNC; circles: experimental data [228]

which is broader but more confining the counter-ions inside the first neighbours shell. A direct evidence that the observed differences are not artifact of the experimental separation into partial factors can be obtained by rebuilding the total X-ray diffraction pattern from the theoretical $S_{ij}(k)$ and comparing it with the diffraction intensity data. As shown in fig. 37 clear differences are evident in the region of the peak of S_{MN} .

To get some physical insight in the discrepancy between the rigid ion potential and the real interactions in the system, we have to collect pieces of information from many related fields.

Quantum mechanical ab initio calculations for the alkali halides molecules [229] and solids [230] have shown that in this region of interionic distances, highly non linear deformations of the electronic shells take place.

It is well known that in the solid many body interactions do exist which are responsible of the violation of the Cauchy relations. Their presence was demonstrated theoretically by the Hartree-Fock calculations of Löwdin [231].

The lattice dynamics of the solid, and in particular the optical branches, cannot be successfully reproduced by a rigid ion potential. For this particular problem some of the many variations on the phenomenological shell model [232, 233] can achieve very close quantitative agreement with the measured phonon spectrum by allowing suitable deformations of the shells. This provides a many body interaction which is also able to explain the Cauchy relation violations.

In the case of molten alkali halides only the simplest shell model has been introduced in the computer simulation [234]. The resulting modifications of the $g_{ij}(r)$, respect the rigid ion situation, are minor as compared with the discrepancies with the experiments.

In particular no change has been seen in the region above the first peak of g_{+-} .

While new simulations with more sophisticated shell model could assess the possibility of a consistent modelling of both the solid and the liquid, it is important to try to extract more informations as possible from the existing experimental data.

Since the pioneering work of Johnson and March [235], many attempts have been done to get directly an effective pair potential from the experimental structural data by inverting the statistical mechanical (approximate) relations between the pair potential and the structure.

Many authors have claimed about reliable approximate schemes of "inversion" and have applied them to experimental structure factors for monocomponent systems [236]. Much less has been done for multicomponent systems and for molten salts we are aware of only one attempt in the past [237].

We have to note that any inversion scheme has to face with some important practical and theoretical problems:

1. With the integral equation theories the mathematical dependence of the pair potential from the $S(k)$ is not well conditioned. This means that small errors on the input data are magnified on the output. In other words, very precise experimental data are

required particularly at small angles.

2. The experimental data are given only inside a finite interval of wavenumbers; hence some extrapolation scheme is required to perform the necessary Fourier transforms.

3. In general the obtained pair potential can have only the meaning of an "effective" pair potential which is able to reproduce the starting structure but whose connection with thermodynamics is inconsistent with the formulas [1.16, 1.17] valid for a true pair potential.

Most of the existing works on the inversion problem have dealt with the problem of finding an efficient and stable algorithm. An obvious criterium of reliability is that the obtained pair potential, when used to calculate the structure factor, reproduces it at a reasonable extent. It is clear that the fulfilment of this request does not eliminate the problems related to the points 1-3. For these reasons it seems well beyond the present possibilities to carry out an inversion of the molten salts structures with quantitative confidence.

Nevertheless we have explored the potentialities of our MHNC scheme respect a less ambitious program of correlating some specific observed features of the short range order in the melts with gross features of the effective pair potentials.

We have used the consideration of point 3 as a qualitative gauge of the many body effects contained in the extracted potentials.

The reliability of the MHNC results and the observed weak sensitivity of the bridge functions $b_{\alpha\beta}(r)$ to reasonable changes in the pair potentials give us some confidence that our approximate MHNC equation with the same bridges evaluated for the MHNC solution with the

Fumi Tosi potential can be used to gain some qualitative information on the potential in the NaCl above 3 \AA .

We have therefore supplied to the incompleteness of the experimental data at small and large wavenumbers by making use of the theoretical ones. In practice we have done a double cross-over from the MHNC $S_{\alpha\beta}(k)$ to the experimental ones and then back to the MHNC smoothly interpolating with functions centered around 1 and 7 \AA^{-1} . Then we have Fourier inverted these "windowed" structure factors to get the $g_{\alpha\beta}(r)$ and $c_{\alpha\beta}(r)$.

We have checked the stability of this procedure to reproduce the main details of the experimental $g_{\alpha\beta}(r)$ by changing the positions, the shape and the functional form of these crossing functions. Within large limits we get the results shown in fig. 38 for the $g_{\alpha\beta}(r)$. The extracted "pair potentials" are shown in fig. 39 where the trivial Coulomb term has been subtracted.

We stress that these results can be viewed only as semiquantitative. However the oscillations above 3 \AA seem to have correlation with the previously discussed features of the experimental pair distribution functions.

In particular the cation-anion effective interaction shows an attractive part in the outer region of the first neighbour shell. It turns out to be larger by a factor 5 than the van der Waals attractive terms in the potential 4.1. These features, as compared with the previous discussion, strongly suggest that the effective pair potential reflects the many-body interactions originated from large electronic shell distortions.

We can have a partial check of the many body origin

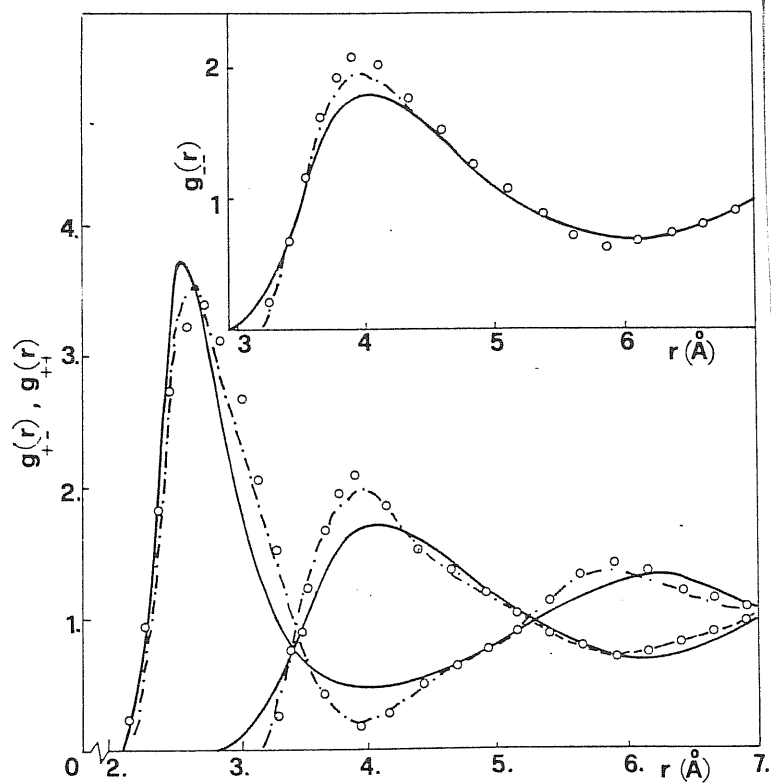


fig. 38. Pair distribution function in molten NaCl. Full curve: MHNC with the Tosi-Fumi potential 4.1; circles: experimental data; dashed curve: empirical $g_{ij}(r)$ constructed as described in the text.

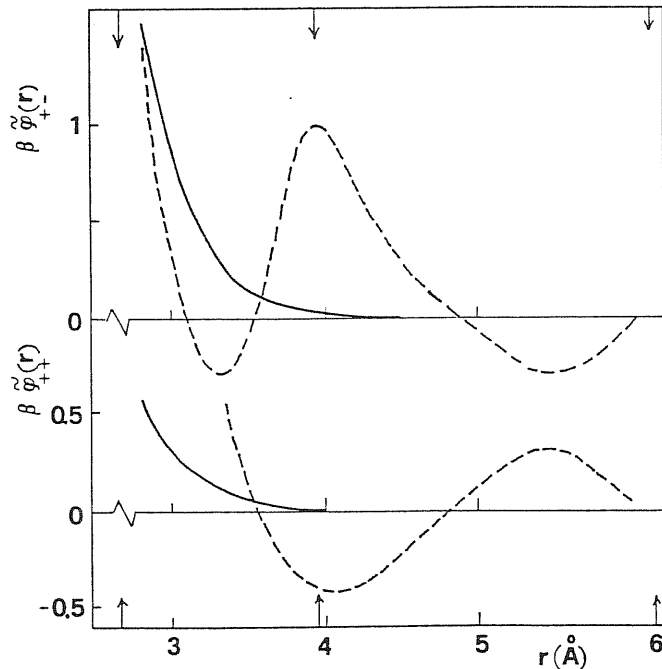


fig. 39. Effective short-range potential for NaCl (coulomb part subtracted). Full curve: Tosi-Fumi potential; dashed curve: inversion from the experimental data (see text). The arrows correspond to the positions of the first peak, first minimum and second peak of $g_{+-}(r)$.

of the obtained potential by treating it as a true two-body interaction and evaluating the internal energy through the formula 1.16. We find a shift of U by about 30 kJ/mol which is probably beyond the reasonable uncertainty that may be induced on this quantity from the uncertainty on the coefficient of 4.1.

A similar analysis on other systems for which experimental liquid structure of comparable quality is available (RbCl, CsCl) becomes more difficult since these systems are composed of more polarizable ions and a static-crystal-potential approach to the liquid structure yields progressively worse results. In any case the qualitative trends of the effective potentials seem to parallel those illustrated for NaCl.

The quantitative indication we get from this analysis is that in the liquid the main effects of many-body interactions are displayed in the range between 2 and 4 Å. It seems worth to try to properly take into account such indications in any attempt to improve the rigid-ion potentials introducing electronic polarization effects.

Finally we shall comment on our understanding of the structural properties of more complex salts as the divalent-cation dihalides. For many of them accurated neutron scattering experiments have been carried out (BaCl_2 [238], ZnCl_2 [239], CaCl_2 [240], SrCl_2 [241], MgCl_2 , MnCl_2 [242]). These systems have interesting physical behaviors below the melting point: BaCl_2 and SrCl_2 show a fast-ion conduction phase, the ZnCl_2 has a glassy state.

Looking at the experimental structure factors shown in fig.32, the most evident differences are in the relative shape of the cation-cation and anion-anion

structure factors. In particular BaCl_2 and SrCl_2 display the strongest correlations in the cationic component as reflected in the dominance of the main peak of its partial structure factor. There are strong indications that the relative disorder of the anions is connected with the super-ionic behavior observed in the solid [243].

The comparison of the experimental and the simulated correlation functions for Sr-Sr and the quite large distance of the first peak suggest their coulombic origin. In fig. 40. we have compared the simulated and the experimental $g_{\text{SrSr}}(r)$ and $S_{\text{SrSr}}(k)$ with an oversimplified model in which the anionic component has been reduced into a rigid neutralizing background. By using the MHNC theory for the DCP we have evaluated the $g(r)$ and $S(k)$ for $\Gamma=200$ (as determined directly from the temperature $T=1150^\circ\text{K}$, the density n and the double valence of Sr^{++}) and for $\Gamma=73$ which is the value obtained by screening the direct $\text{Sr}^{++}-\text{Sr}^{++}$ interaction with the electronic (high frequency) dielectric constant ($\epsilon=2.72$) [244].

The comparison is strongly suggesting that dielectric screening of the Sr-Sr coulombic repulsion is occurring in the molten SrCl_2 . Of course, while it is reasonable to use a dielectric constant at the large interionic separations of the peak of g_{SrSr} , a more detailed account of the spatial dependence of the screening properties required to deal with the real system.

The progressive qualitative changes going to CaCl_2 and ZnCl_2 , MgCl_2 , MnCl_2 and in particular the modifications of the relative strengths of the cation-cation and anion-anion correlations point to an increased importance of strong polarization effects or,

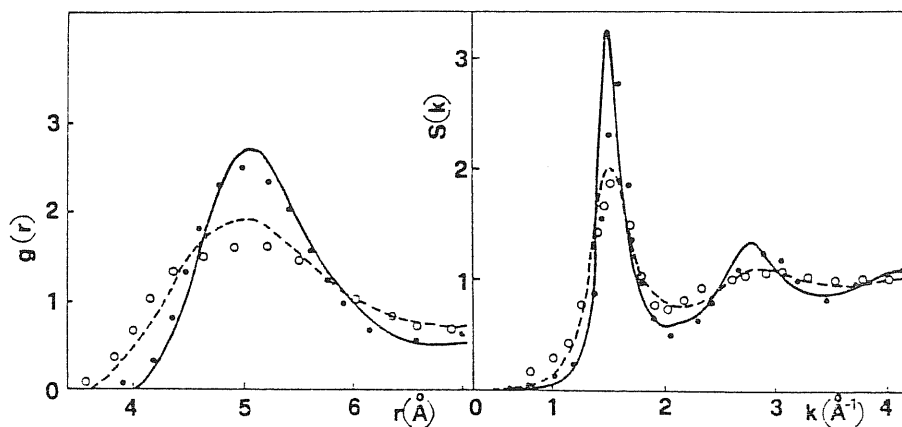


fig. 40. Pair distribution function $g(r)$ and structure factor $S(k)$ of a OCP at coupling $\Gamma = 200$ (full curve) and $\Gamma = 73$ (dashed). Dots: simulation data (DeLeeuw); circles: experiment [228] for the Sr-Sr correlations.

in chemical language, of a less ionic character of the bond. The modelling of the real interactions in these systems appears a formidable task but some qualitative insight in the structural implications of effective pair potentials can be gained by using simple HNC theory and reasonable simple model interactions. In particular model potentials which embody non-additivity effects of the excluded volumes would allow the modelling of the particular coordination properties of these systems.

APPENDIX A. Functional derivative relations.

If A^{exc} is the excess free energy functional connected to the grand partition function Ξ through

$$A = A^{exc} + A^{id} = -\log \Xi + \int d\mathbf{r}_i u(\mathbf{r}_i) \rho(\mathbf{r}_i)$$

$$\frac{\delta A^{exc}}{\delta \rho(\mathbf{r}_2)} = \log z(\mathbf{r}_2) + \log p(\mathbf{r}_2) = c^{(1)}(\mathbf{r}_2) \quad (u(\mathbf{r}_2) = \beta\mu - \beta\psi(\mathbf{r}_2))$$

and using in $c^{(2)}(1,2) = \frac{\delta c^{(1)}(1)}{\delta \rho(2)}$

$$c^{(2)}(1,2) = -\frac{1}{z(1)} \frac{\delta z(1)}{\delta \rho(2)} + \frac{1}{p(1)} \delta(\mathbf{r}_1 - \mathbf{r}_2)$$

hence

$$\frac{\delta \log z(1)}{\delta \rho(2)} = \frac{1}{p(1)} \delta(\mathbf{r}_1 - \mathbf{r}_2) - c^{(2)}(1,2)$$

From the identity

$$\int \frac{\delta p^{(1)}(1,4)}{\delta \log z(3)} \frac{\delta \log z(3)}{\delta p^{(1)}(2,4)} d\{3\} = \delta(\mathbf{r}_1 - \mathbf{r}_2)$$

and using 1.34 we have

$$\int \left\{ \frac{1}{p(3)} \delta(\mathbf{r}_3 - \mathbf{r}_2) - c^{(2)}(3,2) \right\} \left\{ p(1) \delta(\mathbf{r}_1 - \mathbf{r}_3) + \gamma_2(1,3) \right\} d\{3\} = \delta(\mathbf{r}_1 - \mathbf{r}_2)$$

from which

$$\frac{\gamma_2(1,2)}{p(2)} - p(1) c^{(2)}(1,2) - \int \gamma_2(1,3) c^{(2)}(3,2) = 0$$

i. e. at $\psi=0$, having $\gamma_2 = p^2 h(r)$, $c^{(2)} = c(r)$, $p(r) = p = \rho$ we get

$$h(r) = c(r) + \rho \int d\mathbf{r}' h(|\mathbf{r} - \mathbf{r}'|) c(r')$$

APPENDIX B. Diagrammatic definitions.

In order to make more clear the terminology we use and the connection with the diagrammatic methods we briefly introduce some definitions [58].

At low density we can usually expand the thermodynamic and structural properties of a fluid in powers of the density. The terms in the so obtained virial expressions, which are integrals of some functions, can be associated to some graphs. This allows a complete classification of the integrals in terms of their complexity as measured by the topological connectivity properties of the corresponding graphs. Moreover it is possible to develop methods of formal manipulation of series of graphs which simplify the resummation process.

A graph G of order p consists of a finite non empty set $V(G)$ of p points together with a specified set X of q unordered pairs of distinct points (no loop which connects a point to itself). It can be represented by a diagram in which points are represented by points or circles and the pairs by bonds between points.

A circle $f_j(r_j)$ will represent the function $f_j(r_j)$; a bond $\underline{F_x}$ is the graphical representation of a two-argument function $F_x(r_i, r_j)$. A diagram which is composed of white circles $f_1(r_1), \dots, f_m(r_m)$ and bonds $\underline{F_x}, \underline{F_0}, \dots$, etc. connecting circles =

$1/m! \{$ the sum of all the topologically different diagrams which one obtains from the given diagram by attaching coordinates r_{-m+1}, \dots, r_{-1} to the black circles in an arbitrary way $\}$. The total number of the diagrams appearing on the r.h.s. of the definition is given by

$m!/s$ where s is the symmetry number of the original diagram defined as the number of permutations of the coordinates of the black circles which do not lead to a topologically different diagram. Therefore we have that the previous diagram can be written as:

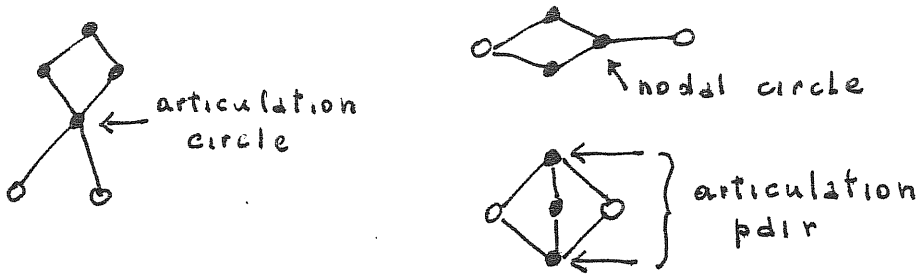
$1/s*\{$ any one of the diagrams which are obtained from the original one by attaching coordinates r_{-m1}, \dots, r_{-m+m} to the black circles in an arbitrary way $\}$.

A connected diagram is the diagram which contains at least two circles and in which there exists at least one path to reach any circle in the diagram from any other circle. In general a diagram will be composed of separate parts, each of which is a connected diagram or one circle.

n-fold connected diagram: it is a connected diagram in which there exist at least n independent paths to reach any circle from any other one.

Articulation circle (pair of circles): it is such a circle (pair of circles), in a connected diagram, that if one removes the circle (pair of circles) and, if exist, the bonds connecting them, the diagram divides into two or more separate parts such that at least one part contains no white circles.

Nodal circle: a black circle, in a connected diagram containing just two white circles, that if one removes it, the diagram divides into two or more separate parts in such a way that the two white circles are in different graphs.



Starting from these definitions, the virial series for the free energy, the one-particle density and the pair correlation function and some formal manipulation rules it is possible to derive an equation for $g(r)$ (see 1.40):

$$g(r) = e^{-\beta\phi(r) + h(r) - c(r) - b(r)}$$

where $c(r)$ and $b(r)$ have a functional definition as series of integrals over h functions. In particular $c(r)$ is connected to $g(r)$ through the diagrammatic equivalent of the OZ equation and for $b(r)$ we have the following definition:

$b(r) = \{$ sum of all the connected diagrams which are composed of two white circles O_{r_1}, O_{r_2} , black circles ρ_0 and bonds $h(r, r')$ and which have no articulation point, no nodal point and no articulation pairs of circles and in which the bond connecting O_{r_1} and O_{r_2} is not allowed to appear).

Some simple diagrams appearing in the definition of b are shown below.



We note that this set of diagrams is completely neglected in the HNC approximation and it is exactly the set of diagrams which are not simply evaluable (see note [45]).

The extension of all the previous results to multicomponent fluids is trivial: every two body function will have n more arguments which select the species of the particle at the positions $\underline{r}_1, \dots, \underline{r}_n$ and every integration has to be intended as an integration over the coordinates and a summation over the species.

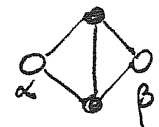
For example the OZ relations will hold


$$h_{\alpha\beta}(r) = c_{\alpha\beta}(r) + \sum_{\gamma} \rho_{\gamma} \int h_{\alpha\gamma}(r') c_{\gamma\beta}(r-r') d\underline{r}'$$

the relation

$$g_{\alpha\beta}(r) = \exp \left[-\beta \phi_{\alpha\beta}(r) + h_{\alpha\beta}(r) - c_{\alpha\beta}(r) - b_{\alpha\beta}(r) \right]$$

where

$$b_{\alpha\beta}(r) = \text{diagram} + \dots$$


$$\text{diagram} = -\frac{1}{2} \sum_{\delta} \rho_{\gamma} \rho_{\delta} \int d\underline{r}' \int d\underline{r}'' h_{\alpha\gamma}(r') h_{\alpha\delta}(r'') h_{\beta\gamma}(r-r') h_{\beta\delta}(r-r'') h_{\gamma\delta}(r'-r'')$$


APPENDIX C. Long wavelength behavior of the structure factor of the 2-D OCP.

Let us study the response of the system to an external field $V^{ext}(\underline{r})$: taking into account the polarization field induced, the equilibrium condition is:

$$qE^{\perp} - \nabla V^{ext} = \nabla \delta\mu \quad (1)$$

where q is the electric charge and $\delta\mu$ the shift of the chemical potential. From 1 and using $\delta\mu = \frac{\partial\mu}{\partial\rho}|_{T,A} \delta\rho$ (ρ is a number density and A the surface area) we get:

$$q \nabla E^{\perp} = \nabla^2 (V^{ext} + \frac{\partial\mu}{\partial\rho}|_{T,A} \delta\rho) = -q \nabla^2 \phi \quad (1')$$

since $\phi(r) = q \int \frac{\delta\rho(r')}{|r-r'|} d^2r'$ if $\delta\rho(r') = \delta\rho(x',y') \delta(z')$ $\tilde{\phi}(k, z=0) = \frac{2\pi q}{k} \delta\tilde{\rho}(k)$

and 1' becomes

$$q k^2 \tilde{\phi}(k) = 2\pi q^2 k \delta\tilde{\rho}(k) = -k^2 \left(\tilde{V}^{ext}(k) + \frac{\partial\mu}{\partial\rho}|_{T,A} \delta\tilde{\rho}(k) \right)$$

and solving for $\delta\tilde{\rho}(k)$

$$\delta\tilde{\rho}(k) = \frac{-k}{2\pi q^2 + \frac{\partial\mu}{\partial\rho}|_{T,A} \cdot k} \tilde{V}^{ext}(k)$$

Then the long-wavelength limit of the response function is

$$\chi(k) = \frac{-1}{\frac{2\pi q^2}{k} + \frac{\partial\mu}{\partial\rho}|_{T,A}}$$

and, through the fluctuation-dissipation theorem we have

$$S(k) = \frac{-\chi(k)}{\beta\rho} = \frac{1}{\frac{k_D}{k} + \beta\rho \frac{\partial\mu}{\partial\rho}|_{T,A}}$$

where k_D is the Debye wavelength.

APPENDIX D. Numerical solutions of the integral equations.

We illustrate in details the methods used to solve numerically the integral equations of the theory of liquids i.e. the coupled system of the Ornstein-Zernike equation

$$h_{ij}(r) = c_{ij}(r) + \sum_k \rho_k \int dr' h_{ik}(r') c_{kj}(r-r')$$

D. 1

and the closure which gives an other (approximate) relation between h_{ij} and c_{ij} .

In the following we shall discuss the HNC closure explicitly but many of the observations will hold also for other usual closures (MSA, PY etc); in particular the extension to the MHNC closure is trivial because the parametrized bridge functions enter as an extra pair interaction which is added to the true potential

The system we have to solve is then the D1 coupled with

$$h_{ij}(r) = \exp(-\beta \phi_{ij}(r) + h_{ij}(r) - c_{ij}(r)) - 1 \quad \text{D.2}$$

This system is highly non linear as it is evident by introducing the functions $\gamma_{ij} = h_{ij} - c_{ij}$ and rewriting the as

$$\gamma_{ij}(r) = \sum_k \rho_k \int dr' \left[\exp(-\beta \phi_{ik}(r') + \gamma_{ik}(r')) - 1 \right] \left[\exp(-\beta \phi_{kj}(r-r') + \gamma_{kj}(r-r')) - \gamma_{kj}(r-r') \right]$$

The existing numerical methods to solve D1, D2 can be collected in three main groups:

1. minimization
2. serial solution
3. iterative solution

The method 1 [245] is based on the existence of a derivation of the integral equations from an extremum condition from some suitable functional. For this method

the convergency difficulties often encountered in the other methods are not crucial but its main drawbacks can be summarized as follows:

a) it is not clear what is the characterization of the set of functions in which the minimum has to be found; the problem is far from being academic since these functionals can have deep unphysical minima in correspondence with unphysical correlation functions (for exemple $g_{ii}(r)$ or $S_{ii}(k)$ negative);

b) as usual in variational methods it is difficult to estimate sharply the distance from the minimum of an approximate solution;

c) good minimization routines are required but in any case already 8/10 parameters make the calculation heavy;

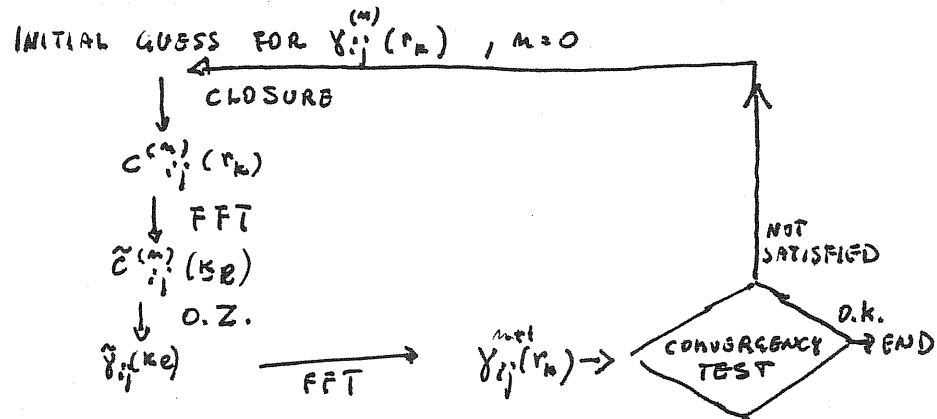
d) it is not easy to find a set of trial functions of simple evaluation and which give physical solutions also on the smallest subsets.

The method 2 [246] is based on a rewriting of D1 and D2 such that the solution can be found as a series of functions. Notwithstanding the claims of the authors about the stability properties of the algorithm, it has not been used in the literature but in the original papers.

The method 3 is by far the most used in the literature. Due to the almost unavoidable degree of instability of any algorithm of this kind, it is difficult to design a sufficiently efficient and robust implementation which does not require a careful control of the performances and results.

The main advantages of this methods are the availability of very fast and flexible algorithms and the possibility of getting an arbitrary large degree of accuracy. The possibility of fast algorithms hinges on

the acknowledgment that the the convolution integrals in D1 can be evaluated in a time which increases proportionally to $N \log N$ (where N is the number of mesh points), instead N^2 as in the simplest implementation, by using the fast fourier transform (FFT) techniques [247]. The iteration scheme is then



In the case of hard core potentials the $c_{ij}(r)$ are discontinuous (but not the $\gamma_{ij}^{(m)}$) and some care has to be put in the fourier transform from $c_{ij}(r)$ to $\tilde{c}_{ij}(k)$. In these cases it is sufficient to add a step function to eliminate the discontinuity in the numerical integrand and next the analytical transform of the step function from the numerical transform.

An other delicate point is the presence of long tail in the potential (as in the coulomb case). In this case also a suitable adding and subtracting of the asymptotic long-range tail allows a reasonable accuracy of the calculation.

The simplest and more accurate way is to use the functions $\beta e^{-\frac{1}{2}\alpha r} \operatorname{erf}(\alpha r)$ and their fourier transforms with a careful choice of α .

In the practical use the previous scheme does not converge until the input guess functions $\gamma_{ij}^0(r_m)$ are not very close to the final solution. The usual way to

cope with this instability is a "mixing" of old and new estimations for the functions γ to be put as input in the new iteration. The simplest one-step mixing is

$$\gamma_{input}^{(n)} = (1-\lambda) \gamma_{input}^{(n-1)} + \lambda \gamma_{output}^{(n-1)}$$

with $0 < \lambda < 1$. Usually very small values (10^{-3}) are required at the first iterations and after can be slowly increased. Automatic ways to fix the optimal choice of λ do exist. For example the Ng's method is based on the requirement that the "distance" between the mixed input and the result of the iteration is minimum relatively to λ . The method is simple to be implemented and very efficient but in some difficult cases (like for molten salts) it involved an extremely large number of iterations (up to 5000!) which can give unacceptable computer times and, more important, can introduce important round-off errors.

The best available algorithm has been developed by Gillan [248]. It is mainly a finite-element-weighted-residual method [249] in which the determination of the finite elements is done through the Newton-Raphson solution of the involved non-linear equations while the solution is refined through the iterative Picard method only on the (small) orthogonal complement to the element-projected part. The main idea is to project the functions $\gamma_{ij}(r)$ on a set of simple functions like the "rough" (or "hat") functions in such a way to decompose γ as

$$\gamma_{ij}(r) = \sum_{\alpha} a_{\alpha}^{ij} P_{\alpha}(x) + \Delta \gamma_{ij}(x)$$

At this point the D1, D2 system of equation for the a at fixed $\Delta \gamma_{ij}$ is solved using the Newton-Raphson method (whose convergency is quadratic) to get new a_{α}^{ij} . The result of the Picard iteration on the function $\gamma_{ij}'(r) = \sum_{\alpha} a_{\alpha}^{ij} P_{\alpha}(r) + \Delta \gamma_{ij}$ is decomposed again into a

projected part and a rest

$$\gamma_{ij}''(x) = \sum_{\alpha} b_{\alpha}'' P_{\alpha}(x) + \Delta \gamma_{ij}'(x)$$

new b_{α}'' are obtained from the equations D1, D2 at fixed $\Delta \gamma_{ij}'$ and the procedure is continued up convergency respect both the projected part and the rest.

The method has an impressive stability which implies also a small (up to two order of magnitude) number of total iterations to get convergency and a small dependency on the quality of the initial guess for $\gamma_{ij}^0(r)$. The main drawback is in the longer man-time required for the practical implementation of the algorithm.

We add some comments on the typical values of the numerical parameters used in this kind of calculation. The number of mesh points is between 512 and 4096 the lowest limit being suggested by precision requirements and the upper one being connected to the storage and computer time limitations. With these numbers of points a typical range for the direct space range is $10 \div 100a$ where a is the ion sphere radius ($k \frac{\pi a^3}{3} = \frac{1}{\rho}$). The usage of the FFT implies that the k -space mesh is fixed by N and $\delta r : \delta k = 2\pi \delta r / N$.

Finally we further stress that the occasional convergency of the iterations to unphysical situations (negative $S(k)$) requires a constant control of the results.

APPENDIX E. Ionic structure factor in the EIP model.

At the simplest level of approximation the electron-ion interaction is described by a model-potential $V_{ei}(r)$ that is supposed sufficiently weak to be treated at the lowest order in the perturbations. An ionic fluctuation of density

$\rho_i(k, \omega)$ is viewed by the electrons as the source of an external perturbation. The induced density is

$$\rho_e(k, \omega) = \chi_e(k, \omega) V_{ei}(k) \rho_i(k, \omega) \quad |$$

where $\chi_e(k, \omega)$ is the electronic linear response function. It is related to the dielectric function through

$$\frac{1}{\epsilon(k, \omega)} = 1 + \frac{4\pi e^2}{k^2} \chi_e(k, \omega)$$

The adiabatic approximation is equivalent to take for $\chi_e(k, \omega)$ its static value $\chi_e(k)$.

If the ionic fluctuation of density is induced by an external potential $V_i^{ext}(k, \omega)$ coupled to the ions, we can describe the response of the electronic and ionic component as:

$$\rho_i(k, \omega) = \chi_i(k, \omega) V_i^{ext}(k, \omega)$$

$$\rho_e(k, \omega) = \chi_{ei}(k, \omega) V_i^{ext}(k, \omega)$$

and comparing with | we find

$$\chi_{ei}(k, \omega) = \chi_e(k) V_{ei}(k) \chi_i(k, \omega)$$

We can also consider the ionic density fluctuation as the response of a bare ionic plasma to an internal potential due to the external V_i^{ext} and to some polarization term due to the electrons:

$$\rho_i(k, \omega) = \chi_i^0(k, \omega) \left[V_i^{ext}(k, \omega) + V_{ei}(k) \rho_e(k, \omega) \right]$$

from which we obtain

$$\chi_i(k, \omega) = \frac{\chi_i^0(k, \omega)}{1 - V_{ei}^2 \chi_e \chi_i^0(k, \omega)}$$

or from the fluctuation and dissipation theorem

$$S(k) = \frac{S_0(k)}{1 + \beta \rho \tilde{\chi}(k) S_0(k)}$$

where

$$\tilde{\chi}(k) = \frac{V_{e_i}^2(k)}{\frac{4\pi e^2}{k^2}} \left(\frac{1}{\epsilon(k)} - 1 \right)$$

APPENDIX F. Numerical implementation of the ORPA.

We have worked directly with the minimization of the functional F respect the parameters q, s, c . We have used a standard library routine for the search of the minimum (MINUIT [250]).

Some care has to be put in the evaluation of the analytical fourier transform of the optimization function particularly at small wavenumbers, due to the large cancellations between large terms. Let us write

$$\Delta u(r) = \vartheta(\sigma-r) \left\{ q - s \left(1 - \frac{r}{\sigma}\right) + \left(1 - \frac{r}{\sigma}\right)^2 \sum_n c_n P_n \left(\frac{2r}{\sigma} - 1\right) \right\}$$

where the parameters q and s collect all the discontinuity at σ of the function and of its first derivative. We have

$$\Delta \tilde{u}(k) = \frac{4\pi}{k} \int_0^\sigma \Delta u(r) r \sin kr dr = \frac{4\pi\sigma^2}{k} \left\{ q j_1(k\sigma) - s \Sigma(k\sigma) + \sum_n c_n \Theta_n(k\sigma) \right\}$$

$$\text{where } \Sigma(k\sigma) = \frac{\sin k\sigma}{(k\sigma)^2} - \frac{\cos k\sigma}{k\sigma} - \left[\frac{2}{(k\sigma)^2} \sin k\sigma + \left(\frac{2}{(k\sigma)^3} - \frac{1}{(k\sigma)} \right) \cos k\sigma - \frac{2}{(k\sigma)^3} \right]$$

$$\text{and } \Theta_n(x) = \frac{1}{16} \left\{ \sin \frac{x}{2} \operatorname{Re} \mathcal{L}_n \left(\frac{x}{2} \right) + \cos \frac{x}{2} \operatorname{Im} \mathcal{L}_n \left(\frac{x}{2} \right) \right\}$$

$$\mathcal{L}_n(a) = \int_{-1}^1 (1-\xi-\xi^2+\xi^3) P_n(\xi) e^{ia\xi} d\xi \quad 1$$

from which, after some tedious algebra we get the explicit formulas:

$$\begin{aligned} \mathcal{L}_n(a) = & \frac{(n+3)(n+2)(n+1)}{(2n+5)(2n+3)(2n+1)} E_{n+3}(a) - \frac{(n+2)(n+1)}{(2n+3)(2n+1)} E_{n+2}(a) + \\ & + \left[\frac{(n+1)(n+2)^2}{(2n+5)(2n+3)(2n+1)} + \frac{(n+1)^3}{(2n+3)(2n+1)^2} + \frac{(n+1)n^2}{(2n+1)^2(2n-1)} - \frac{n+1}{2n+1} \right] E_{n+1}(a) + \\ & + \left[1 - \frac{(n+1)^2}{(2n+3)(2n+1)} - \frac{n^2}{(2n+1)(2n-1)} \right] E_n(a) + \left[\frac{(n+1)^2 n}{(2n+3)(2n+1)^2} + \frac{n^3}{(2n+1)^2(2n-1)} + \frac{n(n-1)}{(2n+1)(2n-1)(2n-3)} - \frac{n}{2n+1} \right] E_{n-1}(a) + \\ & - \frac{n(n-1)}{(2n+1)(2n-1)} E_{n-2}(a) + \frac{n(n-1)(n-2)}{(2n+1)(2n-1)(2n-3)} E_{n-3}(a) \end{aligned}$$

and

$$E_n(a) = \begin{cases} \frac{q \eta a}{a} \sum_{k=0}^{n/2} \frac{(-1)^k}{a^{2k}} P_n^{2k} + \frac{2 \cos a}{a} \sum_{k=1}^{n/2} \frac{(-1)^{k-1} P_n^{2k-1}}{a^{2k-1}} & \text{for } n \text{ even} \\ -2i \frac{\cos a}{a} \sum_{k=0}^{(n-1)/2} \frac{(-1)^k}{a^{2k}} P_n^{2k} + 2i \frac{\eta a}{a} \sum_{k=1}^{(n+1)/2} \frac{(-1)^{k-1} P_n^{2k-1}}{a^{2k-1}} & \text{for } n \text{ odd} \end{cases}$$

$$P_n^m = \frac{1}{2^m} \frac{(n+m)!}{m!(n-m)!}$$

From 1 we can derive the small k expansion of $\Delta u(k)$:

$$\Delta u(k) \sim U + U'' k^2 + U^{IV} k^4 + O(k^6)$$

where

$$U = 4\pi r^3 \left\{ \frac{q}{3} - \frac{s}{12} + \frac{c_0}{30} - \frac{c_2}{105} + \frac{c_4}{360} \right\}$$

$$U'' = 4\pi r^3 \left\{ -\frac{q}{30} + \frac{s}{180} - \frac{c_0}{630} - \frac{c_1}{2520} + \frac{c_2}{2520} + \frac{c_3}{3780} - \frac{c_4}{4480} - \frac{c_5}{16632} - \frac{c_6}{720+2} \right\}$$

$$U^{IV} = 4\pi r^3 \left\{ \frac{q}{840} - \frac{s}{6720} + \frac{c_0}{30240} + \frac{c_1}{75600} - \frac{c_2}{20+900} + \frac{c_3}{1663200} - \frac{c_4}{393120} + \frac{c_5}{1081080} + \frac{c_6}{1140} \right\}$$

U and U'' are exact while in U^{IV} the contributions up to the 6-th Legendre polynomial have been included.

For the quadrature, an optimized gaussian integration [251] has been used to have a constant precision in the evaluation of the functional.

We have looked for the minimum of F_{RPA} inside a relative precision of 10^{-5} increasing progressively the number of coefficients until the maximum deviation from zero inside the core is few percent of the height of the peak of $g(r)$ and the variation of the height of the peak of $S(k)$ is smaller than the 1%. Up to six parameters are sufficient to guarantee this precision.

A problem which is often encountered in every ORPA calculation, also with the hard sphere reference system, is related to the presence of values of the coefficients q, s, c_m for which the structure assumes unphysical values ($1 - \rho c(k) < 0$) and the RPA functional is not defined. The

problem is important because the same RPA ($q=s=c_w=0$) corresponds to such catastrophic situation for some thermodynamic state. Moreover, also starting from a "physical point", it can happen that the search for the minimum goes through the unphysical region. To avoid this problem we have introduced a penalty function method: the integrand has been redefined as

$$\begin{cases} \beta p \bar{v}(k) S_0(k) - \log \{ S_0(k) (1 - p \bar{E}(k)) \} & \text{if } 1 - p \bar{E}(k) > 0 \\ 10^6 & \text{if } 1 - p \bar{E}(k) < 0 \end{cases}$$

in such a way that unphysical points have to pay an extremely high contribution to the integral. The method, extremely simple and very efficient, has worked well for all the calculations we have done.

APPENDIX G. Evaluation of $B_4(\tau)$.

We have used the Legendre polynomial expansion method employed by Bacquet and Rossky [221] or Iyetomi and Ichimaru [111]: three of the five pair correlation functions which appear in the integrand have been expanded as

$$h_{ij}(r_{23}) = \sum_{b=0}^{\infty} A_b^{ij}(r_{12}, r_{13}) P_b(\cos \vartheta_{123})$$

and using the orthonormality of the Legendre polynomials we end with

$$b_{ij}^4(r_{12}) = -\frac{1}{2} n^2 \sum_{k,e} x_k x_e \int_0^{\infty} \int_0^{\infty} \int_0^{\infty} dr_{13} dr_{14} r_{13}^2 r_{14}^2 h_{ik}(r_{13}) h_{ie}(r_{14}) A_b^{kj}(r_{12}, r_{13}) A_b^{li}(r_{12}, r_{14}) A_b^{ke}(r_{13}, r_{14})$$

The integrals are numerically evaluated using the Simpson's rule and up to 400 points and checking the sensitivity to the upper limit truncation. We evaluated the contributions up $b=6$ but $b=4$ is already sufficient to give a reasonable precision.

Typical computer times on the GOULD 32/97 computer of the SISSA/ICTP Computer Centre are about 1 hour of CPU for the full $b_{ij}^4(\tau)$.

BIBLIOGRAPHY

REFERENCES.

- 1 P. Ballone, G. Pastore, M. Rovere, M. P. Tosi, J. Phys. C 18, 4011 (1985); P. Ballone, G. Pastore, M. Rovere, M. P. Tosi, in "Festkoerper Probleme XXV.
- 2 G. Pastore, P. V. Giaquinta, J. S. Thakur, M. P. Tosi, J. Chem. Phys. (1985)
- 3 G. Pastore, G. Senatore, M. P. Tosi, Physica B111, 283 (1981)
- 4 G. Pastore, M. P. Tosi, Physica B124, 383 (1984)
- 5 P. Ballone, G. Pastore, M. P. Tosi, J. Phys. C 17, L333 (1984)
- 6 P. Ballone, G. Pastore, M. P. Tosi, J. Chem. Phys. 81, 3174 (1984)
- 7 G. Pastore, P. Ballone, M. P. Tosi, J. Phys. C (1985)
- 8 G. P. Malescio, G. Pastore, P. Ballone, M. P. Tosi, Phys. Chem. Liq. 15, 31 (1985)
- 9 P. Ballone, G. Pastore, J. S. Thakur, M. P. Tosi unpublished
- 10 P. A. Egelstaff "An Introduction to the Liquid State" (Academic Press, London, 1967) J. A. Barker, D. Henderson, Rev. Mod. Phys. 48, 587 (1976); D. Henderson ed. "Physical Chemistry. An advanced treatise" Vol VIII A (Academic Press, London, 1971); N. H. March, M. P. Tosi "Atomic Dynamics in Liquids" (McMillan Press Ltd., London 1976); N. H. March, M. P. Tosi, "Coulomb Liquids" (Academic Press, London, 1984); H. N. V. Temperley, J. S. Rowlinson, G. S. Rushbrooke "Physics of Simple Liquids" (North Holland Co., Amsterdam 1968); J. P. Hansen, I. R. McDonald, "Theory of Simple Liquids" (Acad. Press, London 1976).
- 11 Ref. 10 and more specifically J. R. D. Copley, S. W. Lovesay, Rep. Prog. Phys. 38, 461 (1975); K. Furukawa Rep. Prog. Phys. 25, 395 (1962)
- 12 P. C. Martin, in "Probleme a N corps. Many-Body Physics" ed. by C. DeWitt, R. Balian (Gordon and Breach, NY 1968)p. 37;
- 13 D. Forster "Hydrodynamic Fluctuations, Broken Symmetry and Correlation Functions" (Benjamin Inc., Reading 1975);
- 14 R. Kubo, Rep. Progr. Phys. 29, 255 (1966);
- 15 L. van Hove, Phys. Rev. 95, 249 (1954)
- 16 J. E. Enderby, P. A. Egelstaff, D. M. North, Phil. Mag. 14, 961 (1966)
- 17 See for example the review paper by J. E. Enderby, J. Phys. C15, 4609 (1982) and references therein contained or R. L. McGreevy, E. W. J. Mitchell, J. Phys. C15, 5537 (1982)
- 18 Y. Waseda, K. Hirata, Bull. Res. Inst. Min. Met. Tohoku University 31, 8 (1975)
- 19 Y. Waseda, S. Tamaki, Phil. Mag. 32, 951 (1975); J. Phys. F7, L151 (1977).

20 Y. Waseda, "Novel Applications of Anomalous (Resonance) X-ray Scattering for Structural Characterization of Disordered Materials" Lecture Notes in Physics 204 (Springer-Verlag, Berlin, 1984)

21 F. Paasche, H. Olbrich, G. Rainer-Harbach, P. Lamperter, S. Steeb, Z. Natur. 37a, 1215 (1982)

22 P. A. Egelstaff, N. H. March, N. C. McGill, Can. J. Phys. 52, 1651 (1974)

23 P. J. Dobson, J. Phys. C11, L295 (1978); M. Johnson referred in N. H. March, M. P. Tosi, Phys. Chem. of Liq. 10, 211 (1980); S. Takeda, S. Tameki, Y. Waseda, J. Phys. Soc. Jpn. 54, 2552 (1985)

24 H. Olbrich, H. Ruppertsberg and S. Steeb, Z. Naturforsch. 38a, 1328 (1983) report negative evidence of significant discrepancies between n and X for Li; moreover by updating the experimental data used by Egelstaff et al. with more recent ones their conclusions, strongly based on the heights of the first peak of $S(K)$, become weaker.

25 W. van der Lugt, ref(33) and private communication

26 M. J. Huijben, W. van der Lugt, Acta Cryst. A35, 431 (1979)

27 A. J. Greenfield, J. Wellendorf, N. Wiser, Phys. Rev. A4, 1607 (1971)

28 See e.g. N. W. Ashcroft, N. D. Mermin, Solid State Physics, (Holth, Rinehart, Winton, N. Y. 1976)

29 "EXAFS and Near Edge Structure" Ed. A. Bianconi, L. Incoccia, S. Stipcich, (Springer-Verlag Berlin 1983); "EXAFS Spectroscopy. Techniques and Applications" Ed. B. K. Teo, D. C. Joy (Plenum N. Y. 1981).

30 See further discussion in Ch. 2 about the 2-D systems.

31 See e.g. discussion in J. P. Hansen, I. R. McDonald, "Theory of Simple Liquids" ref (17), p. 200-206.

32 J. G. Kirkwood, J. Chem. Phys. 3, 300 (1935)

33 D. Levesque Physica 32, 1985 (1966)

34 See e.g. D. Ruelle "Statistical Mechanics" (Benjamin Inc., Reading 1969)

35 L. S. Ornstein, F. Zernike, Proc. Akad. Sci. (Amsterdam) 17, 793 (1914) F. Zernike, Proc. Akad. Sci. (Amsterdam) 18, 1520 (1916) reprinted in "The equilibrium Theory of Classical Fluids" Ed. H. L. Frish and J. L. Lebowitz (Benjamin Inc. N. Y. 1964) part III p. 3, 18.

36 J. P. Hansen, I. R. McDonald ref(17) and R. K. Pathria "Statistical Mechanics" Pergamon Press, Oxford 1972.

37 A. B. Bathia, D. E. Thornthon, Phys. Rev. B2, 3004 (1970)

38 The partial structure factors we are using are defined via 1.4 as $S_{\alpha\beta}(k) = k_B T \langle n_{\alpha}(k) n_{\beta}(-k) \rangle / \sqrt{\rho_{\alpha} \rho_{\beta}}$

39 See the related discussion in A. Weyland, Physica 113A, 77

(1982); A. Weyland, Phys. Lett. A93, 81 (1982).

40 F. H. Stillinger, R. Lovett, J. Chem. Phys. 48, 3858 (1968)

41 D. J. Mitchell, D. A. McQuarrie, A. Szabo, J. Groeneweld
J. Stat. Phys. 17, 15 (1977)

42 See L. Verlet, Phys. Rev. 165, 201 (1968) and G. Stell in
"Statistical Mechanics" Ed. Berne (Plenum, N.Y. 1982)

43 A justification of 1.27 is that it is exact (for the whole range) for weak interactions (see p. 26) then its physical meaning is that distant particles have to interact weakly and this is reasonable far from the critical point.

44 T. Morita, Progr. Theor. Phys. 20, 920 (1958); J. M. J. van Leeuwen, J. Groeneweld, J. de Boer, Physica 25, 192 (1959); T. Morita, K. Hiroike, Progr. Theoret. Phys. (Kyoto) 23, 1003 (1960); E. Meeron, J. Math. Phys. 1, 192 (1960); G. S. Rushbrooke, Physica 26, 259 (1960); L. Verlet, Nuovo Cimento 18, 77 (1960);

45 Actually the HNC approximation can be characterized from a computational point of view as the sum of the terms of the virial series which includes all and only those terms which can be evaluated using some calculating device, such a digital computer, which can only integrate over the coordinates of one particle at a time and which can only store one or two particle functions. (See for ex. R. J. Baxter, Ann. of Phys. 46, 509 (1968))

46 See e.g. N. N. Bogolyubov in "Studies in Statistical Mechanics" Ed. J. DeBoer, G. E. Uhlenbeck, vol. 1 (Amsterdam 1962) pag. 1. and for a more detailed and formal discussion: G. Stell in "Phase Transitions and Critical Phenomena" Ed. C. Domb, M. S. Green (Academic Press, London 1976) pag. 205.

47 S. W. Gibbs, "Elementary Principles in Statistical Mechanics" (Reprinted by Dover Publ. Inc. N. Y. 1960) theorem III pag 131; the result can be extended to quantum statistical mechanics as in N. D. Mermin, Phys. Rev. 137, A1441 (1965)

48 cfr. Stell or Baxter or J. K. Percus in H. L. Frisch, J. L. Lebowitz ref. 49.

49 J. K. Percus, Phys. Rev. Lett. 8, 462 (1962) and in "The Equilibrium Theory of Classical Fluids", (Benjamin Inc. N. Y. 1964) part II, p. 33; L. Verlet, Physica 32, 304 (1966)

50 The derivation follows that in H. Iyetomi, Progr. Theor. Phys. 71, 427 (1984)

51 for diagrammatic expansion techniques, besides Hansen McDonald: R. Abe, J. Phys. Soc. of Japan 14, 10 (1959); A. Munster, "Statistical Thermodynamics", Ch. X (Springer, Berlin 1969); T. Morita, K. Hiroike, Progr. Theor. Phys. 23, 1003 (1960); H. C. Andersen in Berne (ref. [52]); T. Morita, K. Hiroike, Progr. Theor. Phys. 25 537 (1961); T. Morita, Progr. Theor. Phys. 23, 829 (1960); V. Balescu, "Equilibrium and Non-equilibrium Statistical Mechanics" (Wiley Int., NY 1975); I. R. McDonald, S. P. O'Gorman, Phys. Chem. Liq. 8, 57 (1978); G. Stell in ref [49].

52 B. J. Berne Ed: "Statistical Mechanics", Plenum Press N. Y. 1977; K. Binder Ed.: "Monte Carlo Methods in Statistical

Mechanics", Topics in Current Physics v. 7 Springer-Verlag, Berlin 1979; K. Binder Ed.: "Applications of MonteCarlo Methods in Statistical Mechanics" Topics in Current Physics v. 36 Springer-Verlag, Berlin 1984.

53 M. Kac, G. E. Uhlenbeck, P. C. Hemmer, J. Math. Phys. 4, 216 (1963); VanKampen, Phys. Rev. 135, 362 (1964); J. L. Lebowitz, D. Penrose, J. Math. Phys. 7, 98 (1966)

54 N. W. Ashcroft, J. Lekner, Phys. Rev. 145, 83 (1966)

55 L. Verlet, Phys. Rev. 163, 201 (1968)

56 One possible empirical definition of simple liquids hinges on the degree of qualitative similarity between the measured $S(k)$ and the hard spheres one.

57 See e. g. D. Henderson, J. A. Barker in "Physical Chemistry. An Advanced Treatise" vol. VIIIA (Academic Press, London 1971) p. 377

58 J. D. Weeks, D. Chandler, H. C. Andersen, J. Chem. Phys. 54, 5237 (1971)

59 R. Zwanzig, J. Chem. Phys. 22, 1420 (1954) B. Hafskjold, G. Stell, in "The Liquid State of Matter" E. W. Montroll, J. L. Lebowitz Ed. (North Holland Co. 1982) p. 175;

60 D. Chandler, J. D. Weeks, Phys. Rev. Lett. 25, 149 (1970)

61 J. D. Weeks, D. Chandler, H. C. Andersen, J. Chem. Phys. 54, 5237 (1971); Ibid. 55, 5421 (1971)

62 H. C. Andersen, D. Chandler, J. Chem. Phys. 53, 547 (1970)

63 H. C. Andersen, J. D. Weeks, D. Chandler, Phys. Rev. A4, 1597 (1971)

64 D. Chandler, H. C. Andersen, J. Chem. Phys. 54, 26 (1971)

65 H. C. Andersen, D. Chandler, J. Chem. Phys. 55, 1497 (1971)

66 H. C. Andersen, D. Chandler, J. D. Weeks, J. Chem. Phys. 56, 3812 (1972)

67 H. C. Andersen, D. Chandler, J. Chem. Phys. 57, 1918 (1972)

68 H. C. Andersen, D. Chandler, J. D. Weeks, J. Chem. Phys. 57, 2626 (1972)

69 H. C. Andersen, D. Chandler, J. D. Weeks, Adv. Chem. Phys. 34, 105 (1975)

70 G. Stell, J. J. Weis, Phys. Rev. A21, 645 (1980)

71 An useful introduction can be found in R. D. Watts in "Statistical Mechanics. A Specialist Periodical Report" (The Chemical Society, London 1973) p. 1.

72 J. K. Percus, G. J. Yevick, Phys. Rev. 110, 1 (1958); G. Stell, Physica 29, 517 (1963)

73 The first appearance of the RHNC eqns is in F. Lado, Phys. Rev. 135, 1013A (1964)

74 L. L. Lee, J. Chem. Phys. 62, 4436 (1976)

75 D. McGowan, Phys. Lett. A76, 264 (1980)

76 The MSA was introduced in J. K. Percus, G. J. Yevick, Phys. Rev. 136, B290 (1964); J. L. Lebowitz, J. K. Percus, Phys. Rev. 144, 851 (1966). It is expressed by 1.59 disregarding if the actual potential has or not a hard core. This implies that for soft potentials the region around will be particularly inaccurate. To improve on the drawbacks of MSA many authors have tried to modify 1.59 using the Percus-Yevick closure inside. See e.g. A. H. Narten, L. Blum, R. H. Fowler, J. Chem. Phys. 60, 3378 (1974); W. G. Madden, S. A. Rice, J. Chem. Phys. 72, 4208 (1980). In some cases this form of MSA seems to give better results but more investigations would be necessary to assess this point. Moreover a different name would generate less confusion since this MSA has a different structure than the usual (for example no analytical solution is known).

77 See appendix D for details about the solution methods.

78 MSA analytical solutions and related methods can be found in: M. S. Wertheim, J. Math. Phys. 5, 643 (1964); J. L. Lebowitz, Phys. Rev. 133, A815 (1964); R. J. Baxter, J. Chem. Phys. 52, 4550 (1970); P. J. Leonard, D. Henderson, J. A. Baxter, Mol. Phys. 21, 107 (1971); W. R. Smith, D. Henderson, Mol. Phys. 19, 411 (1970); J. W. Perram, Mol. Phys. 30, 1505 (1975); K. Hiroike, J. Phys. Soc. Jpn. 27, 1415 (1969); J. L. Lebowitz, O. Zomick, J. Chem. Phys. 54, 3335 (1972); D. Penrose, J. L. Lebowitz, J. Math. Phys. 13, 604 (1972); for hard spheres and their mixtures. P. T. Cummings, J. Phys. F9, 1477 (1979) for oscillating Yukawian potential. E. Waisman, J. L. Lebowitz, J. Chem. Phys. 56, 3086 (1972); L. Blum, Mol. Phys. 30, 1529 (1975); M. Parrinello, M. P. Tosi, Chem. Phys. Lett. 64, 579 (1979); K. Hiroike, Mol. Phys. 33, 1195 (1977); L. Blum, J. S. Hoye, J. Phys. Chem. 81, 1311 (1977); for charged hard spheres and their mixtures with and without neutralizing background. L. Blum, J. Stat. Phys. 24, 661 (1980); E. R. Smith, Mol. Phys. 38, 823 (1979); for Yukawa-like potentials.

79 W. Olivares, D. A. McQuarrie, J. Chem. Phys. 65, 3604 (1976)

80 See e.g. M. S. Wertheim, J. Math. Phys. 8, 927 (1967); L. Verlet, Physica 30, 95 (1964); ibidem 31, 959 (1965); L. Verlet, D. Levesque, ibidem 36, 254 (1967) and the RHNC of Lado ref. [73].

81 (TC) P. Hutchinson, W. R. Conkie, Mol. Phys. 21, 881 (1971); ibidem 24, 567 (1972). F. J. Rogers, D. A. Young, Phys. Rev. A30, 999 (1984) (MHNC); Y. Rosenfeld, N. W. Ashcroft, Phys. Rev. A20, 1208 (1979)

82 J. S. Hoye, J. L. Lebowitz, G. Stell, J. Chem. Phys. 61, 3253 (1974) J. S. Hoye, G. Stell, J. Chem. Phys. 67, 524 (1977)

83 The functional form Yukawa-like is partly constrained by the requirement of maintaining the possibility of analytical solution (i.e. the allowed forms should be Yukawian or exponentials) and partly, in the case of hard sphere or Coulomb potentials, it is suggested by density gradient expansion results for the asymptotic behavior of $h(r)$ (M. Fisher, J. Math. Phys. 6, 1643 (1965)).

84 L. Verlet, J. J. Weis, Phys. Rev. A5, 937 (1972);

- D. Henderson, G. W. Grunke, J. Chem. Phys. 63, 601 (1975)
- 85 S. M. Foiles, N. W. Ashcroft, L. Reatto, J. Chem. Phys. 80, 4441 (1984)
- 86 F. Lado, J. Chem. Phys. 59, 4830 (1973) F. Lado, Phys. Lett. 89A, 196 (1982)
- 87 J. P. Hansen, G. Zerach, Phys. Lett. 108A, 277 (1985)
J. Wiechen, J. Phys. C18, L717 (1985)
- 88 B. Jancovici, Phys. Rev. Lett. 46, 386 (1981)
- 89 D. J. Stevenson, E. E. Salpeter, Ap. J. 35, 221 (1977);
ibidem 35, 239 (1977)
- 90 L. Mestel, M. A. Ruderman, Mon. Not. R. Astr. Soc. 136, 27 (1967);
H. M. Van Horn, Ap. J. 151, 227 (1968)
- 91 G. Baym, C. Pethick, Ann. Rev. Nucl. Sci. 25, 27 (1975)
- 92 M. Baus, J. P. Hansen, Phys. Rep. 59, 1 (1980)
- 93 E. H. Lieb, N. Narnhofer, J. Sta. Phys. 12, 291 (1975)
- 94 P. Vieillefosse, J. P. Hansen, Phys. Rev. A12, 1106 (1975)
- 95 The first Monte Carlo study of the DCP was undertaken by S. G. Brush, H. L. Sahlin, E. Teller, J. Chem. Phys. 45, 2102 (1966). In that paper the superiority of the Ewald method on other possible way of computing the configurational energy was assessed. More precise calculations were done by J. P. Hansen, Phys. Rev. A8, 3096 (1973); E. L. Pollock, J. P. Hansen, Phys. Rev. A8, 3110 (1973); D. M. Ceperley, G. V. Chester, Phys. Rev. A15, 755 (1977). A further improvement on the precision is in the studies of W. L. Slattery, G. D. Doolen, H. E. DeWitt, Phys. Rev. A21, 2087 (1980); ibidem A26, 2255 (1982).
- 96 See appendix D;
- 97 J. F. Springer, M. A. Pokrant, F. A. Stevens, J. Chem. Phys. 58, 4863 (1973);
- 98 K. Ng, J. Chem. Phys. 61, 2680 (1974)
- 99 R. G. Palmer, J. D. Weeks, J. Chem. Phys. 58, 4171 (1973)
- 100 See for example McGowan, J. Stat. Phys. 32, 123 (1983)
- 101 M. J. Gillan, J. Phys. C 7, L1 (1974); Y. Rosenfeld, J. Phys. C15, L125 (1982); R. G. Palmer, J. Chem. Phys. 73, 2009 (1980); V. DeAngelis, A. Forlani, M. Giordano, J. Chem. Phys. C13, 3649 (1980)
- 102 J. P. Hansen, ref. 95
- 103 W. L. Slattery, G. D. Doolen, H. E. DeWitt, Phys. Rev. A26, 2255 (1982) other fitting formulas can be found in the ref. [95], while tentative explanations of the dependence of the internal energy are in H. E. DeWitt, Phys. Rev. A14, 1290 (1976) and H. E. DeWitt, Y. Rosenfeld, Phys. Lett. 75A, 79 (1979).
- 104 Estimated as standard deviations of subsets of the complete runs.
- 105 K. Ng, ref [98] ; H. Iyetomi, S. Ichimaru, Phys. Rev. A27, 1734 (1983) and H. E. DeWitt, private communication.

- 106 H. E. DeWitt, private communication.
- 107 D. K. Chaturvedi, G. Senatore, M. P. Tosi, N. Cimento 62B, 375 (1981)
- 108 The GMSA as developed in [107] has two main related problems: the theory is not self-contained because it requires the external information on the equation of state and for Γ smaller than some value around 20 (the exact value depends on the fitting formula used for the equation of state) there is no more solution to the equations. The solution is lost in the same region of coupling in which the differences between the Monte Carlo $g(r)$ and $g_{GMSA}(r)$ become large. At the same time this region of distances becomes more important for the evaluation of the internal energy.
- 109 F. J. Rogers, D. A. Young, H. E. DeWitt, M. Ross, Phys. Rev. A28, 2990 (1983)
- 110 F. Lado, Phys. Lett. 89A, 196 (1982)
- 111 H. Iyetomi, S. Ichimaru, Phys. Rev. A25, 2434 (1982)
H. Iyetomi, S. Ichimaru, Phys. Rev. A27, 3241 (1983)
- 112 Q. N. Usmani, B. Friedman, V. R. Pandharipande, Phys. Rev. B25, 4502 (1982)
- 113 E. E. Salpeter, Austr. J. Phys. 7, 373 (1954) and
S. Ichimaru, Rev. Mod. Phys. 54, 1017 (1982)
- 114 J. P. Hansen, G. M. Torrie, P. Vieillefosse, Phys. Rev. A16, 2153 (1977)
- 115 H. E. DeWitt, W. B. Hubbard, Ap. J. 205, 295 (1976)
- 116 G. Senatore, M. Rovere, M. Parrinello, M. P. Tosi
N. Cimento, 56B, 39 (1980)
- 117 Very recently good performances of the TC scheme for this problem have been reported. F. J. Rogers, H. E. DeWitt in "Conference Record of the 1984 IEEE International Conference on Plasma Science" (IEEE, NY 1984)p. 123
- 118 F. Nicolo, in "Nonlinear Equations in Classical and Quantum Field Theory" ed. N. Sanchez, Lecture Notes in Physics (Springer Verlag, Berlin 1985)p. 301
- 119 R. B. Laughlin Phys. Rev. Lett. 50, 1395 (1983)
- 120 H. Zabel, A. Magerl, A. J. Dianoux, J. J. Rush,
Phys. Rev. Lett. 50, 2094 (1983)
- 121 J. Haberle, S. Franco, Z. Naturforsch. 23a, 1439 (1968);
S. Franco, J. Haberle, Z. Naturforsch. 25a, 134 (1970);
S. Margulies, P. Debrunner, H. Frauenfelder, Nucl. Instr. and Meth. 21, 217 (1963)
- 122 C. C. Grimes, Surf. Sci. 73, 397 (1978)
- 123 R. Williams, R. S. Crandall, Phys. Lett. 36A, 35 (1971)
- 124 F. M. Peeters, Phys. Rev. B30, 159 (1984)
- 125 R. S. Crandall, R. Williams, Phys. Lett. 34A, 404 (1971)
- 126 C. C. Grimes, G. Adams, Phys. Rev. Lett. 42, 795 (1979)

127 D. S. Fischer, B. I. Halperin, P. M. Platzman,
Phys. Rev. Lett. 42, 798 (1979)

128 M. Baus, J. Stat. Phys. 19, 163 (1978)

129 A. L. Fetter, Phys. Rev. B10, 3739 (1974); H. Totsuji,
J. Phys. Soc. Japan 39, 253 (1975); ibidem 40, 857 (1976);
J. Chalupa, Phys. Rev. B12, 4 (1975); ibidem B13, 2243
(1976); P. M. Platzman, N. Tsoer, Phys. Rev. B13, 3197 (1976)

130 F. Lado, Phys. Rev. B17, 2827 (1978);

131 R. W. Hockney, T. R. Brown, J. Phys. C8, 1813 (1979)

132 H. Totsuji, H. Kakeye, Phys. Rev. A22, 1220 (1980)

133 R. C. Gann, S. Chakravarty, G. V. Chester, Phys. Rev. B20, 326
(1979)

134 M. Baus, J. P. Hansen ref [92]

135 R. H. Morf, Phys. Rev. Lett. 43, 931 (1979)

136 R. K. Kalia, P. Vashishta, S. W. DeLeeuw, Phys. Rev. B23,
4794 (1981)

137 J. P. Hansen, D. Levesque, J. J. Weis, Phys. Rev. Lett. 43, 979
(1979)

138 L. Bonsall, A. A. Maradudin, Phys. Rev. B15, 1959 (1977)

139 S. Chakravarty, C. Dasgupta, Phys. Rev. B22, 369 (1980)

140 A. Alastuey, B. Jancovici, J. Stat. Phys. 24, 443 (1981)

141 R. E. Peierls, Helv. Phys. Acta 7, 81 (1923);
Ann. Inst. Poincaré' 5, 177 (1935)

142 N. D. Mermin, Phys. Rev. 176, 250 (1968)

143 B. Jancovici, see ref [140]. To be rigorous the theorem is
proved assuming that the T.L. exists for the internal energy
per particle.

144 B. I. Halperin, D. R. Nelson, Phys. Rev. Lett. 41, 121
(1978); ibidem 41, 519 (1978); D. R. Nelson, B. I. Halperin,
Phys. Rev. B19, 2457 (1979); see also A. Holz,
J. T. N. Medeiros, Phys. Rev. B17, 1161 (1978).

145 F. F. Abraham in "Ordering in Two Dimension" S. Sinha
Ed., (North Holland Inc.) 1980 p. 155 see also the
discussion in Gann et al. [133]

146 J. M. Kosterlitz, D. J. Thouless, J. Phys. C6, 1181 (1973)

147 W. G. Hoover, W. T. Ashurst, R. J. Olivers, J. Chem. Phys. 60,
4043 (1974)

148 At present there is no parametrization of computer
experiment results for a hard disk system. The PY equation has
been solved numerically (no analytical solution is
available in 2D) following the previous work by D. G. Chae,
F. H. Ree, T. Ree, J. Chem. Phys. 50, 1581 (1969) and F. Lado,
J. Chem. Phys. 49, 3092 (1968); we note that the comparison PY
versus simulation seems to be better in 2D than in 3D.

149 The $D_{NSA}(r)$ are defined only for $r > \sigma_{NSA}$. Since their
precise values for $r < \sigma_{NSA}$ are decreasingly important going to

$r = 0$ due to the presence of the cross-over function $f(r)$, we have continued them with a straight line. In any case the final results are not dependent from the exact form of b inside the core.

- 150 J. G. Kirkwood, E. Monroe, *J. Chem. Phys.* 9, 514 (1941)
- 151 T. V. Ramakrishnan, M. Youssuf, *Phys. Rev.* B19, 2775
(1979) M. Youssuf, *Phys. Rev.* B23, 5871 (1981) A. D. Haymet,
D. W. Oxtoby, *J. Chem. Phys.* 74, 2559 (1981) M. Rovere,
M. P. Tosi, *J. Phys.* C18, 3445 (1985)
- 152 J. M. Caillol, D. Levesque, J. J. Weis, J. P. Hansen,
J. Stat. Phys. 28, 925 (1982)
- 153 T. V. Ramakrishnan, *Phys. Rev. Lett.* 48, 541 (1982)
- 154 G. J. Jones, U. Mohanty, *Mol. Phys.* 54, 1241 (1985)
- 155 [154], and M. Rovere, private communications.
- 156 In the spirit of the discussion of Rosenfeld and Ashcroft about the role of the bridge functions, we can interpretate the eq. 2.26 as an exact equation in an unknown periodic external field which exactly erases the higher order correlation terms and with its presence stabilizes the long-range translational order.
- 157 M. Bretz, J. G. Dash, D. C. Hickernell, E. O. McLean,
D. E. Vilches, *Phys. Rev.* A8, 1589 (1973) R. L. Siddon,
M. Schick, *Phys. Rev.* A9, 907 (1974) S. Sokolowski, W. Steele,
J. Chem. Phys. 82, 3413 (1985)
- 158 M. Plischke, *Can. J. Phys.* 59, 802 (1982) M. Plischke,
W. D. Leckie, *Can. J. Phys.* 60, 1139 (1982) R. Clarke, in
"Ordering in Two Dimensions", S. Sinha Ed. (North Holland
Inc. 1980) p. 53; H. Zabel, *ibidem*, p. 611
- 159 A good discussion of the known theoretical and numerical results for CHS as primitive model for ionic liquid can be found in the paper of B. Hafskjold and G. Stell in "The liquid State of Matter" E. W. Montroll and J. L. Lebowitz Eds. (North Holland Co. 1982) p. 175
- 160 R. Caminiti, *J. Chem. Phys.* 77, 5682 (1982)
- 161 R. Caminiti, *Z. Naturforsch.* 36a, 1062 (1981)
R. Caminiti, G. Johanson, *Acta. Chem. Scand.* A35, 373 (1981)
- 162 T. W. Melnyk, B. L. Sawford, *Mol. Phys.* 29, 891 (1975)
- 163 F. E. Rosztocy, D. Cubicciotti, *J. Phys. Chem.* 69, 1687
(1965) B. Makowsky, N. Nicoloso, W. Freyland,
Ber. Bunsenges. Phys. Chem. 88, 297 (1984)
- 164 W. Kantzig, M. Labbert, *J. Physique* 37, C7-39 (1976);
- 165 S. Soprirejan, G. C. Kennedy, *Am. J. Sci.* 260, 115 (1962);
K. S. Pitzer, M. C. P. deLima, D. R. Schreiber, *J. Phys. Chem.* 81,
1854 (1985)
- 166 For the neutral case the relevance of a non additive hard sphere system as reference has been underlined by D. Levesque, J. H. Nixon, M. Silbert, J. J. Weis, *J. Physique* 41,
C8-317 (1980)
- 167 D. J. Adams, I. R. McDonald, *J. Chem. Phys.* 63, 1900 (1975)

- 168 see ref. [162]
- 169 J. L. Lebowitz, D. Zomick, J. Chem. Phys. 54, 3335 (1971)
D. Penrose, J. L. Lebowitz, J. Math. Phys. 13, 604 (1972)
- 170 J. H. Nixon, M. Silbert, Mol. Phys. 52, 207 (1984)
- 171 Actually the very idealized model in which $\sigma_{11} = \sigma_{22} = 0$ and $\sigma_{12} \neq 0$ is the continuous analogous of the Widom and Rowlinson lattice model (B. Widom, J. S. Rowlinson, J. Chem. Phys. 52, 1670 (1970)) which shows a phase separation behavior.
- 172 CHS additive: B. Larsen, Chem. Phys. Lett. 27, 47 (1974);
J. C. Rasaiah, D. N. Card, J. P. Valleau, J. Chem. Phys. 56, 248 (1972);
B. Larsen, J. Chem. Phys. 68, 4511 (1978);
J. C. Rasaiah, H. L. Friedman, J. Chem. Phys. 48, 2742 (1968);
ibidem, 50, 3965 (1969); F. J. Rogers, J. Chem. Phys. 73, 6272 (1980);
- 173 A. H. Narten, H. A. Levy, Science 165, 447 (1969);
- 174 The EXAFS and related techniques or the differential scattering seem particularly promising to this aim.
- 175 N. Shimoji, "Liquid Metals" (Academic Press, London 1977)
- 176 R. Evans in "Microscopic Structure and Dynamics of Liquids" Ed. A. J. Dianoux, J. Dupuy (Plenum, NY 1979)p. 417;
N. W. Ashcroft, D. Stroud Sol. St. Phys. 33, 1 (1978);
N. W. Ashcroft in "The Liquid State of the Matter" Ed. E. W. Montroll, J. L. Lebowitz (North Holland Co. 1982)p. 141;
- 177 V. Heine and coworkers in Sol. St. Phys. 24 (1970)
- 178 K. K. Hon, N. H. Ashcroft, G. V. Chester Phys. Rev. B19, 5103 (1979);
J. M. Gonzales Miranda, V. Torra, Phys. Lett. 103A, 126 (1984);
J. M. Gonzales Miranda, J. Phys. F (1985) in press
- 179 H. Hasegawa, J. Phys. F 6, 649 (1976)
- 180 L. Dagens, M. Rasolt, R. Taylor, Phys. Rev. B11, 2717 (1975)
- 181 N. W. Ashcroft, Phys. Lett. 23, 48 (1966)
- 182 Some of the most frequently used dielectric functions in the liquid metal literature are in the papers of: F. Toigo, T. O. Woodruff, Phys. Rev. B2, 3958 (1970);
D. J. N. Geldart, S. H. Vosko, Can. J. Phys. 44, 2137 (1966); see also the next two references.
- 183 P. Vashishta, K. S. Singwi, Phys. Rev. B6, 875 (1972). In this paper a simple analytical fit is given for the local field function $Q(q)$. A comparison with the tabulated results shows discrepancies in the dielectric function up to 10%. For this reason we have always used a direct numerical interpolation of the tabulated values.
- 184 K. S. Singwi, M. P. Tosi, R. H. Land, A. Sjolander, Phys. Rev. 176, 589 (1968);
- 185 S. Ichimaru, K. Utsumi, Phys. Rev. B 24, 7385 (1981)
- 186 D. M. Ceperley, B. J. Alder, Phys. Rev. Lett. 45, 566 (1980);
D. M. Ceperley, Phys. Rev. B 18, 3126 (1978);
L. J. Lantto, ibidem, 22, 1380 (1980); J. C. Zabolitsky,

- Phys. Rev. D 22, 2353 (1980)
- 187 G. Baym, Phys. Rev. 135, A1691 (1964)
- 188 J. M. Ziman, Phil. Mag. 6, 1013 (1961)
- 189 T. E. Faber "Theory of Liquid Metals" (Cambridge Univ. Press 1972)
- 190 P. Bohm, T. Staver, Phys. Rev. 84, 836 (1951); see also D. Pines "Elementary Excitations in Solids (NY 1964)
- 191 F. Postogna, M. P. Tosi N. Cimento 55B, 399 (1980); see Appendix C
- 192 M. P. Tosi, in "Electron Correlations in Solids, Molecules and Atoms" Ed. J. T. Devreese, F. Brouers (Plenum Publ. Co. 1983)
- 193 S. A. Trigger, Phys. Lett. 56A, 325 (1976)
- 194 N. Montella, G. Senatore, M. P. Tosi, Physica B124, 22 (1984); D. K. Chaturvedi, G. Senatore, M. P. Tosi, Lett. N. Cimento 30, 47 (1981); D. K. Chaturvedi, M. Rovere, G. Senatore, M. P. Tosi, Physica 111B, 11 (1981)
- 195 Since an electron responds to a potential which includes a contribution from the exchange and correlation effects, the screening corrections which enter in $V_e(k)$ are different from those which enter in the effective inter-ionic potential. If an external field is screened by the "electronic" dielectric function will be $\epsilon(k, \omega) = \epsilon(k, \omega) (1 + G(k) \hbar^2 / k^2 \chi_0(k, \omega))$. (see e. g. R. W. Shaw, J. Phys. C 3, 1140 (1970))
- 196 J. M. Ziman in "The Properties of Liquid Metals" Ed. P. D. Adams, H. A. Dover, S. G. Epstein (Taylor and Francis, London 1967) p. 551; H. Endo, Phil. Mag. 8, 1403 (1963); J. Hennephof, C. van der Marel, W. van der Lugt, Physica 94B, 101 (1978); J. M. Dickey, A. Mayer, W. H. Young, Proc. Phys. Soc. 92, 460 (1967); S. Y. Lien, J. M. Sivetsen, Phil. Mag. 20, 759 (1969)
- 197 B. P. Ablas, M. van der Lugt, H. J. L. van der Velck, J. Th. M. De Hosson, C. van Dijk, Physica 101B, 177 (1980); M. J. Huijben, W. van der Lugt, W. A. M. Reinart, J. Th. M. De Hosson, C. van Dijk, Physica 97B, 338 (1979);
- 198 T. E. Faber, J. M. Ziman, Phil. Mag. 11, 153 (1965)
- 199 J. C. Wheeler, D. Chandler, J. Chem. Phys. 53, 1645 (1971)
- 200 J. Hennephof, W. van der Lugt, G. W. Wright, Physica 52, 279 (1971); J. Hennephof, C. van der Marel, W. van der Lugt, Physica 94B, 101 (1978);
- 201 G. Senatore, M. P. Tosi, Phys. Chem. Liq. 11, 365 (1982)
- 202 A. Rahman, Phys. Rev. Lett. 32, 52 (1974); Phys. Rev. A9 1667 (1974)
- 203 D. L. Price, K. S. Singwi, M. P. Tosi, Phys. Rev. B2, 2983 (1970)
- 204 R. A. McDonald, R. D. Mountain, R. C. Shukle, Phys. Rev. B20, 4012 (1979) R. D. Mountain, Phys. Rev. A26, 2859 (1982).
- 205 H. Minoo, C. Deutsch, J. P. Hansen, J. Physique Lett.

38, L191 (1971)

206 D. L. Price, K. S. Singwi, M. P. Tosi, Phys. Rev. B2, 2983 (1970)

207 I. L. McLaughlin, W. H. Young, J. Phys. F12, 245 (1982);
R. E. Jacobs, H. C. Andersen, Chem. Phys. 10, 73 (1975);
N. K. Aillawadi, Phys. Rep. 57, 241 (1980); R. Kumaravadivel,
R. Evans, J. Phys. C9, 3877 (1976).

208 G. Kahl, J. Hafner, Z. Phys. B58, 283 (1985)

209 R. Kumaravadivel, M. P. Tosi, N. Cimento D4, 39 (1984)

210 Y. Waseda, Z. Naturforsch. 38a, 509 (1983)

211 C. G. Matthai, N. H. March, Phys. Chem. Liquids 11, 207 (1982)

212 M. Rasolt, Phys. Rev. B29, 3703 (1984)

213 For example it is well known (C. J. Fethick, Phys. Rev. B2, 1789 (1970) and W. Jones, J. Phys. C6, 2833 (1973)) that the consistency between the fluctuation and the virial routes to the compressibility involves non linear effects of the electron-ion interactions.

214 A. P. Copestake, R. Evans, J. Phys. C15, 4961 (1982);
G. Pastore unpublished.

215 M. C. Abramo, C. Caccamo, G. Pizzimenti, M. Parrinello,
M. P. Tosi, J. Chem. Phys. 68, 2889 (1978); M. Rovere,
M. Parrinello, M. P. Tosi, P. V. Giaquinta, Phil. Mag. B39, 167 (1979)

216 M. P. Tosi, F. G. Fumi, J. Phys. Chem. of Sol. 25, 45 (1964)

217 All the alkali halides but the heavier cesium halides have the NaCl structure at normal pressure

218 J. E. Mayer, J. Chem. Phys. 1, 270 (1933)

219 R. H. Lyddan, R. G. Sachs, E. Teller, Phys. Rev. 59, 673 (1941)

220 L. V. Woodcock, K. Singer, Trans. Faraday Soc. 67, 12 (1971)
L. V. Woodcock, Proc. R. Soc. London A328, 83 (1972)
M. Dixon, M. J. L. Sangster, Phil. Mag. 35, 1049 (1977)
J. W. E. Lewis, K. Singer, L. V. Woodcock, J. Chem. Soc. Faraday Trans. II 71, 41 (1975)

221 M. Dixon, M. J. Gillan, Phil. Mag. B43, 1099 (1981)

222 The examination of the first peak of the like $g(r)$ in the charged hard sphere liquid clearly reveals that the modulation seen also in the case of soft repulsion is due to a double possible arrangement of three ions: linear (e.g. $+ - +$) or bent ($+ - +$). In this sense we are probing the effects of three-body correlations on the two-body $g_{ii}(r)$.

223 R. Bacquet, P. J. Rossky, J. Chem. Phys. 79, 1419 (1983)

224 G. Casanova, R. Eggenhoffner, F. G. Fumi, Boll. SIF 115, 74 (1978) and [221].

225 The parameters were determined by R. W. Busing, Trans. Amer. Crystallogr. Ass. 6, 57 (1970) from an analysis of crystal data for alkaline-earth halides.

226 S. W. de Leeuw, Ph.D. Thesis, University of Amsterdam 1976; S. W. de Leeuw, Mol. Phys. 36, 103 (1978) S. W. de Leeuw, Mol. Phys. 36, 765 (1978)

227 The explicit dependence of $b_{\alpha\beta}(r)$ from the density has been taken into account.

228 F. G. Edwards, J. E. Enderby, D. I. Page, J. Phys. C8, 3483 (1975); S. Biggins, J. E. Enderby, J. Phys. C14, 3129 (1981); E. W. J. Mitchell, P. F. J. Poncet, R. J. Stewart, Phil. Mag. 34, 721 (1976);

229 L. A. Curtiss, C. W. Kan, R. L. Matcha, J. Chem. Phys. 63, 1621 (1975)

230 S. Froyen, M. L. Cohen, Phys. Rev. B29, 3770 (1984) G. Bobel, G. Cortona, C. Sommers, F. G. Fumi, Acta Cryst. A39, 400 (1983)

231 P. O. Lowdin, Adv. Phys. 5, 1 (1956)

232 J. R. Hardy, A. M. Kato, "The lattice dynamics and Statics of Alkali Halides Crystal" (Plenum Press N. Y. 1969)

233 R. K. Singh, Phys. Rep. 85, 259 (1982)

234 M. J. L. Sangster, M. Dixon, Adv. Phys. 25, 247 (1976); M. Dixon, M. J. L. Sangster, J. Phys. C9, 15 (1976); ibidem, C8, L8 (1975); ibidem, C9, 909 (1976); G. Jacucci, Phys. Rev. A13, 1581 (1976);

235 M. D. Johnson, N. H. March, Phys. Lett. 3, 313 (1963)

236 N. K. Ailawadi, Phys. Rep. 57, 241 (1980); M. W. C. Darma-wardana, G. C. Aers, Phys. Rev. B28, 1701 (1983); W. Schommers, Phys. Lett. A43, 157 (1973); D. Levesque, J. J. Weis, L. Reatto, Phys. Rev. Lett. 54, 451 (1985)

237 Y. Waseda, T. Sakuma, Metal. Phys. Seminar 2, 313 (1977); see also Y. Waseda, "The Structure of non Crystalline Materials" (McGraw Hill, NY 1980);

238 F. G. Edwards, J. E. Enderby, R. A. Howe, D. I. Page, J. Phys. C11, 1053 (1978)

239 S. Biggins, J. E. Enderby, J. Phys. C14, 3129 (1981)

240 S. Biggins, J. E. Enderby, J. Phys. C14, 3577 (1981)

241 R. L. McGreevy, E. W. J. Mitchell, J. Phys. C. 15 5537 (1982)

242 S. Biggins, M. Gay, J. E. Enderby, J. Phys. C17, 977 (1984);

243 M. Rovere, M. P. Tosi, Solid State Communications, 55, 1109 (1985)

244 W. Olivares, McQuarrie, J. Chem. Phys. 65, 3604 (1976)

245 P. J. Rossky, S. Dale, J. Chem. Phys. 68, 3391 (1978); ibidem, 73, 2457 (1980)

246 J. W. Cooley, J. W. Tuckey, Math. Comp. 19, 297 (1965); see also A. J. Starshek, R. D. Larsen, Phys. and Chem. of Liq. 2, 45 (1970)

247 H. J. Gillan, Mol. Phys. 38, 1781 (1979); G. M. Abernethy,

M. J. Gillan, *ibidem* 39, 837 (1980)

248 See e.g. C. A. J. Fletcher, "Computational Galerkin Methods" Springer-Verlag, Berlin 1984"

249 F. James, M. Ross, CERN Computer Centre Program Library.

250 T. N. L. Patterson, "Collected Algorithms from CACM" Algorithm 468 (1974).